The Dissertation Committee for Carolyn M. Cooper Certifies that this is the approved version of the following Dissertation:

A Mechanistic Exploration of Oil Recovery via Selective Oil Permeation

Committee:

Lynn E. Katz, Supervisor

A. Frank Seibert, Co-Supervisor

Kerry A. Kinney, Co-Supervisor

Benny D. Freeman

Desmond F. Lawler

A Mechanistic Exploration of Oil Recovery via Selective Oil Permeation

by

Carolyn M. Cooper

Dissertation

Presented to the Faculty of the Graduate School of

The University of Texas at Austin

in Partial Fulfillment

of the Requirements

for the Degree of

Doctor of Philosophy

The University of Texas at Austin

May 2023

Acknowledgements

I first want to thank my three advisors: Dr. Lynn Katz, Dr. Kerry Kinney, and Dr. Frank Seibert. The opportunity to benefit from your knowledge and kindness has been truly incredible. I would also like to acknowledge my committee members, Dr. Benny Freeman and Dr. Desmond Lawler, for the insight they provided throughout the process.

I would also like to express the sincerest thanks to collaborators in the Innovation at the Nexus of Food-Energy-Water Systems National Research Traineeship Program (Dr. Charles Werth, Laura Klopfenstein, Dr. Ali Fares, Dr. Ripendra Awal, Dr. Jacob Troutman), the National Alliance for Water Innovation (Dr. Tzahi Cath, Dr. Shankar Chellam, Dr. James Rosenblum, James McCall), and Kuwait University (Dr. Abdalrahman Alsulaili and Sara Alshawish) for broadening my understanding of water treatment and the intersectionality of reuse.

I have deeply appreciated the Katz group's support, particularly Alex Wu, Dr. Aurore Mercelat, Benjamin Kienzle, Cameron McKay, Evie Wang, Dr. Justin Davis, Laura Lee, Dr. Matthew Landsman, Sheik Mohammad Nomaan, and Tulasi Ravindran. The encouragement of my friends, both inside and outside academia, has been vital.

I must thank my husband (Dennis Budde), family (especially Dr. Keith Cooper, Dr. Linda Torczon, Christine Cooper, Al Budde, and Nancy Budde), and dog (Bluebell Cooper-Budde) for tolerating my endless rambling about water treatment and climate change. You do not need to read this dissertation – you're already too aware of its contents.

Finally, I want to thank all the fierce, independent women in my life, particularly my mother (Dr. Linda Torczon), sister (Christine Cooper), and my grandmothers (Rayna Cooper and Mary Jo Torczon) all of whom made sure I knew anything was possible. I truly would not be here without your example.

Abstract

A Mechanistic Exploration of Oil Recovery via Selective Oil Permeation

Carolyn M. Cooper, PhD

The University of Texas at Austin, 2023

Supervisors: Lynn E. Katz, A. Frank Seibert, and Kerry A. Kinney

Oil-water separations are necessary for the reuse of oil-laden wastewater. For example, oil and gas produced water may have influent oil concentrations of up to 2,000 mg/L that must be reduced to <10–35 mg/L to meet regulatory requirements for non-industrial reuse. However, many conventional oil-water separation processes are unable to achieve these effluent concentrations. Selective oil permeation is a promising membrane-based oil-water separation approach that may be able to meet these treatment goals. The process differs from traditional membrane-based oil-water separations by permeating oil (instead of water) through the hydrophobic membrane. Exploitation of the preferential oil wetting of the membrane surface minimizes viscous fouling and generates an oil permeate stream.

Previous investigation of selective oil permeation has demonstrated its ability to recover oil over extended durations. Researchers have hypothesized that mechanistic competition between coalescence and permeation controls oil recovery, results in the development of an oil film at the membrane surface, and leads to transport phenomena that deviate from traditional pore flow models. However, further verification is necessary to validate the existence of hypothesized mechanisms within the process and verify its

applicability to produced water treatment. Few studies have investigated mechanistic interactions or process performance (i.e., oil flux, oil recovery, permeate quality) for oil concentrations less than 1%. Even fewer have probed relationships between process performance, operating conditions, and water quality characteristics. Understanding the answers to these outstanding questions is crucial to defining the opportunity space for selective oil permeation.

This dissertation is the first set of studies to present results that (1) characterize and provide guidance for enhancing the membrane conditioning process, (2) identify how the operative mechanisms are impacted by system characteristics, operating conditions, and water quality characteristics within this lower oil concentration range, and (3) apply selective oil permeation to produced water. Achieving the outlined objectives will both expand our understanding of the role of the two key mechanisms underlying selective oil permeation (coalescence and permeation) and begin to define the opportunity space for oil recovery via selective oil permeation.

Table of Contents

List of Tables

List of Figures

Chapter 1: Introduction

Introduction and Research Objectives

Oil-water separations are crucial to achieving the circular water economy. Oily wastewaters like oil and gas produced water, wastewater from petroleum refineries and petrochemical facilities, and metalworking fluids may have influent oil concentrations of 2–560 mg/L, 12–20,000 mg/L, and 20–200,000 mg/L, respectively.[1–5] Recycling and beneficial reuse (*e.g.*, crop irrigation, surface discharge, municipal reuse) of these wastewaters may require effluent total oil concentrations of <10–35 mg/L to meet regulatory requirements.[4,5] Furthermore, effective oil-water separations can enable advanced treatment processes by mitigating oil fouling or allowing for additional valorization through resource recovery of the oil.

Conventional oil-water separations are traditionally categorized as primary, secondary, or tertiary processes. Primary oil-water separations encompass gravity separation of free oil (≥ 150 µm). Secondary oil-water separations target dispersed oil (> 50 µm) using chemical or centrifugal methods. Tertiary oil-water separations remove emulsified oils (≤ 50 µm) via either adsorption or filtration methods.[4,6,7] However, conventional methods often have long retention times, low removals of emulsified oils, use extraneous chemicals, and occupy a large footprint.[8] Consequently, researchers have explored the application of membranes (where water permeates through the membrane pores) to achieve a high quality water permeate and smaller footprint.[6] However, membrane-based oil-water separations often suffer from viscous oil fouling of the membrane surface.[6,9–16]

Selective oil permeation differs from traditional membrane-based oil-water separations by permeating oil (instead of water) through a hydrophobic membrane. Permeation of oil through the membrane pores exploits the preferential oil wetting of the membrane surface to minimize viscous fouling[17,18] and generate an oil permeate stream.[19,20] Selective oil permeation has been shown to directly separate insoluble oils (*e.g.*, algal oils,[17,21] Isopars,[22] gas oil,[20] naphthenic oil,[23] kerosene,[24,25] dodecane,[23] isododecane,[26] tetradecane[19]) from oil-water emulsions. These analyses have demonstrated the importance of various operational parameters (*e.g.*, influent flow rate, transmembrane pressure, oil concentration) and solution characteristics (*e.g.*, oil viscosity, interfacial tension) on oil recovery[18,19,22,23,26] and permeate quality.[19,20] The observed relationships between operating parameters, solution characteristics, and oil recovery have been attributed to mechanistic competition between the approach of oil droplets to the membrane surface, coalescence of the oil onto the membrane surface, the permeation of oil through the membrane pores, and finally release of the oil from the permeate-side of the membrane.[22–24,27,28]

However, studies of selective oil permeation have failed to address many questions crucial to the application of selective oil permeation to produced water. This dissertation presents research that advances our fundamental understanding of the mechanisms, process variables, operating conditions, and water quality characteristics that impact process performance. Through this, we seek to define the opportunity space for selective oil permeation. The first objective assesses the efficacy of selective oil permeation within a concentration range relevant to produced water treatment (2–565 mg/L) in the context of operative mechanisms. The second objective evaluates the influence of water quality characteristics on key transport mechanisms and process performance. The third objective investigates water breakthrough in selective oil permeation through the lens of the Young-

Laplace equation. Finally, the fourth objective directly applies selective oil permeation to real produced water to verify research outcomes from Objectives 1, 2, and 3. This dissertation constitutes the first set of studies to present results that (1) characterize and relate the mechanisms of oil removal to the membrane conditioning process, (2) identify how the operative mechanisms are impacted by system characteristics, operating conditions, and water quality characteristics within this lower oil concentration range, and (3) apply selective oil permeation to produced water treatment. Through these studies, selective oil permeation is demonstrated to be an effective secondary (or tertiary) oil-water separation process that can meet regulatory requirements for the beneficial reuse of produced water. Achieving the outlined objectives will both expand our understanding of the role of the two key mechanisms underlying selective oil separation (coalescence and permeation) and define the opportunity space for oil recovery from produced water and oil spills via selective oil permeation.

DISSERTATION STRUCTURE

The dissertation is divided into chapters and organized as follows:

Chapter 2: Expanding Produced Water Reuse via Conventional and Membrane-Based Oil-Water Separations

Chapter 2 includes a review of existing produced water treatment challenges and how these relate to oil-water separation methods. Conventional and emerging oil-water separation methods are then reviewed to inform the discussion of oil-water separations via selective oil permeation. The selective oil permeation literature is

then discussed to highlight observed relationships, the existing mass transfer model, and outstanding questions.

Chapter 3: Materials and Methods

Chapter 3 provides a brief overview of the experimental approach, materials, and equipment used during experimentation.

Chapter 4: Selective Oil Permeation for Oil Recovery from Low Oil Concentrations

Chapter 4 investigates the behavior of selective oil permeation under a variety of operating parameters (*e.g.*, transmembrane pressure and influent flow rate) and influent feed characteristics (*e.g.*, oil concentration, viscosity, interfacial tension) for oil water emulsions containing $\leq$ 200 mg/L oil. Oil concentrations within this range are of particular importance due to the limited research conducted within this range as well as their relevance to produced water treatment. This chapter also explores how underlying mechanisms influence membrane conditioning and performance. Ultimately, the original mass transfer for selective oil permeation is updated to describe oil flux and oil recovery for lower oil concentrations over a broader range of influent flow rates.

Chapter 5: Effects of Water Quality on Selective Oil Permeation Performance

Chapter 5 describes the behavior of selective oil permeation with oil-water emulsions of varying pH, salinity, and surfactants (*i.e.*, non-ionic, anionic, and cationic). Analysis of variance (ANOVA) is then applied to the results to elucidate the significance of the observed relationships among these properties and macroscopic performance (*i.e.*, oil flux and oil recovery).

Chapter 6: Predicting Water Breakthrough during Selective Oil Permeation

Chapter 6 explores water breakthrough in selective oil permeation through the lens of the Young-Laplace equation to identify appropriate operating conditions (*e.g.*, transmembrane pressure, interfacial tension) and membrane properties (*e.g.*, nominal pore size, breadth of pore size distribution) that may optimize oil recovery. Experimental results are then compared to theoretical estimates from the Young-Laplace equation to provide operational and design guidelines for transmembrane pressure selection in selective oil permeation systems.

Chapter 7: Oil Recovery from Produced Water via Selective Oil Permeation

Chapter 7 presents the first published data for oil recovery from produced water via selective oil permeation. The results are then compared to theoretical expectations to better understand the broader opportunity space for selective oil permeation.

Chapter 8: Conclusions and Recommendations

Chapter 8 summarizes findings from the proceeding chapters. It also provides potential avenues for future research to expand our understanding of selective oil permeation.

Chapter 2: Expanding Produced Water Reuse via Conventional and Membrane-Based Oil-Water Separations

ABSTRACT

Pretreatment of produced water is necessary to support advanced treatment processes that can enable toxicity reduction for beneficial reuse. While conventional treatment processes are often effective, expanding produced water reuse will require autonomous, modular, high-throughput treatment trains. The expansion and integration of membrane technologies into produced water treatment might help achieve the circular water economy – particularly for desalination and targeted constituent removal. Yet, their ability to replace conventional pretreatment technologies is not well understood. This review considers conventional and membrane-based pretreatment processes for oil-water separations in the context of expanding produced water reuse. In particular, we identify the limitations of conventional oil-water separation processes, discuss existing conventional oil-water separation membrane technologies, and define areas of research that would facilitate the application of selective oil permeation to produced water treatment.

INTRODUCTION

Produced water is one of the main byproducts of the oil and gas production process. While produced water can refer to any sub-surface water brought to the surface during oil and gas production, produced water is often defined as the residual water after primary separations (*e.g.,* downhole oil-water separators, free water knockout) from the hydrocarbon resource.[29] Globally, approximately 250 million barrels of produced water are generated daily.[2] The majority of produced water is currently disposed of into the subsurface or reused within the oil and gas industry.[30] As water scarcity increases, interest in the beneficial reuse of produced water (*i.e.,* reuse outside of the oil and gas industry for applications including irrigation, surface water discharge, municipal reuse) will increase. However, the temporal and spatial variability of produced water complicates its management. These constraints ultimately necessitate fit-for-purpose treatment to meet effluent water quality requirements and adequately address toxicity .[2,31–36]

Effective pretreatment is necessary for the implementation of advanced treatment methods (*e.g.,* advanced oxidation processes, membranes) that can address recalcitrant and toxic constituents. In particular, produced water contains total oil and grease (TOG) concentrations ranging from approximately 2–565 mg/L that must be reduced to <5–44 mg/L to protect the formation during disposal, downstream equipment, treatment train efficacy, and the environment depending on the ultimate end-use.[37,38] However, many conventional pretreatment techniques often cannot meet these effluent requirements necessary for offshore produced water or advanced treatment process.[39,40]

Most research and revies of produced water management have detailed current and novel treatment and advanced treatment processes (*e.g.,* biological treatment,[41–45] membranes,[46–55] desalination,[56–58] adsorption,[59–62] advanced oxidation processes[63–65]).[2,3,36,40,66–74] Few have provided a comprehensive review of pretreatment methods.[7,46,75–

[77] This literature review focuses solely on produced water and crude oil characteristics, conventional oil-water separations, and membrane-based oil-water separations to motivate the exploration of selective oil permeation.

CRUDE OIL AND PRODUCED WATER COMPOSITION

Crude oil contains thousands of organic species (*e.g.*, alkanes, alkenes, alkynes, aromatics, polynuclear aromatics, resins, asphaltenes, and other complex hydrocarbon compounds[78–80]) that affect produced water composition, management, and toxicity.[78] Crude oil is nearly always generated as a water-in-oil emulsion. Demulsification of water-in-oil emulsions can occur via physical, chemical, or biological treatment approaches. Zolfaghari *et al.* provide a thorough review of these approaches.[81]

Produced water traditionally contains free oil ($\geq$ 150 µm), dispersed oil (> 50 µm), emulsified oil ($\leq$ 50 µm), or dissolved oil in water.[82,83] *N*-alkanes within the C_{10} to C_{30} range are the most prevalent groups, with the majority falling between C_{14} and C_{18}.[79,80] Dispersed oils traditionally consist of less-soluble compounds (*e.g.*, heavy alkyl phenols, polyaromatic hydrocarbons). Dispersed oil concentration within a raw produced water varies by factors including the density of oil, the interfacial tension between the water and oil, the efficacy of onsite physical separation equipment, the quantity of oil precipitation, and the shear history of the droplet itself.[2,84] Oil-in-water emulsion characteristics may vary physical characteristics of both the oil and water, agitation (*e.g.*, three-phase flows at high velocities, shear generated by pumps), and the presence of emulsifying agents.[83] In produced water, oil-in-water emulsions are often stabilized by produced water characteristics like hydraulic fracturing chemicals (*e.g.*, surfactants, emulsifiers) or solids (*e.g.*, Pickering emulsions), further complicating treatment.[81] In contrast, dissolved oils often include higher solubility and lower molecular weight compounds (*e.g.*, BTEX,

phenols, aliphatic hydrocarbons, carboxylic acid).[72] The concentration and composition of dissolved oils vary by factors including the type of oil, the volume of water generated, and the age of the well.[2]

Produced water also includes a plethora of inorganics, organics, microorganisms, solids, radioisotopes, and dissolved gasses that complicate its management. A multitude of studies[85–88] and reviews[1,2,31,33,74,80,89,90] have characterized produced water. The United States Geologic Survey also provides a Produced Water Geochemical Database that showcases the wide variability of produced water quality in the United States.[91] A summary of selected produced water characteristics is shown in **Table 1**.

Table 1: Selected produced water characteristics.[1,2,31] Abbreviations are as follows: Chemical Oxygen Demand (COD), Total Dissolved Solids (TDS), Total Organic Carbon (TOC), Total Oil and Grease (TOG), and Total Suspended Solids (TSS).

Parameter	Concentration	Parameter	Concentration
pH [a]	4.3 – 10	Na^{+} [a,b]	0 – 150,000 mg/L
TDS [b]	100 – 400,000 mg/L	Ca^{2+} [b]	0 – 74,000 mg/L
TSS [b]	1.2 – 1000 mg/L	Cl^{-} [a]	0 – 270,000 mg/L
TOC [a,b,c]	0 – 1,700 mg/L	HCO_3^{-} [a]	0 – 270,000 mg/L
COD [b]	1,220 – 2,600 mg/L	Li^{+} [b]	0.038 – 64 mg/L
TOG [a]	2 – 565 mg/L	B^{3+} [b]	5 – 95 mg/L

References: [a] Fakhru'l-Razi et al. 2009; [b] Al-Ghouti et al. 2019;[c] Benko et al. 2008

NON-MEMBRANE OIL-WATER SEPARATIONS

Oily wastewaters often require primary, secondary, and even tertiary oil-water separations to achieve the necessary effluent oil concentrations. Primary oil-water separations remove free oil via gravity separations (*e.g.*, gravity settlers, API (American

Petroleum Institute) separators, and plate coalescers). Removal of dispersed oils and emulsions is accomplished during secondary oil-water separations via centrifugal or flotation methods. Finally, tertiary, or polishing, oil-water separations traditionally implement membranes, adsorption, or biological treatment processes.[92]

Table 2 shows the characteristics, advantages, and disadvantages of selected conventional oil-water separation processes. Many commonly used primary oil-water separations (*e.g.*, skim tanks, gun barrel tanks, API separators) have become mainstays in produced water treatment due to their minimal maintenance requirements and simple structures.[6,93] The efficiency of these separations can be increased through internal coalescence devices in processes (*e.g.*, corrugated plate inceptor (CPI)) that reduce the equipment size and minimum droplet removal.[6,94] Separation efficiency can be further optimized by adjusting both equipment parameters (*e.g.*, geometry, material surface properties) and operational characteristics (*e.g.*, fluid velocity).

Stokes' Law governs many of the methods for enhancing primary and secondary gravity-based oil-water separations:

$$V_R = \frac{(\rho_w - \rho_o) \times g \times {d_{drop}}^2}{18\mu} \quad (1)$$

Where V_R is the rise rate of a droplet, (m/s), ρ_w is the mass density of water (kg/m^3), ρ_o is the mass density of oil (kg/m^3), g is the gravitational acceleration (m/s^2), d_{drop} is the oil droplet diameter (m), and μ is the viscosity (N-s/m^2) of water. For example, increasing oil droplet size through coalescence (*e.g.*, API separators, CPI), adjusting viscosity and density via temperature variation, or modifying the density of particles through the addition of gas (*e.g.*, induced gas flotation) can increase oil removal efficiency. Microwaves, ultrasonic,

electrostatic, chemicals, product recycles, or mechanical barriers may also be used to enhance gravity settler performance.[95,96]

Secondary oil-water separation technologies focus on de-emulsification to remove dispersed oil droplets. Centrifugal treatment methods (*e.g.*, centrifuges, hydrocyclones) are a common approach for primary or secondary oil-water separations that apply a centrifugal force via a central moving component to generate circular motion of the solution. As a result of the applied force, the lighter phase moves towards the center of the separation device while the heavier phase moves towards the outer edge. Gas flotation methods (*e.g.*, dissolved gas flotation, dissolved air flotation (DAF), induced gas flotation) mechanically separate enlarged oil droplets by generating or injecting gas bubbles into the wastewater. Oil droplets then attach to the hydrophobic gas bubbles and the increase in both particle size and density difference (See **Equation 1**) allows flotation methods to achieve efficient oil-water separations.[97,98] Gas flotation generally achieves higher effluent water quality with shorter retention times and smaller equipment footprints than conventional gravity-based oil-water separation techniques.[98]

Tertiary (or polishing) oil-water separations traditionally implement adsorption (*e.g.*, nutshell filters, granular activated carbon (GAC)), membranes, oxidation, sorption in batch systems, or biological treatment processes.[4,6,7,92] Tertiary oil removal via nonfibrous sorbent materials,[7] fibrous sorbent materials,[99] and coalescence filtration[100] have high oil removal, low processing costs, and relatively simple operation. However, filtration and adsorption methods may yield poor removal of fine emulsions or require substantial hydraulic residence time to achieve higher removals.[99]

Table 2: Common conventional oil-water separation processes for produced water.

Method	Removal Capacity (μm)	Advantages	Disadvantages
Primary Oil-Water Separations			
Gravity Separators[6]	100 – 150	Minimal energy requirements	Low efficiency for small droplet diameters. Spatially inefficient
Gravitational Separators with Plate Separators[6]	30 – 50	Minimal energy requirements	Spatially inefficient
Secondary Oil-Water Separations			
Hydrocyclone[6,101]	10 – 30	Minimal energy and chemical requirements	Residuals management
Gas Flotation[6,75,98]	10 – 20	Minimal chemical requirements	Energy consumption
Tertiary Oil-Water Separations			
Media Filtration and Nutshell[6]	2 – 5	Minimal energy requirements	May require chemicals, may require frequent regeneration and/or replacement of media
Granular Activated Carbon[6,102]	2 – 5	Low energy requirements, treats a wide range of contaminants	May require frequent regeneration and/or replacement of media

MEMBRANE-BASED OIL-WATER SEPARATIONS

Membranes are a versatile and promising treatment technology for produced water treatment. Separation of contaminants or solutes in porous membranes (*e.g.*, microfiltration (MF), ultrafiltration (UF)) predominantly occurs through size exclusion while separation in nonporous membranes (*e.g.*, nanofiltration (NF), reverse osmosis (RO)) follows the solution-diffusion model. Several membrane processes have been explored within the context of produced water treatment.[47–55] However, this review focuses on water permeation through MF and UF membranes, as they are the most often applied to pretreatment.

Water transport through MF and UF membranes can be described via porous media fluid flow models like the Hagen-Poiseuille model or Ergun equation as follows:

$$J_w = \frac{\varepsilon \rho_w {r_{pore}}^2}{8\mu}\left(\frac{\Delta P}{L}\right) \quad (2)$$

Where J_w is the water flux, ε is membrane porosity, ρ_w is water density, r_{pore} is pore radius, μ is water viscosity, ΔP is applied transmembrane pressure, and L is membrane thickness. As seen in **Equation 2**, transport in porous membranes is influenced by factors including physicochemical properties of the solution (*e.g.*, viscosity, density) as well as membrane characteristics (*e.g.*, porosity, pore radius, membrane thickness). Transport can be further influenced by solute-membrane interactions, solute concentration, as well as by phenomenon like concentration polarization.[103]

Membranes, particularly MF and UF, are a promising tertiary oil-water separation method due to their ability to remove small oil droplets (< 1 μm) and high oil removals.[6,104] Membrane-based oil-water separations, where water permeates through the membrane, have been successfully demonstrated in both polymeric[105] and ceramic membranes.[106,107]

While both MF and UF have been evaluated for oil-water separations, UF is often considered more effective due to its lower propensity for oil breakthrough.[108]

Bench-scale studies using synthetic oil-water emulsions have determined relationships between operating characteristics (*e.g.,* transmembrane pressure, crossflow velocity, temperature) and solution characteristics (*e.g.,* oil concentration, pH, oil composition) on water flux and oil or total organic carbon (TOC) removal. Many of the experimental observations within these systems demonstrate the tradeoffs between water flux, oil rejection, and membrane fouling. Crucially, these tradeoffs can often be optimized through careful consideration of operating and solution characteristics.[10] Salahi *et al.* evaluated oil-water separations in refinery wastewater using the Taguchi method in a PAN UF membrane to determine that higher temperature, higher pH, moderate transmembrane pressure, and low crossflow velocity lessened flux decline.[15] Chakrabarty *et al.* found that higher transmembrane pressures increase flux, decrease oil rejection, and increase the rate of flux decline.[105] Hu and Scott observed an increase in water flux with increasing crossflow velocity – and consequently Reynolds Number – in three membranes (PTFE, PVDF, and regenerated cellulose). Water flux was found to be stable at 55°C.[11] Chakrabarty *et al.* also found flux to decline with increased oil concentrations due to concentration polarization and pore blocking.[105] However, Huang *et al.* only noted a significant decline in flux for the highest oil concentration examined (10.5%) using a Sepa1 CF II Med/High foulant lab scale crossflow membrane filtration unit.[109] These and other studies have provided a basis for understanding operating and solution characteristics helpful in optimizing membrane-based oil-water separations.

While the investigation of empirical relationships using synthetic water is crucial to improving the efficacy of membrane-based oil-water separations for pretreatment of produced waters, it is also essential to evaluate MF and UF membranes using real produced

waters. Abbasi *et al.* synthesized mullite and mullite-alumina ceramic membranes and evaluated oil rejection in both synthetic and real produced water. Oil rejection and flux were found to be substantially lower for real produced waters (70.8 – 84.0%, 41.3–91.5 L/m^2-h) than synthetic wastewaters (81.3–93.8%, 72.7–244.0 L/m^2-h).[110] Ahmad *et al.* optimized the synthesis of polyvinyl chloride/bentonite UF membranes to achieve 98.6% oil rejection from Digboi Oil Field produced water.[111] Results from these studies are promising, but reveal the importance of understanding how the complexity inherent to produced water effects the opportunity space for membrane-based treatment.

There are also several promising examples within the literature of membrane-based oil-water separations in real produced waters at the pilot-scale. A summary of selected studies is provided in **Table 3**. An early study by Bilstad *et al.* observed >95% total hydrocarbon removal from produced water via a PVDF UF membrane.[112] Yong *et al.* documented five years of operation of a produced water treatment train (skim tank + DAF + multimedia filtration + UF) for reinjection of treated water in Liaohe Oilfield. The UF system required backwashing every thirty minutes and chemical cleaning once every 24 hours to achieve the stringent effluent standards (<1 ppm TOG and total suspended solids (TSS)). While this study is promising, minimal information was provided regarding membrane longevity.[113] Lee *et al.* analyzed a similar treatment train (skim tank + desanding hydrocyclone + deoiling hydrocyclone + cartridge filter + UF) that reduced influent oil concentrations in West Texas produced water from 100–1,000 ppm to less than 2 ppm. Yet, Lee *et al.* noted the importance of hydrocyclone performance in minimizing oil fouling of the UF membrane.[114] Visvanathan *et al.* investigated three separate treatment trains (multimedia gravity filter + MF/UF/NF + RO) to assess the potential for RO treatment of produced water generated from natural gas production. While UF provided adequate removal of oil and grease, dissolved organics fouled the RO membrane – ultimately

necessitating pretreatment with NF to provide stable operations.[115] Ersahin *et al.* evaluated a more extensive pretreatment train for RO desalination of produced water (chemical precipitation + sand filter + GAC + UF + RO) to achieve approximately 94% chemical oxygen demand (COD) removal.[116] Ultimately, pilot-scale studies with real produced waters often demonstrate the promise of UF membranes for oil-water separations when paired with adequate pretreatment.

Table 3: Selected studies of the application of pressure-driven membrane technologies in the pilot-scale treatment of produced water. Abbreviations are as follows: Inlet oil concentration ($C_{oil,in}$), Hydrocarbon (HC), Microfiltration (MF), and Ultrafiltration (UF).

Feed Water	Process	$C_{oil,in}$	Performance
Produced Water (Snorre Field)[112]	UF	Total HC: 50 mg/L	Total HC: 95%
Natural Gas Produced Water (Thailand)[115]	MF, UF	393.3 mg/L	Not Reported[1]
Produced Water (USA)[114]	UF	~100–1,100 mg/L	< 2 mg/L
Produced Water (Daqing Field)[117]	UF	50–200 mg/L	90%
Produced Water[118]	UF	52–458 mg/L	25%
Produced Water[113]	UF	0.64 mg/L	0.42 mg/L
Produced Water[119]	MF	100 mg/L	<5 mg/L
Produced Water (Arabian Gulf) [120,121]	MF, UF	38–57 mg/L	73–86%
Produced Water (Germany)[122]	MF	94.4 mg/L	>95%[2]
Produced Water (Iran)[123]	UF	15–25 mg/L	80.8%[3]

Notes:
1) MF and UF pretreatment did not provide sufficient oil and grease removal to allow for operation of RO system without substantial fouling.
2) Removals provided for integrated treatment train of MF/NF
3) Removals provided for integrated treatment train of electrocoagulation + UF + RO

Fouling in Traditional Membrane-Based Oil-Water Separations

Membrane fouling is a major challenge in the application of membranes to produced water treatment. Fouling is often defined by the sorption and accumulation of contaminants (*e.g.,* organics, particles, colloids, inorganics, biological) at the membrane surface or within the pores. Accumulation of these contaminants often results in pore

constriction, pore blocking, and cake layer formation that reduce membrane efficiency (*e.g.*, decreased flux, increased transmembrane pressure, increased required energy input). Oil fouling of membranes is often described using traditional fouling models that consider cake filtration, deep bed filtration, complete blocking, and intermediate blocking of the membrane pore. Jepsen *et al.* details various fouling models (*e.g.*, Hermia's Blocking Laws, Resistance Based) and extensions of these models (*e.g.*, critical-flux extension, concentration extension, etc.) that have been employed to model oil fouling of membranes.[50]

Membrane-based oil-water separations often suffer from rapid, viscous fouling of the membrane surface that limits long-term performance.[6,9–16] Membrane fouling during oil-water separations depends on many factors including membrane morphology (*e.g.*, pore size), membrane surface characteristics (*e.g.*, surface chemistry, surface charge), and operating conditions (*e.g.*, water quality, contaminants, transmembrane pressure, crossflow velocity). While optimization of operating conditions (*e.g.*, crossflow velocity) may help reduce fouling rates, physical and chemical cleaning methods, surface shearing (*e.g.*, crossflow, vibrating membranes), additional pretreatment, and membrane modification have been explored to further limit flux decline.

One primary approach for reducing membrane fouling is to increase the hydrophilicity of the membrane surface to increase water adsorption and limit oil droplet attachment and film formation. Researchers have probed this approach through the addition of hydrophilic additives, surface modifications, and novel materials that exploit surface properties like wettability.[124–138] Babayev *et al.* modified PES UF membranes with zwitterionic polymer 3-(3,4-Dihydroxyphenyl)-L-alanine, which resulted in a decrease in flux decline from 38.4% to 16% during 5 hour experiments with Permian Basin produced water (3,200 mg/L COD; 156 mg/L TOC; 191,505 mg/L TDS).[139] Wandera *et al.*

grafted poly(N-isopropylacrylamide) (PNIPAAm)-block-poly(oligoethylene glycol methacrylate) to regenerated cellulose UF membranes. Modified membranes exhibited approximately 40% lower water flux than the unmodified membranes in a synthetic produced water (5,000 mg/L oil and grease, 82.23 mg/L TOC, 543 mg/L TDS), but exhibited a slower rate of flux decline per unit volume of water treated.[140] Naderi *et al.* tailored polyacrylonitrile UF membranes by combining dimethylformamide and N-methyl-2-pyrrolidone using a solvent mixture strategy. When tested with a synthetic produced water, changes in the membrane morphology due to alteration in the polymer concentration and solvent ratio effected both the oil rejection (89.5–99.6%) and water flux (583–399 L/m^2-h).[141] This tradeoff between oil rejection and water flux is well-documented in the literature.[140–144] Further, these approaches may result in fragile membranes, may not be appropriate for use with complex wastewaters, or are not readily commercially available.[8,137]

Researchers have also explored altering the hydrodynamics of membrane processes to minimize oil fouling. As previously noted, increasing turbulence at the membrane surface decreases the foulant deposition rate. However, there are a limited number of studies investigating the addition of hydrodynamic altering approaches (*e.g.*, vibration, bubbling, ultrasound) to membrane-based produced water treatment. Zhen *et al.* increased water flux by 83–164% via a static mixer inside a UF membrane treating Daqing oilfield produced water.[145] Hemmati *et al.* observed a flux increase of up to 170% when air sparging was introduced in MF membranes treating refinery wastewater.[146] While these results are promising, further exploration of hydrodynamic techniques is necessary in order to understand the practicality of these approaches in reducing fouling in produced water.

In the case of flux decline due to oil fouling, various cleaning techniques have been developed to minimize and mitigate membrane fouling (*e.g.*, back-pulsing,[147,148] chemical

cleanings,[149] ultrasound[150]). Yet, even when cleaning techniques are implemented, irreversible fouling hypothesized to be due to oil fouling of the membrane pores may continue to limit membrane performance.[105] Ultimately, minimizing and mitigating oil fouling of membranes remains a crucial hurdle to broad implementation of membrane processes for oil-water separations in real produced water treatment trains.

Integrated Treatment Approaches

Despite substantial advances in membrane technology, conventional treatment techniques are still often necessary for initial bulk phase separations for suspended solids and oil during pretreatment. As discussed in the previous sections, many researchers have paired MF/UF membranes with conventional pretreatment separations to mitigate fouling and enhance removal of bulk contaminants (*e.g.*, TSS, TOG, TOC). However, novel integration of conventional, membrane-based, and advanced treatment processes may better address toxic and recalcitrant constituents.

Lab and pilot scale studies of oil removal from produced water via membranes have largely demonstrated the importance of pretreatment in integrated membrane systems.[55,151] For example, membrane-integrated pretreatment trains for oil-water separations (*e.g.*, coalescer bed/MF,[152] resin composite/MF,[153] ozonation/MF,[154] DAF/O_3/MF,[155] UV/H_2O_2/MF,[155] O_3/UF[156]) have provided promising results for enhancing oil-water separations in produced water. Improvements in pretreatment provided by these integrated pretreatment methods are particularly crucial when considering the potential for advanced integrated treatment trains that may be able to leverage high-efficiency pretreatment to more efficiently desalinate water, remove specific constituents, and reduce toxicity. However, integration has not eliminated the issue of fouling for complex wastewaters.

Ultimately, minimizing and mitigating oil fouling of membranes remains a crucial hurdle to broad implementation of membrane processes for oil-water separations.

SELECTIVE OIL PERMEATION

Selective oil permeation differs from traditional membrane-based oil-water separations by permeating oil through the hydrophobic membrane pores while retaining the water (**Figure 1**). Permeation of oil through the membrane exploits the preferential oil wetting of the membrane surface to minimize viscous fouling[17,18] and generate a high-quality oil permeate stream.[19,20] Minimization of viscous fouling has allowed for extended operation of the membrane systems with oil recoveries higher than 95% from a variety of systems (*i.e.*, submicron lipids from saltwater, submicron lipids from freshwater, and Isopar M from freshwater).[18,157] However, the potential for biological fouling remains a factor that can affect the longevity of membrane modules.[18]

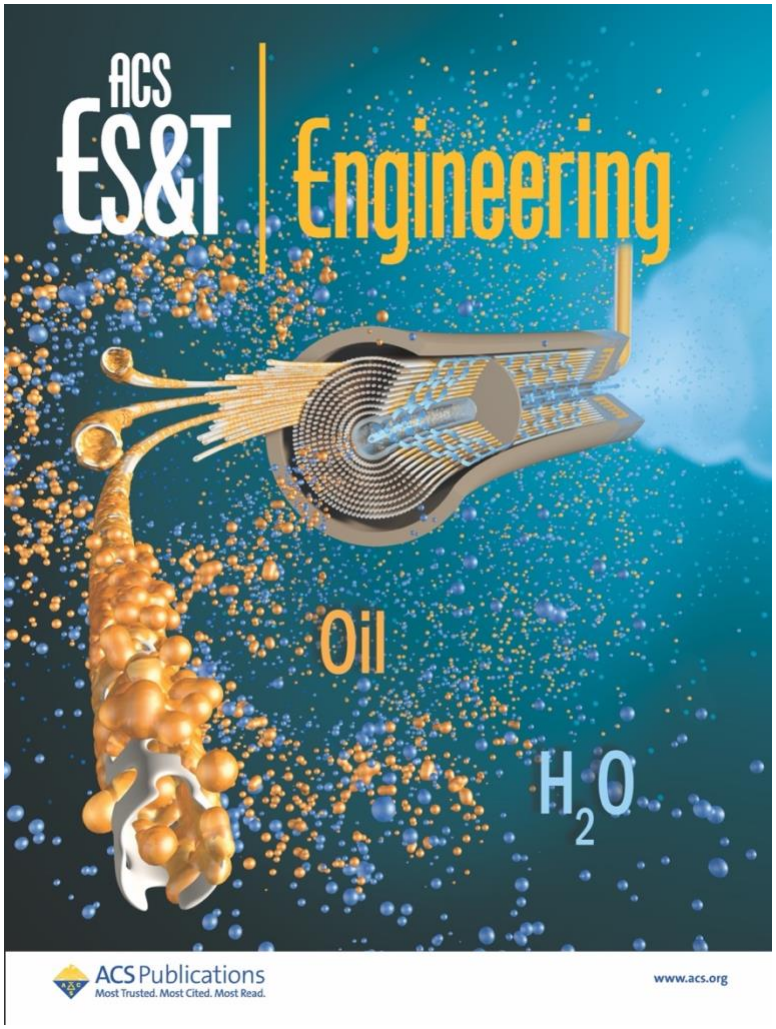

Figure 1: Supplementary Cover associated with Mercelat *et al.* with representation of selective oil permeation process.[22]

Researchers have investigated the selective oil permeation process in numerous hydrophobic membranes including polypropylene,[19,22,23,26] polyvinylidene fluoride,[28] polyethylene,[158] and poly(tetrafluoroethylene).[20,24] Selective oil permeation has been shown to directly separate insoluble oils (*e.g.*, algal oils,[17,21] Isopars,[22] gas oil,[20] naphthenic oil,[23] kerosene,[24] dodecane,[23] isododecane,[26] tetradecane,[19]) from oil-water emulsions. These analyses have demonstrated the importance of various operational parameters (*e.g.*,

influent flow rate, transmembrane pressure, oil concentration) and solution characteristics (*e.g.*, oil viscosity, interfacial tension) on oil recovery[18,19,22,23,26] and permeate quality.[19,20] Macroscopic performance (*i.e.*, oil recovery, oil flux, permeate quality) from these studies has served as the main evidence for mechanistic behavior. Broadly, these studies have hypothesized that oil flux is controlled by the approach of the oil droplet to the membrane fiber, coalescence of an oil droplet onto the membrane surface, permeation of the oil through the membrane pores, and release of the oil from the permeate side of the membrane.[22–24,28] A diagram of the hypothesized mechanisms is shown in **Figure 2**.

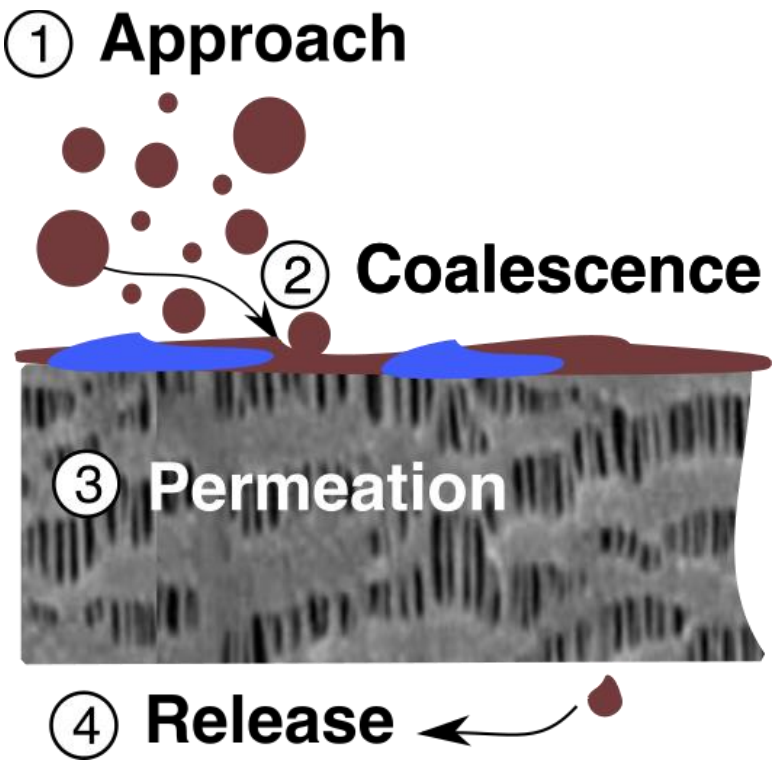

Figure 2: Diagram of hypothesized mechanisms within the selective oil permeation process. Scanning electron microscope image from Mercelat *et al.*[18,22]

Recent work by Mercelat *et al.* demonstrated that evidence of the dominance of competition between coalescence and permeation is particularly pronounced in the

difference in macroscopic behavior between oil-disperse (C_{oil} < 30%) and oil-continuous (C_{oil} > 30%).[22] For example, as anticipated by the Ergun equation (**Equation 2**), Mercelat *et al.* observed an increase in oil flux and recovery with increasing transmembrane pressure for oil-continuous experiments.[22] However, for oil-disperse solutions, oil flux and recovery declined with increasing transmembrane pressure. Mercelat *et al.* hypothesized that this reduction in oil flux and recovery was due to the rate of permeation exceeding the rate of coalescence and reducing the oil-wetted surface area (or an oil film) of the membrane.[22] Furthermore, Mercelat *et al.* hypothesized that the development of an oil film aids in coalescence, supports permeation, and ultimately controls macroscopic performance.[22] Incorporating the presence of an oil film at the membrane surface alters the previously hypothesized mechanisms as now oil droplets must coalesce *with the oil film* at the membrane surface and permeation subsequently occurs *from the oil film* (**Figure 2**). As such, the development and expansion of the oil film may aid in oil recovery, while destabilization and reduction in the oil film can reduce long-term oil flux.

Within the experimental conditions evaluated in this dissertation ($C_{oil} \leq 500$ mg/L), coalescence of oil droplets onto the membrane surface (not within the bulk fluid) is anticipated to be the operative mechanism. Adhesion and coalescence of oil droplets onto hydrophobic fiber surfaces has been investigated as part of the coalescence filtration literature.[100] Early coalescence filtration literature examining the removal of water from water-in-oil emulsions using fibrous filter beds provides a basis for understanding coalescence of droplets onto fiber surfaces.[159] Hazlett and others found that coalescence required approach (or direct interception) of droplets onto the fiber surface.[159] The efficiency of this approach is influenced by factors including diffusion, inertial impaction, electrostatics, and gravity.[159] Hazlett mathematically modeled inertial impaction efficiency using an empirical model developed by Landahl and Hermann.[159,160] Interception and

diffusion within these systems was modeled using the following equations originally developed by Langmuir:

Interception:

$$E_s = \frac{1}{2(2-\ln Re)} \times \left[2(1+R)\ln(1+R) - (1+R) + \frac{1}{1+R}\right] \quad (3)$$

Where E_s is the collection efficiency of a single fiber, Re is the Reynolds Number ($Re = {\rho v L}/{\mu}$ where ρ is density, v is velocity, L is the characteristic length, and μ is the dynamic viscosity), R is the interception parameter (d_p/d_f), d_p is the particle diameter (cm), and d_f is the fiber diameter (cm).

Diffusion:

$$E_s = 2.16\left[\frac{1}{2(2-\ln Re)}\right]^{1/3}\left(\frac{D}{V d_f}\right)^{2/3} \quad (4)$$

Where D is the diffusion coefficient ($D = {kT}/{3\pi\eta d_p}$ where k is the Boltzman constant, T is absolute temperature, and η is the absolute viscosity), and V is the flow velocity (cm/s). These approach mechanisms were shown to dictate the efficiency of the fiber coalescence process by controlling the approach of particles to the fiber surface.

While depth filtration (*i.e.*, capturing of droplets at the fiber surface due to interception) underlies the approach mechanism within selective oil permeation, surface filtration and wetting coalescence (*i.e.*, oil droplets adhering to and becoming engulfed into oil films at the fiber surface) may provide insight into the development of the oil film at the fiber surface. Attachment and coalescence of the oil droplet to the membrane fiber requires the drainage and rupture of the thin continuous phase film between the oil droplet

and the fiber surface (or the oil droplet and the oil droplet/film already adhered to the fiber surface).[159] The rates of this coalescence process have been shown to be affected by both mechanical factors and electrostatics.[23,161] Furthermore, an increase in the number of droplets at the fiber surface may alter the effective diameter of the fiber itself – thereby increasing approach efficiency. Interestingly, surface coalescence of oil-in-water emulsions have been shown to exhibit a saturation style relationship among factors including oil separation efficiency and oil concentration.[100] A similar saturation style relationship between oil flux and oil concentration in selective oil permeation further supports the parallels between the coalescence filtration and selective oil permeation literature. In both processes, constraints imposed by the effective fiber surface area (via either the amount of oil present in the feed or the actual fiber surface area) can ultimately limit oil removal.

Mercelat *et al.* developed the initial model to describe oil flux during selective oil permeation. One crucial challenge in modeling selective oil permeation mass transfer is the deviation in the impact of operating parameters (*e.g.*, transmembrane pressure) between oil-continuous and oil-disperse solutions. Ultimately, an initial model was developed to describe the oil film as the fractional wetted surface area of the membrane (a_e/a_t), which may be proportional to the hypothesized oil film.[18,22] The fractional wetted surface area of the membrane was observed to exhibit a saturation-style relationship with oil concentration, which is consistent with observations of saturation from the coalescence filtration literature.[100] In this process, the fractional wetted surface area of the membrane can be limited by either the amount of oil present in the feed at low oil concentrations or the actual membrane surface area at high oil concentrations. As such, Mercelat *et al.* envisioned oil flux ($J_{o/w,}$ m^3/m^2-s) as a fraction of pure oil flux that is related to the fractional wetted surface area of the membrane (a_e/a_t) as follows:

$$J_{O/W} = J_{Oil} \cdot \frac{a_e}{a_t} \quad (5)$$

Where J_{oil} is the pure oil flux (m^3/m^2-s) described by the Blake-Kozeny viscosity component of the Ergun equation as follows:

$$J_{Oil} = \frac{P_T \times d_{pore}^2 \times \left(\frac{1-\varepsilon}{\varepsilon}\right)^{\frac{2}{3}} \times \varepsilon^3}{150 \times L \times \mu \times (1-\varepsilon)^2} \quad (6)$$

Where P_T is the applied transmembrane pressure (Pa), d_{pore} is the average pore diameter (m), ε is the membrane porosity, L is the membrane wall thickness (m), and μ is the oil viscosity (Pa-s). Ultimately, Mercelat *et al.* developed the following model describing the fractional wetted surface area of the membrane.[18,22]

$$\frac{a_e}{a_t} = \frac{1.65 \times 10^{12} \cdot C_{oil} \cdot \mu \cdot {P_T}^{-1.6} \cdot v^{0.3}}{1 + 2.66 \times 10^{15} \cdot C_{oil} \cdot \mu^{1.1} \cdot {P_T}^{-2.1} \cdot v^{0.4}} \quad (7)$$

Where C_{oil} is the volume fraction of oil and the liquid velocity, v (m/s), is defined as $v = \frac{Q_{shell}}{\frac{\pi}{4} d_{mod}^2}$. This model provided good prediction (+/-20%) of the experimental data taken in the study.[22] Additional details regarding the development of this model are presented in Chapter 6 of Mercelat's dissertation.[18]

SUMMARY OF RESEARCH OBJECTIVES

While previous studies of selective oil permeation have demonstrated the efficacy of the process, further research is necessary to understand how factors inherent to produced water treatment impact selective oil permeation performance. In particular, the following sections focus on (1) how operative mechanisms influence macroscopic performance for oil concentration ranges relevant to produced water, (2) how water quality impacts oil

recovery and flux in selective oil permeation, and (3) how water permeation (or water breakthrough) can be predicted and avoided. A summary of the selective oil permeation literature in relation to these three topics is shown in **Table 4**.

Table 4: Summary of the selective oil permeation literature.[19,20,22–28,158] Abbreviations are as follows: Flat Sheet (FS) and Hollow Fiber (HF).

	Type	C_{in} < 1%	pH	Salinity	Surfactant	Water Permeation
Unno *et al.* 1986[1]	FS					
Ueyama *et al.* 1987	FS				✓	
Magdich *et al.* 1988	HF		✓	✓	✓	✓
Daiminger *et al.* 1995	HF				✓	
Tirmizi *et al.* 1996[2]	HF				✓	✓
Kong *et al.* 1999	FS	✓				
Leiknes *et al.* 2000[3]	HF		✓	✓	✓	✓
Ezzati *et al.* 2005[2]	FS				✓	✓
Mercelat *et al.* 2021	HF	✓				

[1] While Unno *et al.* 1987 does not directly investigate oil-water separations, it provides important insight into the process by expanding on Unno *et al.* 1986 to evaluate permeation and release of liquids (including water).[27]

[2] Water breakthrough intentionally induced and monitored via Karl Fischer Titration.

[3] Wastewater mixtures characteristics varied, but water quality parameter variation was not systematic.

Mechanistic Competition in Oil-Disperse Solutions

Macroscopic experimentation has identified divergent macroscopic and mechanistic behavior between oil-disperse (C_{oil} < 30%) and oil-continuous (C_{oil} > 30%) solutions. Oil-continuous solutions are traditionally limited by permeation and

release.[18,22,23] Oil flux from pure oil solutions is well described by traditional pore flow models (**Equation 4**).[18,22] Researchers have shown that the dominance of permeation in oil-continuous solutions appears to be a function of oil concentration, viscosity, and transmembrane pressure.[18,22] For example, for oil-continuous solutions, increasing the transmembrane pressure increases recovery.

While may of the same operating characteristics (*e.g.*, transmembrane pressure, oil viscosity) influence selective oil permeation performance for oil-disperse solutions, they may result in divergent macroscopic behavior. For example, increasing the transmembrane pressure during oil recovery from an oil-disperse solution decreases recovery.[22] This observation supports the dominance of approach of oil droplets to the membrane surface and coalescence of oil droplets onto the membrane surface for oil-disperse solutions.[18,22–25,27] This limitation is intuitive as, in oil-disperse solutions, if the mass flow rate of oil is substantially below the membrane's permeation capacity, oil flux will be limited by the probability that an oil droplet approaches and coalesces at the membrane surface. Early work in the coalescence filtration literature postulated a similar series of steps for attachment (*i.e.*, interception, diffusion, inertial impaction) or coalescence (*i.e.*, deformation, film formation, and thin film rupture) mechanisms in oil removal from oil-water emulsions in porous media.[100,159,162–167] Broadly, approach is influenced by oil concentration, module geometry,[168] and system hydrodynamics.[23] While the rate of coalescence cannot exceed the rate of approach, the coalescence rate may also be dependent on factors including surface energy,[169] surface roughness,[169] electrostatics, and interfacial phenomena[161] that have been shown to control the rate of drainage of the thin film formed between the coalescing fluids in coalescence filtration. However, the full influence of these individual parameters on coalescence rates within the selective oil permeation processes has not been characterized.

To evaluate the relevance of selective oil permeation to produced water, it is necessary to assess both the applicability of selective oil permeation within the relevant oil concentration range (2–565 mg/L) and understand the mechanisms that underly the observed macroscopic behavior. While Magdich's results questioned the relevance of selective oil permeation for oil concentrations less than 1%,[23] Mercelat *et al.* and Kong *et al.* successfully recovered oil from ranges relevant to secondary and tertiary oil-water separations (~20–500 mg/L).[6,22,28] To understand the relevance of selective oil permeation for produced water, it is necessary to evaluate how operative mechanisms impact macroscopic performance within this lower concentration range. Further, it is necessary to understand the impact of oil characteristics (*e.g.*, viscosity) within this lower concentration range. In particular, while coalescence will often dominate mass transfer for oil disperse solution, we hypothesize that permeation and release may become the dominant mass transfer mechanism for higher viscosity oils. Further, interactions between the four hypothesized mechanisms (*i.e.*, approach, coalescence, permeation, release) may result in macroscopic behavior that deviates from results presented by Mercelat *et al.* and Kong *et al.*

Impact of Water Quality

Produced water quality has been shown to vary substantially (See **Table 1**).[2,31–33] Further, the usage of chemical additives (*e.g.*, surfactants, crosslinkers, gelling agents, breakers, biocides) during unconventional oil and gas production has the potential to undermine the selective oil permeation process.[33,158,170] Multiple studies have investigated the effect of anionic (*e.g.*, Pet Mix #9,[23] Alkylbenzene Sulfonic Acid (ABSA),[23] Sodium Dodecyl Sulfate (SDS)[23,25]) and nonionic (*e.g.*, Triton X-102,[23] Span 80,[19,20] Igepal CO 610,[19] and ECA5025[19]) surfactants. The analyses examining surfactants have generally

shown that both anionic and nonionic surfactants hinder oil removal[23] and increase the water content in the oil permeate due to the decrease in interfacial tension and potential fouling of the membrane surface.[19,158] However, only a few studies have investigated the influence of common water quality parameters like pH and ionic strength on selective oil permeation performance.[23,158] For example, Seibert observed successful oil recovery from concentrated saline non-flocculated lysed algae.[157] However, Magdich and Leiknes *et al.* achieved less successful results when treating other complex emulsions.[23,158]

As previously noted, oil recovery and flux in selective oil permeation is predominantly controlled by coalescence and permeation. Pure oil permeation is consistent with pore flow models and is unlikely to be impacted by water quality (outside of conditions that impact membrane morphology, undermine membrane module integrity, or obstruct the membrane pores pores).[18] However, the rate of coalescence may be impacted by water quality parameters that influence the individual mechanisms within coalescence (*i.e.*, deformation, film formation, and thin film rupture). Furthermore, the tendency of dispersed droplets to recombine (*i.e.,* emulsion instability) can also be further divided into approach (or flocculation) involving interception, diffusion, and inertial impaction as well as coalescence.[23,159,162–167] Consequently, particularly for oil-disperse solutions, we hypothesize that changes in water quality will alter coalescence rates and ultimately impact oil recovery and flux.

Both mechanical and electrical factors have been shown to affect emulsion stability and consequently coalescence rates.[23,161] For example, higher interfacial tension emulsions tend have lower emulsion stability due to a reduction in interfacial energy driving a reduction in interfacial area and thus increased deformability of the droplet.[58,159] An increased mechanical stability of the interfacial film theoretically allows for droplets to resist rupture.[23] From an electrostatics perspective, electrostatic repulsion between

emulsion droplets dictates how closely two droplets or a droplet and a surface may approach.[23] A reduction in the repulsive forces (*e.g.*, reducing the negative charge of oil droplets within the system, increasing the positive charge of the membrane surface, etc.) would theoretically favor coalescence within selective oil permeation. Previous investigations of water quality effects in selective oil permeation have broadly followed the above outlined mechanisms.[19,20,23,25,26,158] In particular, the literature offers insight into the often-detrimental effects of anionic and nonionic surfactants, particularly when used in high concentrations.[23,25,158] Yet, systematic investigation of pH, salinity, and surfactants may offer further insight into the importance of coalescence mechanisms, how enhanced understanding may allow for process optimization, and opportunity space definition.

Water Permeation

While permeating oil through the hydrophobic membrane limits the typical viscous fouling experienced by comparable hydrophilic systems, the process is susceptible to water fouling of the membrane surface and water permeation through the membrane surface. Many researchers have investigated the competitive permeation of oil and water through hydrophilic membranes with the intent of permeation water. However, few have characterized the competitive permeation of organics and water through hydrophobic surfaces.[171,172] Within selective oil permeation, water has been shown to pass through the membrane pores and contaminate the pure oil permeate.[19,20,23,158] Tirmizi *et al.* and Mercelat *et al.* both indicated that the Young-Laplace equation underlies water permeation in selective permeation.[19,22] In particular, Mercelat *et al.* noted that the permeation of oil through the hydrophobic membrane surface requires the application of a transmembrane pressure between the critical entry pressure of the oil and the critical entry pressure of the water. If the transmembrane pressure is operated below the critical entry pressure of the

oil, no separation will occur. Conversely if the critical entry pressure is above that of water, water may contaminate the oil permeate.[19,22]

Thus far, Tirmizi *et al.* demonstrated the applicability of the Young-Laplace to predicting critical entry pressures in a hydrophobic polypropylene membrane.[19] Two studies have quantified permeate quality within selective oil permeation over a range of experimental conditions.[19,20] Others have unintentionally induced water breakthrough when separating complex oil-water emulsions with high surfactant concentrations at elevated transmembrane pressures.[23,158] While these experiments have provided valuable understanding of methods to induce water breakthrough (*e.g.*, low interfacial tension, high transmembrane pressure), the results have limited ability to help others avoid similar missteps or guide future designers.

CONCLUSION

While previous studies have expanded macroscopic and mechanistic understanding of selective oil permeation, investigations of selective oil permeation have almost exclusively quantified oil flux and recovery from emulsions with oil concentrations greater than 1%.[18,19,22,23,26] However, it is necessary to expand our understanding of macroscopic (*i.e.*, oil flux, oil recovery, permeate quality) and mechanistic behavior to include influent oil concentrations less than 500 mg/L of varying water quality. The following chapters will explore these topics to identify the opportunity space for selective oil permeation.

ACKNOWLEDGEMENTS

This project was funded by the Kuwait Foundation for the Advancement of Sciences under project code CN17-45EV-01. This material is based upon work supported by the National Science Foundation Graduate Research Fellowship under Grant No. DGE

2137420. Much of my understanding of produced water and membranes was informed by work conducted through the Department of Energy's National Alliance for Water Innovation (NAWI), the Department of Energy's Center for Materials for Water and Energy Systems (MWET), and a collaboration with Kuwait University supported by the Kuwait Foundation for the Advancement of Sciences. These collaborations resulted in co-authorship on the following publications:

- Cooper, C. M. *et al.* Oil and Gas Produced Water Reuse: Opportunities, Treatment Needs, and Challenges. *ACS ES&T Eng.* **2**, 347–366 (2022).
- Cath, T. *et al.* *Resource Extraction Sector Technology Roadmap*. (2021).
- Barry, M. E. *et al.* Expanding the Use of Synchrotron Techniques for Water Treatment: From Minerals to Membranes. *Synchrotron Radiat. News* **33**, 3–12 (2020).
- Landsman, M. R. *et al.* Water Treatment: Are Membranes the Panacea? *Annu. Rev. Chem. Biomol. Eng.* **11**, 559–585 (2020).

Chapter 3: Materials and Methods

The following chapter provides a summary of the core materials and methods utilized in this dissertation. **Chapters 4**, **5**, **6**, and **7** contain information regarding the specific materials, methods, and experimental matrices that were used within the relevant chapter.

SYNTHETIC OILS

Experiments utilized Isopar M, Isopar V, Soybean Oil, and 10W-30 Motor Oil to achieve a broad range of viscosities. Specifics of influent oil, oil concentrations, and water used are discussed in each chapter. Oil density was measured in triplicate (**Figure 3A**) using a DE40 Density Meter (Mettler Toledo, Columbus, OH, USA). Viscosities were measured in triplicate (**Figure 3B**) utilizing an NDJ-5S Digital Rotational Viscometer (Vevor Machinery Equipment, San Jose, CA, USA).

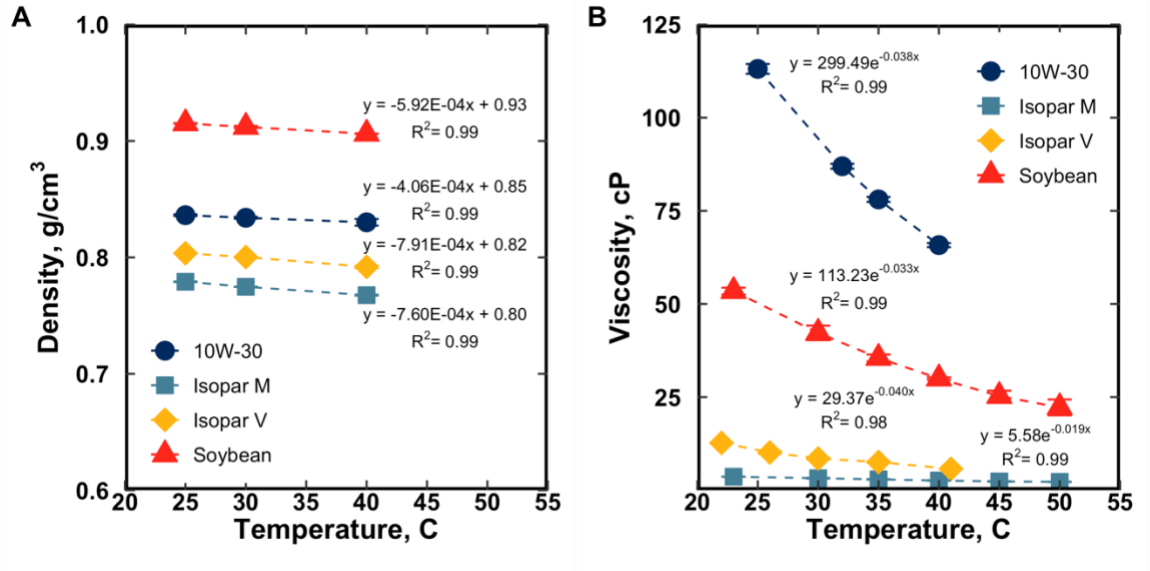

Figure 3: (A) Density and (B) viscosity correlations for synthetic oils used during experiments.

Interfacial tension was measured in triplicate using a 70535 CSC-DuNouy Tensiometer. Interfacial tensions of interest are discussed in their respective chapters. Droplet diameters of the emulsions were measured between the high-shear pump and inlet to Membrane A via an Inline Particle Analyzer (J.M. Canty, Lockport, NY, USA). An exemplar inlet and outlet pore size distributions are shown in **Figure 4**.

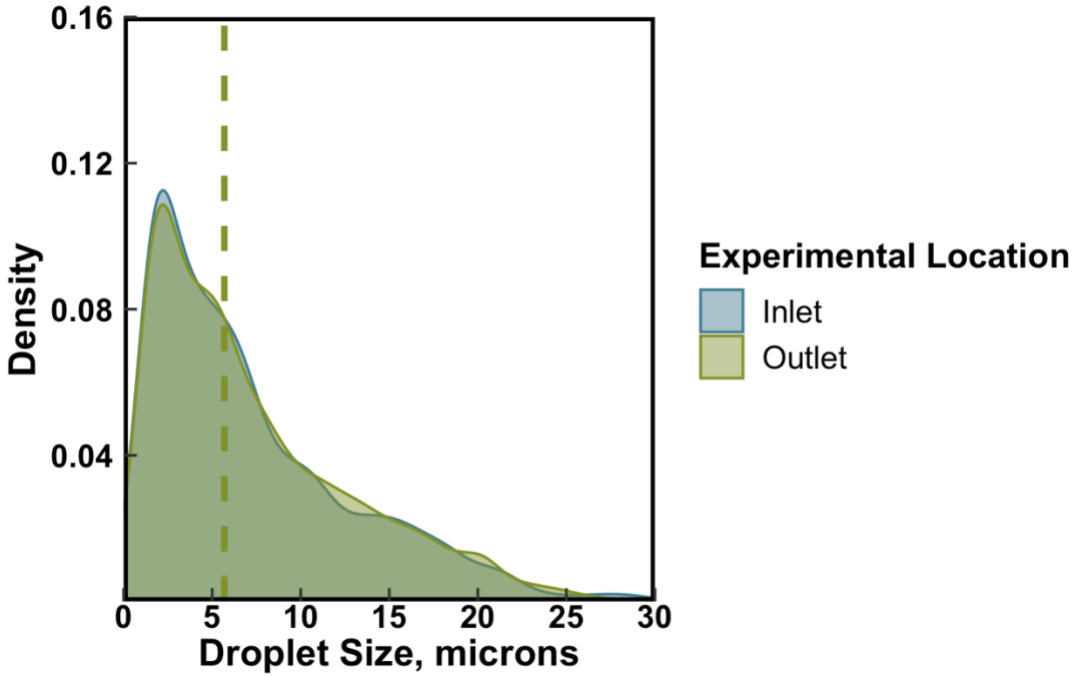

Figure 4: Inlet and outlet pore size distribution for Isopar M in Austin Tap Water.

MEMBRANE MODULES, EXPERIMENTAL FACILITY, AND EXPERIMENTAL APPROACH

All experiments were conducted using the membrane system located at the University of Texas at Austin's Separation Research Program at the J.J. Pickle Research Campus. The skid with the membrane system (**Figure 10**) was located inside a floor-to-

ceiling fume hood. Photographs of the fume hood and experimental set up are presented in **Figure 5**, **Figure 6**, **Figure 7**, and **Figure 11**.

Figure 5: Photograph of floor-to-ceiling fume hood at the J.J. Pickle Research Campus that houses the membrane skid used in this work.

Figure 6: Photograph of membrane skid used in experiments throughout the dissertation.

Two 3M™ Liqui-Cel™ Extra Flow Membrane Contactors of varying size and surface area were utilized to separate oil-water mixtures (3M™, Saint Paul, MN, USA) (**Figure 7**, **Figure 8**, and **Table 5**). All reported permeate quality and oil recovery data were taken from the primary membrane, Membrane A. Membrane A was sized to achieve less than 100% oil recovery to allow for quantitative evaluation of the system performance. In contrast, the guard membrane, Membrane B, was sized to achieve 100% oil recovery to allow for recycle of the system. Membrane modules were run continuously for extended durations throughout this work. As in Mercelat's dissertation, membrane longevity was generally limited by biological fouling and evidenced by factors including low oil recovery, high shell-side differential pressures, and the appearance of biological films during backflushing of the membrane system.

Figure 7: Photograph of Membrane A, Membrane B, and peristaltic oil pump.

Table 5: Hollow fiber module specifications

	Membrane A	**Membrane B**
Module dimensions (cm) [a]	6.4 x 20.3	10.2 x 71.1
Fiber outer diameter (μm) [a]	300	300
Fiber inner diameter (μm) [a]	220	220
Fiber wall thickness (μm) [a]	40	40
Pore size (μm) [a]	0.05	0.05
Porosity (%) [b]	40	40
Contact Angle (°) [c]	120	120
Membrane surface area (m^2) [a]	1.4	20

[a] Supplied by Manufacturer

[b] Mahmud *et al.* 2000

[c] Mercelat *et al.* 2021

Each membrane module consisted of a hydrophobic microporous polypropylene hollow-fiber mat of the commercially available X50 fibers with an internal distributor. The modules contained a central baffle positioned perpendicularly to the shell-side flow to mitigate channeling. A diagram of the device is presented in **Figure 8**. An SEM and pore size distribution of the membrane is shown in **Figure 9.**[18]

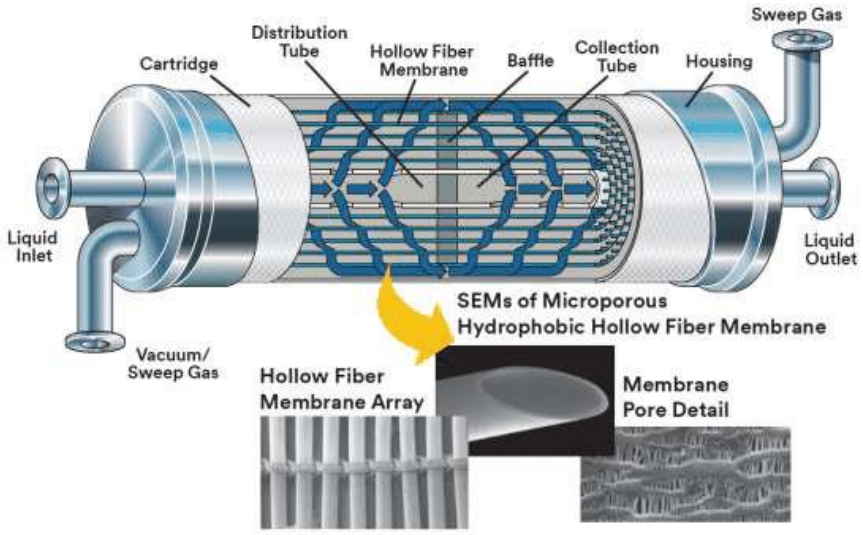

Figure 8: Diagram of 3M^{TM} Liqui-Cel^{TM} Extra Flow Membrane Contactors.[173]

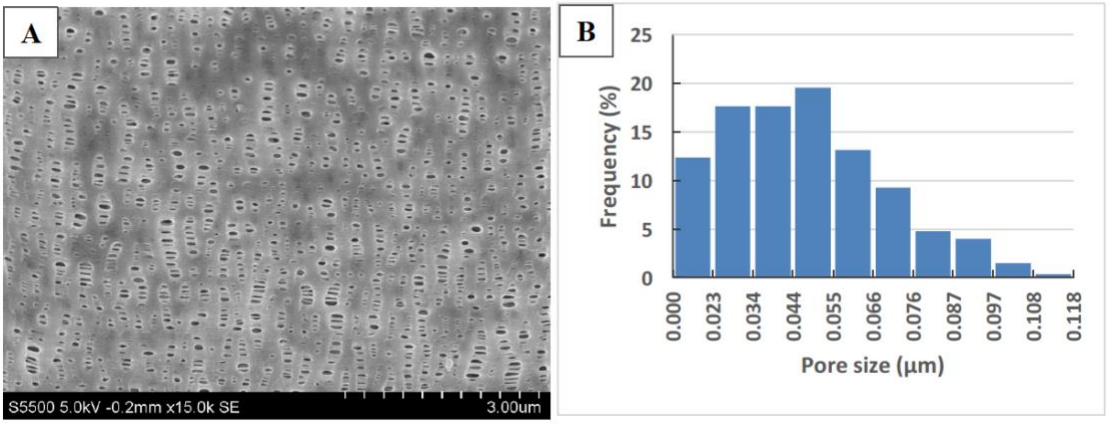

Figure 9: Pore size analysis conducted by Mercelat from SEM picture with gold and palladium. Pore size distribution generated using Image J analysis from Aurore Mercelat's dissertation.[18]

A process flow diagram of the membrane system is shown in **Figure 10**. Inlet oil concentration was controlled via a peristaltic pump that injected a known mass of oil into the suction of the high-shear pump with a variable speed drive (MTH Pump, Plano, IL, USA). The high-shear pump generated the oil-in-water emulsion and propelled the emulsion to Membrane A. The oil-in-water emulsion entered Membrane A through the bottom shell-side port. Transmembrane pressure and water flow rate in Membrane A were controlled using both the variable speed drive and a needle valve downstream of Membrane A. Rosemount pressure transmitters (Emerson, St. Louis, MO, USA) monitored and recorded shell-side pressure while tube-side pressure remained at atmospheric pressure. Transmembrane pressure was then calculated by averaging the inlet and outlet shell-side pressure. As the emulsion passed through Membrane A, oil droplets intercepted the hollow fibers prior to permeation. Effluent water from the shell-side of Membrane A returned to the feed tank. An air diaphragm pump supplied water from the feed tank to Membrane B, which maintained the purity of the feed tank due to its higher flow rate and larger surface area.

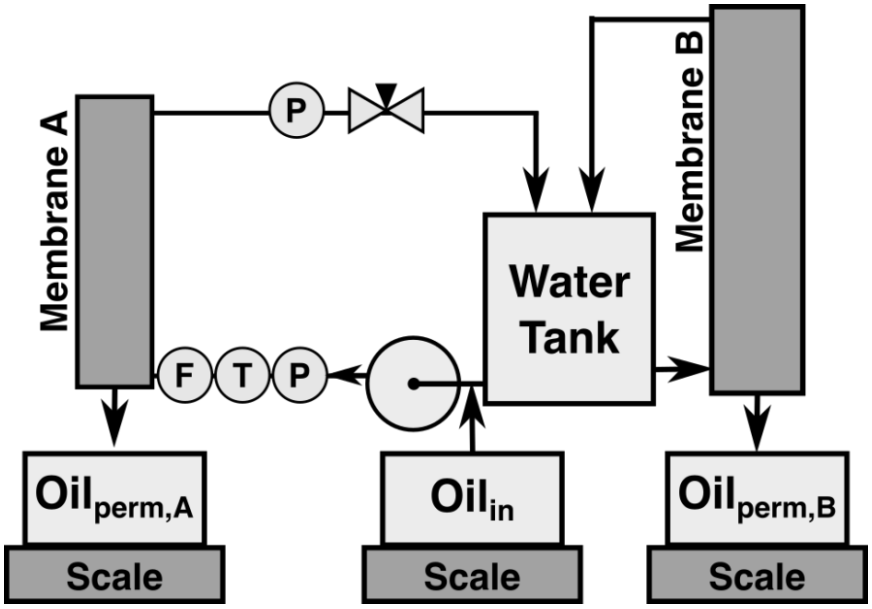

Figure 10: Process flow diagram of experimental apparatus. Membrane A (Dimensions: 6.4 cm x 20.3 cm, Surface Area: 1.4 m^2) serves as the primary membrane while Membrane B (Dimensions: 10.2 cm x 71.1 cm, Surface Area: 20 m^2) serves as the guard membrane. Abbreviations are as follows: pressure transmitter (P), temperature transmitter (T), flow transmitter (F), injected oil (Oil_{in}), oil permeate from Membrane A ($Oil_{perm,A}$), and oil permeate from Membrane B ($Oil_{perm,B}$).

Both injected oil and oil permeate were quantified via weigh scales (**Figure 11**). Oil flux and oil recovery in Membrane A were calculated as:

$$Oil\ Flux\ (\frac{m^3}{m^2-s}) = \frac{\dot{m}_{permeate}}{\rho_{oil} \times A_{membrane}} \quad (8)$$

$$Oil\ Recovery\ (\%) = \frac{\dot{m}_{permeate}}{\dot{m}_{injected}} \cdot 100\% \quad (9)$$

Where $\dot{m}_{permeate}$ was the mass flow of the permeate (g/s), $\dot{m}_{injected}$ was the mass flow of injected oil (g/s), ρ_{oil} was the density of the oil (g/cm^3), and $A_{membrane}$ was the surface area of the membrane (m^2).

Figure 11: Photograph of weigh scales and flow meters.

The mass flow of both permeate and inlet were determined after the system had reached steady state as the average of the last four hours of the experiment (unless otherwise noted in the text in the chapter). For most experimental conditions, steady state was achieved within a few hours (< 4 hours). In this dissertation, experiment duration ranged from 8 hours to 18 days, but generally lasted approximately 12 to 24 hours. Typical operating data from an experiment is shown in **Figure 12**.

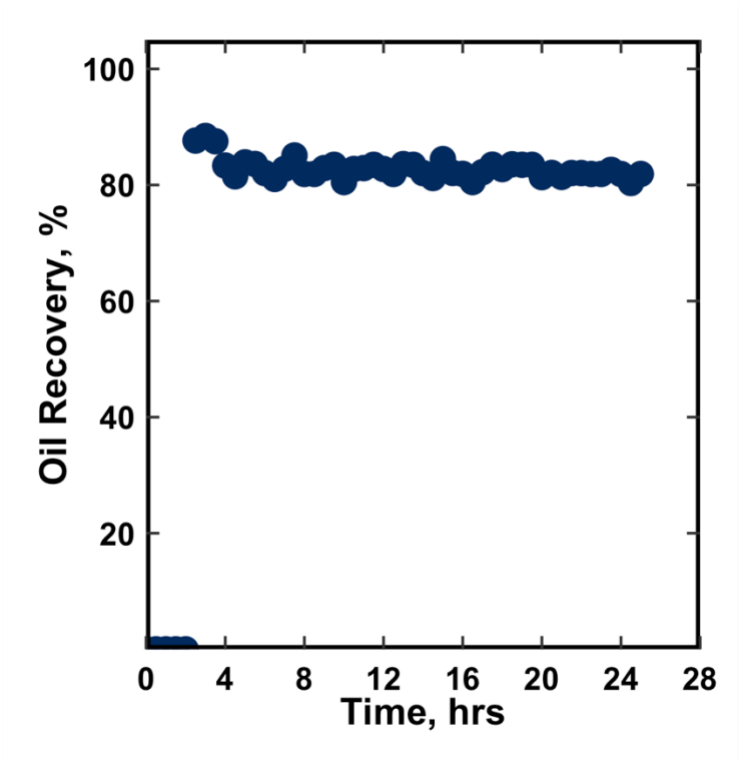

Figure 12: Typical experimental data for single experiment. All data is from Membrane A using Isopar M at an influent oil concentration of 100 mg/L, influent flow rate of 7.6 L/min, and a transmembrane pressure of 1.38 bar.

An Emerson DeltaV data acquisition system allowed for real-time data collection from all described instruments over extended periods (**Figure 13**).

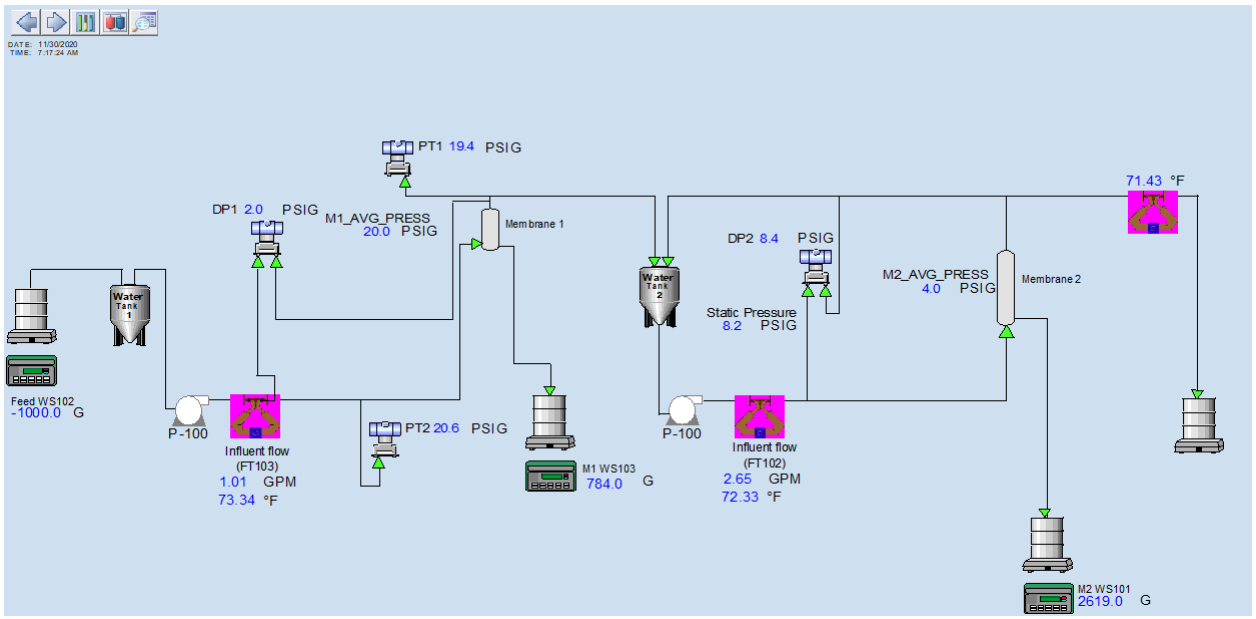

Figure 13: Example of DeltaV Acquisition System Output

Each scale was connected to a computer via a RS232-USB converter. Pressure transmitters and flow transmitters communicated with the Delta V system wirelessly. A schema of the real-time data collection and communication system is shown in **Figure 14**.

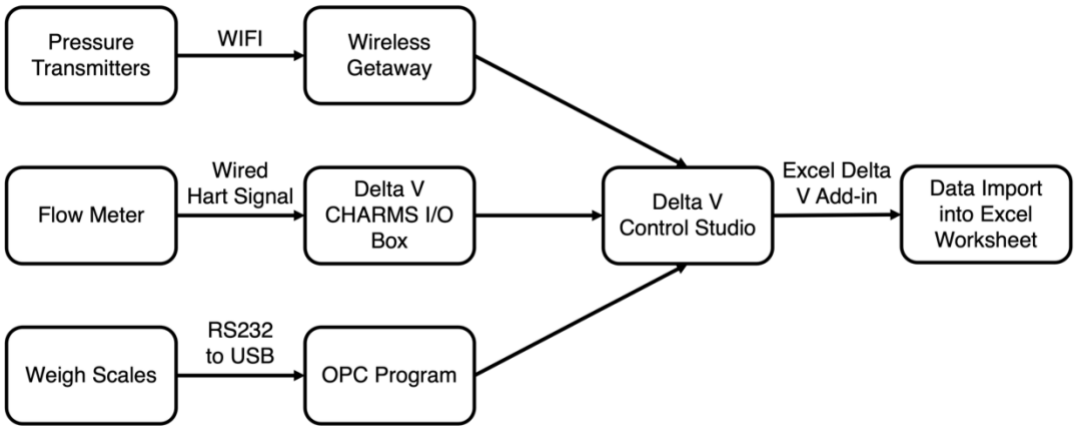

Figure 14: Schema of data acquisition from experimental system adapted from Mercelat.[18]

Data stored in DeltaV was processed via an Excel spreadsheet (**Figure 15**).

Run	Run 90							
Start Date	22-Jan-21							
Membrane names	M4X28-02, New M2.5X8-03	Isopar V				Manual input		
TMP (psi)	19.98	Viscosity, cP	11.31			Data input		
oil feed flow g/min	0.376	Membrane 1 Surface Area, m2	1.4					
Influent flow (gpm)	0.50		Density (g/ml)			Calculated cells		
Oil/water emulsion	Oil concentration, PPM	200	0.805	11.18012422				
	Water concentration, %	99.98	1					
	IPA concentration wt.%	0						
Main Pump setting: VSD	1058							
Perilstatic pump pump setting:	white pump, oil feed	0.500						

Time	Shell Flow rate	P1 (psi) Small membrane shell	P2 (psi) Small membrane shell	TMP1 AVG(P1,P2)	DP1 (psi) Small membrane shell DP	Shell Side Inlet T	Isopar V μ	Run time
HH:MM	gpm	psi	psi	psi	psi	°C	cP	H:MM:SS
1/22/21 1:30 PM	0.51	19.66	20.41	20.04	0.77	21.84	11.60	0:00:00
1/22/21 2:00 PM	0.50	19.73	20.17	19.95	0.77	21.56	11.71	0:30:00
1/22/21 2:30 PM	0.49	19.58	20.26	19.92	0.77	21.53	11.72	1:00:00
1/22/21 3:00 PM	0.49	19.52	20.47	20.00	0.73	22.35	11.41	1:30:00
1/22/21 3:30 PM	0.50	19.68	20.33	20.00	0.77	22.22	11.46	2:00:00
1/22/21 4:00 PM	0.50	19.70	20.33	20.01	0.78	21.91	11.57	2:30:00
1/22/21 4:30 PM	0.49	19.78	20.37	20.08	0.77	21.53	11.72	3:00:00
1/22/21 5:00 PM	0.50	19.65	20.41	20.03	0.78	21.81	11.61	3:30:00

Figure 15: Exemplar data acquisition spreadsheet.

Experimental matrices are detailed in their respective chapters. Additional details regarding the operation and characteristics of the system are available in Mercelat *et al.* and the corresponding dissertation.[18,22]

Chapter 4: Selective Oil Permeation for Oil Recovery from Low Oil Concentrations

ABSTRACT

Selective oil permeation is an emerging membrane-based oil-water separation process that may help achieve the circular water economy. Previous investigation of selective permeation has demonstrated the efficacy of separating oil-water emulsions by permeating oil (instead of water) through the membrane pores. Researchers have observed that mechanistic competition between permeation and coalescence leads to transport phenomena that deviate from traditional pore flow models for oil-disperse solutions. However, these studies have generally focused on insoluble organic concentrations above 1%, and, for many industrial wastewaters, oil concentrations may be substantially lower. This study investigates the efficacy of selective oil permeation from oil-water emulsions containing oil concentrations less than approximately 200 mg/L by evaluating the effects of both operating parameters (*e.g.*, transmembrane pressure, influent flow rate) and solution properties (*e.g.*, influent oil concentration, interfacial tension, viscosity). Of particular significance, the study demonstrates that process performance improves over time, illustrates the role of membrane conditioning, identifies the presence of optimal and suboptimal operating ranges, and uses the identification of these ranges to rectify discrepancies within the literature.

INTRODUCTION

Oil-water separations are a crucial component in many industrial wastewater treatment trains. For example, petroleum produced water, metalworking fluids, and vegetable oil refinery waters often contain 2–2,000 mg/L, 20–200,000 mg/L, and 480–7,782 mg/L of oil and grease, respectively. While regulatory limits vary by both country and end-use, these concentrations often must be reduced to <10–50 mg/L oil and grease[1] for discharge or external reuse.[4] Achieving these effluent concentrations often requires a series of primary, secondary, and even tertiary oil water separations to adequately address free oil (≥ 150 μm), dispersed oil (> 50 μm), and emulsified oils (≤ 50 μm).[4,6] Moreover, in addition to meeting regulatory requirements, oil-water separations can also mitigate oil fouling of downstream treatment processes and allow for the valorization of the treatment train through resource recovery of the oil.

Tertiary oil removal via nonfibrous sorbent materials,[7] fibrous sorbent materials,[99] and coalescence filtration have high oil removal, low processing costs, and relatively simple operation. However, filtration and adsorption methods may also be labor intensive, have poor removal of fine emulsions, or require substantial hydraulic residence time to achieve higher removals.[99] Traditional membrane-based separations are a promising oil-water separation method due to their low minimum droplet removals (< 1 μm), high oil removals (~99%), and relatively low hydraulic retention times.[4,6] However, they often experience rapid viscous fouling of the membrane surface,[6,9–16] particularly when exposed to complex wastewaters like produced water.[110,112–114] Researchers have endeavored to minimize oil fouling of the membrane surface through novel materials that exploit surface

[1] Oil and grease (or n-hexane extractable material) is measured using EPA Method 1664A. The literature includes other methods (*e.g.*, ASTM D7575) to measure similar fractions of hydrocarbons in water samples using other analytical techniques (*e.g.*, UV-Vis, FTIR, GC). Due to the wide variety of organics that may be present in an oily wastewater sample, these methods may yield different results.

properties like wettability.[124–138] Yet, these approaches may result in fragile membranes, reduced flux, may not be appropriate for use with complex industrial wastewater, or are not readily commercially available.[137]

Selective oil permeation is a membrane-based approach to oil-water separations that differs from traditional membrane-based oil-water separations by permeating oil (instead of water) through the membrane surface.[19,20,22–24,26,157,158] Oil permeation through the membrane generates a high-quality oil permeate stream while minimizing viscous oil fouling of the membrane surface. Analyses of selective oil permeation have demonstrated its ability to separate insoluble oils (*e.g.*, various alkanes,[19,23,26] algal oils,[157] and Isopar [22]) from water without the use of solvent. These studies have also shown the importance of various operational parameters and solution characteristics on oil recovery[18,19,22,23,26] and permeate quality.[19,20] Macroscopic behavior observed during these fundamental studies has developed our mechanistic understanding of the process where oil flux is controlled by one or more of the following: the approach of the oil droplet to the membrane fiber, coalescence of an oil droplet at the oil film on the membrane surface, permeation of the oil through the membrane surface, and release of the oil from the permeate side of the membrane (**Figure 2**).[22–24,27,28]

Only three studies have investigated oil recovery via selective oil permeation from oil concentrations at or below 1%. However, the studies resulted in disagreement within the literature on the viability of selective oil permeation for oil-disperse solutions. Magdich observed that oil removal was limited at low oil concentrations (<1%) and ultimately questioned the relevance of selective oil permeation for oil concentrations within this range.[23] In contrast, Mercelat *et al.* and Kong *et al.* successfully recovered oil from oil concentrations in ranges relevant to secondary and tertiary oil-water separations (~20–500 mg/L).[6,22,28] Selective oil permeation may be well-suited to this range as, for low oil

concentrations (*i.e.*, conditions not limited by membrane surface area), we hypothesize that oil recoveries will increase with decreasing transmembrane pressure and remain constant with increasing flow rate. Thus, understanding the fundamental behavior of the process within this concentration range is crucial to defining the opportunity space for selective oil permeation. Furthermore, while theory suggests that viscosity should have a negative impact on oil flux, few studies have characterized the effect of this parameter at low oil concentration or operating conditions (*i.e.*, influent flow rate, transmembrane pressure). Since common industrial oily wastewaters (*e.g.*, petroleum wastewaters, metalworking wastewaters, food processing wastewaters) may contain oils with a broad set of characteristics,[174] it is necessary to investigate the impact of viscosity on process efficacy over a wider range of oil characteristics to fully comprehend the limitations of selective oil permeation.

This chapter investigates the efficacy of selective oil permeation for oil recovery from oil-water emulsions containing low oil concentrations (50 mg/L to 200 mg/L) by examining the effects of both operating parameters (*e.g.*, transmembrane pressure, influent flow rate) and solution properties (*e.g.*, influent oil concentration, interfacial tension, viscosity). Of particular significance, the study demonstrates that process performance improves over time, illustrates the role of membrane conditioning, identifies the presence of optimal and suboptimal operating ranges, and uses the identification of these ranges to rectify existing discrepancies within the selective oil permeation literature.

SELECTIVE OIL PERMEATION MECHANISMS

Many researchers have investigated both coalescence[26,175–178] and permeation[19,20,28,175,178–181] in hydrophobic membranes. These studies and macroscopic performance (*i.e.*, oil flux, oil recovery, permeate quality) observed during studies of

selective oil permeation have contributed to our mechanistic understanding of selective oil permeation. Broadly, researchers have hypothesized that oil flux is controlled by approach of the oil droplet to the membrane fiber, coalescence of an oil droplet onto the membrane surface, permeation of the oil through the membrane pores, and release of the oil from the permeate side of the membrane.[22–24,27,28] Recent work by Mercelat *et al.* expanded on the hypothesized mechanistic understanding of selective oil permeation by considering the role of an oil film at the membrane surface.[18,22] Incorporating the presence of an oil film at the membrane surface alters the previously hypothesized mechanisms as now oil droplets must coalesce *with the oil film* at the membrane surface and permeation subsequently occurs *from the oil film* (**Figure 2**). Mercelat *et al.* hypothesized that the development of an oil film aids in coalescence, supports permeation, and ultimately controls macroscopic performance.[22] As such, the development and expansion of the oil film may aid in oil recovery, while destabilization and reduction in the oil film can reduce long-term oil flux.[22]

Mercelat *et al.* then developed an initial mass transfer model to predict oil flux during selective oil permeation by considering both permeation (via a traditional pore flow model) and the role of the oil film.[18,22] Mathematically, the model described the oil film as the fractional wetted surface area of the membrane, which may be proportional to the hypothesized oil film.[18,22] The fractional oil wetted surface area of the membrane was observed to exhibit a saturation-style relationship with oil concentration, which is consistent with observations of saturation from the coalescence filtration literature.[100] In selective oil permeation, the fractional wetted surface area of the membrane can be limited by either the amount of oil present in the feed at low oil concentrations or the actual membrane surface area at high oil concentrations. As such, Mercelat *et al.* envisioned oil flux ($J_{o/w,}$ m^3/m^2-s) as a fraction of pure oil flux that is related to the fractional wetted surface area of the membrane (a_e/a_t) as follows:

$$J_{O/W} = J_{oil} \cdot \frac{a_e}{a_t} \quad (10)$$

Where J_{oil} is the pure oil flux (m^3/m^2-s) described by the Blake-Kozeny viscosity component of the Ergun equation as follows:

$$J_{oil} = \frac{P_T \times d_{pore}^2 \times \left(\frac{1-\varepsilon}{\varepsilon}\right)^{\frac{2}{3}} \times \varepsilon^3}{150 \times L \times \mu \times (1-\varepsilon)^2} \quad (11)$$

Where P_T is the applied transmembrane pressure (Pa), d_{pore} is the average pore diameter (m), ε is the membrane porosity, L is the membrane wall thickness (m), and μ is the oil viscosity (Pa-s). Mercelat *et al.* then developed the following model to predict the fractional wetted surface area of the membrane by considering the competition between coalescence and eventual permeation of an oil droplet in the context of saturation:

$$\frac{a_e}{a_t} = \frac{1.65 \times 10^{12} \cdot C_{oil} \cdot \mu \cdot {P_T}^{-1.6} \cdot v^{0.3}}{1 + 2.66 \times 10^{15} \cdot C_{oil} \cdot \mu^{1.1} \cdot {P_T}^{-2.1} \cdot v^{0.4}} \quad (12)$$

Where C_{oil} is the volume fraction of oil and the velocity, *v* (m/s), is defined as $v = \frac{Q_{shell}}{\frac{\pi}{4} d_{mod}^2}$.

This model provided good prediction (+/-20%) of the experimental data generated during the study.[18,22] Additional information regarding the development of the model and its basis is presented in Chapter 6 of Mercelat's dissertation.[18] However, further work is necessary to broaden the applicability of the model, particularly at higher viscosities, lower oil concentrations, and over a broader range of influent flow rates that are important in the design of selective oil permeation systems for produced water treatment (**Table 6**).

Table 6: Comparison of original parameters in Mercelat study to parameters examined in this work.[18]

	Mercelat et al.	**This Work**
Oil Concentration, %	0.02–90	0.005–0.02
Oil Viscosity, cP	1.5–10.7	3.5–116
Influent Flow Rate, L/min	1.9–5.7	1.9–9.5
Transmembrane Pressure, bar	0.7–4.1	0.2–2.8

METHODS

Feed Composition

Experiments utilized Isopar M, Isopar V, Soybean Oil, and 10W-30 Motor Oil to achieve a broad range of viscosities (**Table 7**). No surfactants were added during experiments. Influent oil concentration ranged from 50 mg/L to 200 mg/L by volume in Austin Tap Water. Austin Tap Water is a lime softened, recarbonated water with a pH of 9.6, alkalinity of 62 mg/L as $CaCO_3$ and hardness of 87 mg/L as $CaCO_3$. The tap water has been chloraminated with typical concentrations of chloramines at the tap of approximately 2.5 mg/L as Cl_2. Other water quality characteristics are presented in **Table A10**. Density, viscosity, and interfacial tension were measured in triplicate using a Mettler Toledo DE40 Density Meter, NDJ-5S Digital Rotational Viscometer, and a 70535 CSC-DuNouy Tensiometer.

Table 7: Oil characteristics at 25 degrees Celsius.

	Density, g/cm^3	**Viscosity, cP**	**Interfacial Tension, mN/m**
Isopar M	0.78	3.5	46.3
Isopar V[1]	0.80	10.7	25.3
Soybean	0.92	49.6	32.5
10W-30	0.84	115.8	6.1

[1] Isopar V has a reported interfacial tension of approximately 50 mN/m.

Experimental System

A detailed process flow diagram of the membrane skid is shown in **Figure 16.** Two 3M^{TM} Liqui-Cel^{TM} Extra Flow Membrane Contactors of varying size were utilized to separate oil-in-water emulsions (**Table 8**). Both membranes contained a hydrophobic microporous polypropylene hollow-fiber mat of the commercially available X50 fibers. All reported permeate quality and oil recovery data were taken from the primary membrane, Membrane A, which was sized to achieve less than 100% oil recovery to enable quantitative evaluation of the system at various conditions. In contrast, the guard membrane, Membrane B, was sized to achieve 100% oil recovery to allow for recycle of the system by removing all oil from the water reservoir.

Table 8: Hollow fiber membrane module specifications

	Membrane A	**Membrane B**
Module dimensions (cm) [a]	6.4 x 20.3	10.2 x 71.1
Fiber outer diameter (μm) [a]	300	300
Fiber inner diameter (μm) [a]	220	220
Fiber wall thickness (μm) [a]	40	40
Pore size (μm) [a]	0.05	0.05
Porosity (%) [b]	40	40
Contact Angle (°) [c]	120	120
Membrane surface area (m^2) [a]	1.4	20

[a] Supplied by Manufacturer

[b] Mahmud *et al.* 2000

[c] Mercelat *et al.* 2021

The feed tank was charged with Austin Tap Water. Inlet oil concentration was controlled via a peristaltic pump that injected a known mass flow rate of oil into the suction of the high-shear pump with a variable speed drive (MTH Pump, Plano, IL, USA). The high-shear pump generated the oil-in-water emulsion and propelled the emulsion to Membrane A. The oil-in-water emulsion entered Membrane A through the bottom shell-side port. Transmembrane pressure and water flow rate in Membrane A were controlled using both the variable speed drive and a needle valve downstream of Membrane A. Rosemount pressure transmitters (Emerson, St. Louis, MO, USA) monitored and recorded shell-side pressure while tube-side pressure remained at atmospheric pressure. Transmembrane pressure was then calculated by averaging the inlet and outlet shell-side pressure. As the emulsion passed through Membrane A, oil droplets intercepted the hollow fibers prior to permeation. Effluent water from the shell-side of Membrane A returned to the feed tank. An air diaphragm pump supplied water from the feed tank to Membrane B,

which maintained the purity of the feed tank due to its higher flow rate and larger surface area. No free water was observed in the oil permeate of either Membrane A or Membrane B during the study.

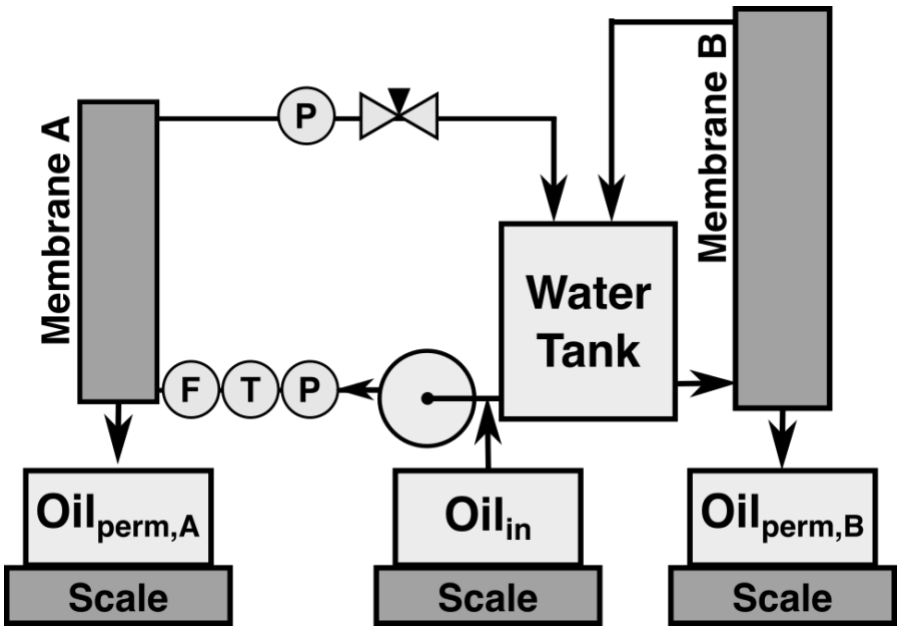

Figure 16: Process flow diagram of experimental apparatus. Membrane A (Dimensions: 6.4 cm x 20.3 cm, Surface Area: 1.4 m^2) serves as the primary membrane while Membrane B (Dimensions: 10.2 cm x 71.1 cm, Surface Area: 20 m^2) serves as the guard membrane. Abbreviations are as follows: pressure transmitter (P), temperature transmitter (T), flow transmitter (F), injected oil (Oil_{in}), oil permeate from Membrane A ($Oil_{perm,A}$), and oil permeate from Membrane B ($Oil_{perm,B}$).

All injected and permeated oil were quantified via an Arlyn D-620T weigh scale (reported resolution of 1.0 gram). Oil flux and oil recovery were calculated as follows:

$$Oil\ Flux\ (\frac{m^3}{m^2-s}) = \frac{\dot{m}_{permeate}}{\rho_{oil} \times A_{membrane}} \quad (13)$$

$$Oil\ Recovery\ (\%) = \frac{\dot{m}_{permeate}}{\dot{m}_{injected}} \cdot 100\% \quad (14)$$

Where $\dot{m}_{permeate}$ was the mass flow of the permeate (g/s), $\dot{m}_{injected}$ was the mass flow of injected oil (g/s), ρ_{oil} was the density of the oil (g/cm^3), and $A_{membrane}$ was the surface area of the membrane (m^2). The mass flow of both permeate and inlet were determined as the average of the last four hours after the system reached steady state. For conditioned membranes, steady state was generally reached within a few hours of operation and experiments lasted approximately 24 hours. A table of the experimental conditions examined is shown in **Table 9**. A DeltaV data acquisition system collected real-time data from all described instruments (Emerson, St. Louis, MO, USA). The R programming environment was utilized for statistical analysis and to generate figures using the ggplot2.

Table 9: Summary of experimental conditions. Except where noted, all conditions were conducted using the four characteristic oils. Abbreviations are as follows: transmembrane pressure (TMP) and flow rate (Q).

	$C_{oil,in}$ (mg/L)	TMP (bar)	Q (L/m)
Conditioning (TMP)*	200	0.2, 0.3, 0.7, 1.2, 1.8, 2.2, 2.8	3.8
Conditioning (Q)*	200	1.4	1.9, 3.8, 5.7, 7.6, 9.5
Oil Concentration	50, 100, 200	0.7	3.8
Fluid Flow Rate	200	1.4	1.9, 3.8, 5.7, 7.6, 9.5
Oil Mass Flow Rate*	50, 100, 200	1.4	1.9, 3.8, 5.7, 7.6, 9.5, 11.4
TMP	200	0.2, 0.3, 0.7, 1.2, 1.8, 2.2, 2.8	3.8

* Only with Isopar M

RESULTS AND DISCUSSION

Experimental results indicate successful oil recovery from oil-water mixtures with varying influent oil concentrations. Further, the potential for cumulative recoveries of more than 99% indicates the potential for complete separation of fine oil-water emulsions if sufficient membrane surface area is provided. Overall, these results support the efficacy of selective oil permeation for secondary and tertiary oil-water separations. Finally, during single extended-duration experiments, the conditioned membrane maintained steady recoveries for periods for nearly 18 days without macroscopic evidence of fouling (**Figure 17**). During an extended-duration experiment shown in **Figure 17**, the experimental system

processed approximately 97,500 L of total volume, which was equivalent to approximately 295,700 Membrane A shell-side volumes (shell-side Membrane A volume is ~330 mL[182]). However, it should be noted that, due to the continuous nature of the experimental system design, the performance of the membrane was observed to improve with respect to time over more than 127 days (**Figure 18**). A summary of the results for the experiments detailed in **Table 9** examining membrane conditioning as well as the impact of oil concentration, transmembrane pressure, and influent flow rate is available in **Table A1**.

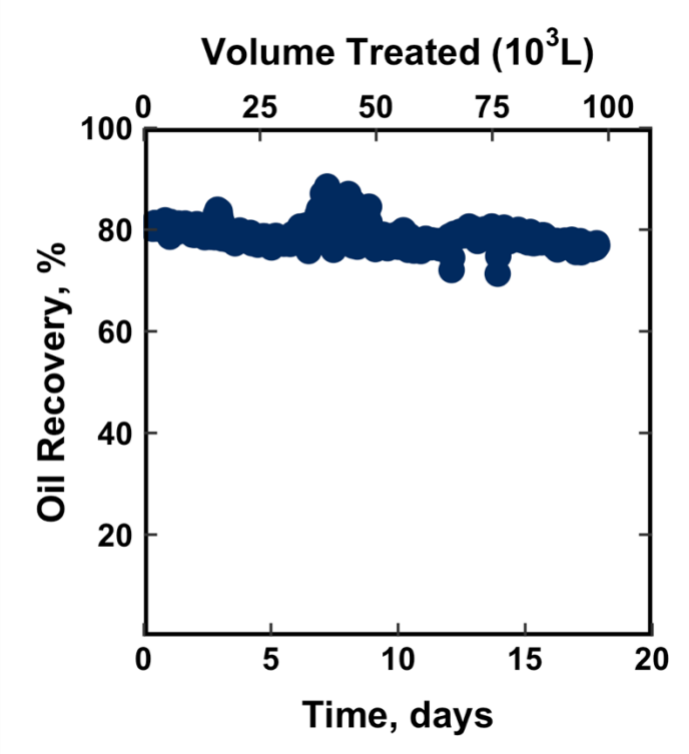

Figure 17: An extended duration experiments with 200 mg/L Isopar M at a transmembrane pressure of 0.34 bar and an influent flow rate of 3.8 L/min. Gaps in data are due to resetting of data acquisition system.

Membrane Conditioning

Mercelat *et al.* hypothesized that the development of an oil film at the membrane surface is critical to membrane performance.[18,22] However, for unused membranes, there is

no oil film at the membrane surface to facilitate coalescence and oil recovery. Thus, for new membranes, we anticipate an increase in oil recovery and flux as an oil film develops at the membrane surface.

In this study, the performance of a new, unconditioned (*i.e.*, not subjected to any surface treatment prior to initial operation) Membrane A was observed to improve substantially over time when separating Isopar M emulsion (**Figure 18**). Oil flux and oil recovery for Isopar M increased from 22.9% to 65.2% at the highest transmembrane pressure (C_{oil} = 200 mg/L, Q = 3.8 L/min, and P_T = 2.75 bar) after the first approximately 67 days of operation. After another approximately 60 days of operation, oil recovery increased to 71.1% for the same set of experimental conditions. The results reported in **Figure 16** are in stark contrast to the often rapid decline seen in traditional membrane-based oil-water separations.[9–16,110,112–114] Furthermore, these results are consistent with the hypothesis that oil wets the membrane surface, forms an oil film, and that the film itself supports the permeation of oil through the membrane surface.

Yet, the temporal changes in membrane performance invites optimization of the membrane conditioning process. Soaking both the shell-side (~330 mL[182]) and lumen-side (~90 mL[182]) of a separate, new Membrane A in Isopar M for 7 days prior to installation and operation improved initial performance substantially (**Figure 18**). The effect of membrane conditioning was most pronounced at the highest transmembrane pressure (C_{oil} = 200 mg/L, Q = 3.8 L/min, and P_T = 2.75 bar), where the initial oil recovery increased from 22.9% to 68.1%. An additional week of conditioning further increased the oil recovery at the same experimental conditions to 77.1%.

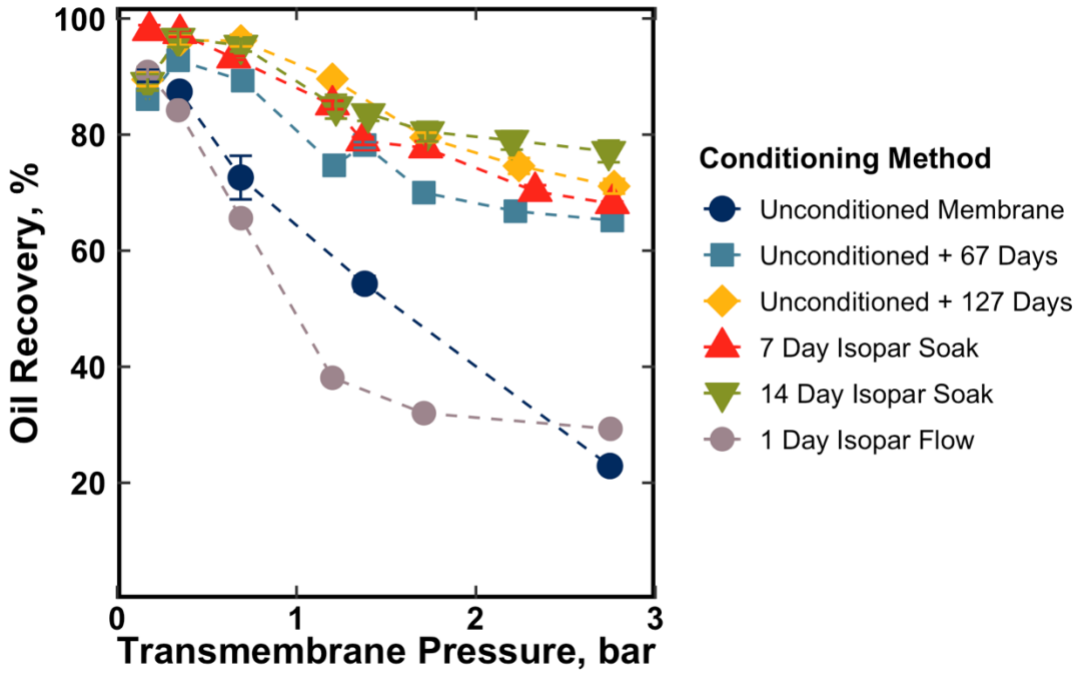

Figure 18: Improvements in oil recovery in an originally unconditioned Membrane A with respect to days of operation or membrane conditioning method. All experiments utilized Isopar M at an influent oil concentration of 200 mg/L and an influent flow rate of 3.8 L/min. Conditioning methods are as follows: "Unconditioned" was not subjected to any surface treatment prior to initial operation; "Unconditioned + 67 Days" was the "Unconditioned" membrane operated continuously for 67 days; "Unconditioned + 127 Days" was the "Unconditioned + 67 Days" operated continuously for an additional 60 days; "7 Day Isopar Soak" was a new membrane soaked in Isopar M for 7 days prior to initial operation; "14 Day Isopar Soak" was the "7 Day Isopar Soak" membrane soaked in Isopar M for an additional 7 days following approximately 14 days of operation; "1 Day Isopar Flow" was the membrane conditioned with pure Isopar M flow for 24 hours at a transmembrane pressure of 0.34 bar and flow rate of 3.8 L/min. Lines are for visual clarity only.

Initially, we hypothesized that pure Isopar M flow through the membrane would offer superior results to soaking the membrane due to the pressure-induced wetting of both the membrane surface and pores. However, permeating pure Isopar M through the

membrane for approximately 24 hours (Q = 3.8 L/min and P_T = 0.34 bar) did not provide similar improvements in membrane performance (**Figure 18**).[18] These results suggest that the membrane wetting (and potentially membrane swelling) may be more effective with soaking rather than constant flow. Perhaps oil film formation is more effective over longer-durations and with no crossflow velocity to disrupt film formation. It should also be noted that membrane soaking prior to operation is not unique to the selective oil permeation, as membranes are often soaked in the wetting liquid before experiments. Further research would be necessary to fully understand fundamental changes at the membrane surface and within the membrane pore that underly the observed performance differences.

Similar improvements were also evident for variation in influent flow rate (**Figure 19**). For the unconditioned membrane, oil recovery was initially observed to increase with increasing flow rate (38.1% at 1.9 L/min to 61.7% at 9.5 L/min as shown in **Figure 19**). Yet, this trend was not present for data taken at either 67 days or on preconditioned membranes. As such, the initially observed increase in oil recovery with increasing influent flow rate may be due to the initial wetting of the membrane surface over the first five days of experiments beginning to establish an oil film. For the first experiment conducted on the conditioned membrane (C_{oil} = 200 mg/L, Q = 1.9 L/min, and P_T = 1.38 bar), oil recovery increased from 38.1% to 77.5% after approximately 67 days of continuous membrane operation. As with membrane performance improvement for transmembrane pressure with respect to time, oil recovery after a week of preconditioning was similarly elevated (75.4% at experimental conditions of C_{oil} = 200 mg/L, Q = 1.9 L/min, and P_T = 1.38 bar) and continued to increase after two weeks of preconditioning (79.1% at experimental conditions of C_{oil} = 200 mg/L, Q = 1.9 L/min, and P_T = 1.38 bar). Thus, it appears that preconditioning of the membrane surface expedites the formation of an oil film at the membrane surface and enhances long-term oil recovery.

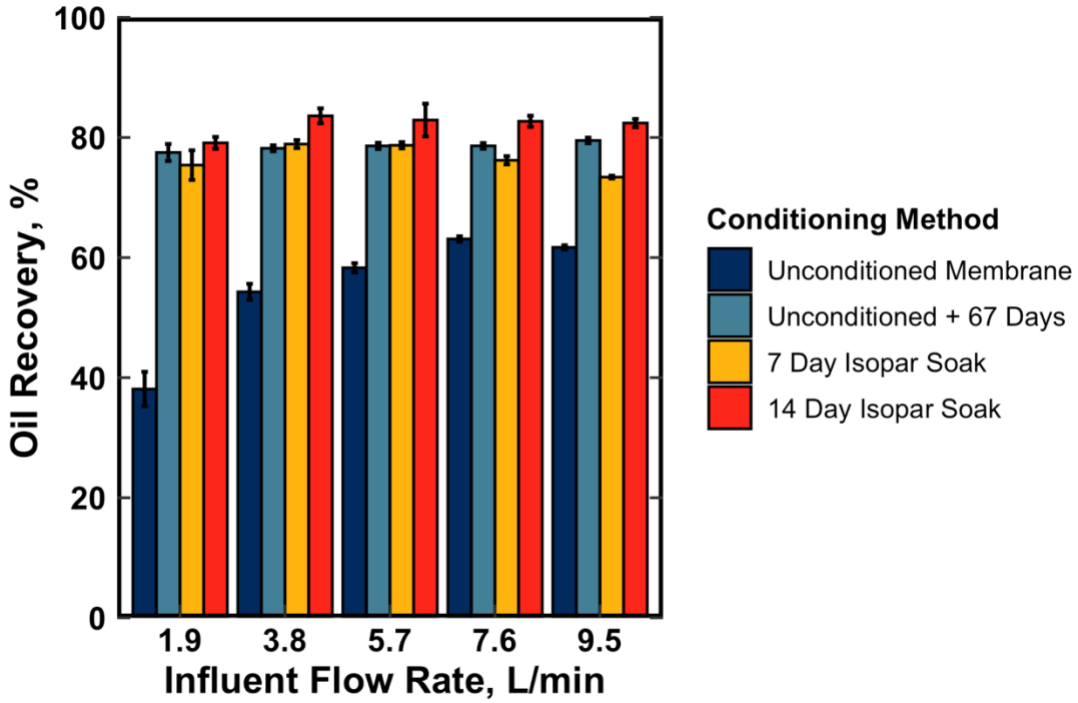

Figure 19: Improvements in initial oil recoveries on an unconditioned and conditioned (*e.g.*, soaked in Isopar M for 7 days prior to initial operation) Membrane A. All experiments used Isopar M at an influent oil concentration of 200 mg/L with a transmembrane pressure of 1.38 bar. Conditioning methods are as follows: "Unconditioned" was not subjected to any surface treatment prior to initial operation; "Unconditioned + 67 Days" was the "Unconditioned" membrane operated continuously for 67 days; "7 Day Isopar Soak" was a new membrane soaked in Isopar M for 7 days prior to initial operation; "14 Day Isopar Soak" was the "7 Day Isopar Soak" membrane soaked in Isopar M for an additional 7 days following approximately 14 days of operation.

These experimental results ultimately highlight a critical benefit of selective oil permeation. Within this study, improvements in oil recovery were observed over more than 127 days of continuous operation indicating the potential for long-term operation of selective oil permeation systems. Observation of substantial improvements in oil recovery with respect to time supports the fundamental benefits (*e.g.*, minimization of viscous oil

fouling at the membrane surface) of selective oil permeation over traditional membrane-based oil-water separations. Furthermore, by demonstrating the potential to precondition the membrane, these results may allow for future selective oil permeation research that more directly exploits wettability of the membrane surface to enhance oil recovery.

Oil Concentration Effect

For oil-disperse solutions, approach and coalescence are anticipated to dominate mass transfer in selective oil permeation.[18,22–25,27] This limitation is intuitive as, in oil-disperse solutions, if the mass flow rate of oil is substantially below the membrane's capacity, oil flux and recovery will be limited by the probability that an oil droplet approaches and coalesces at the membrane surface. Thus, for non-surface area limited experimental conditions (*i.e.*, low oil concentrations), we hypothesize that oil flux will increase directly with the influent oil mass flow rate while oil recovery remains relatively constant.

Experimental oil flux and recovery were consistent with this mechanistic understanding of selective oil permeation. Oil flux increased linearly with increasing influent oil concentration for oil-disperse solutions (**Figure 20A**). Oil recovery varied minimally across the low concentration range examined (**Figure 20B**). Due to the minimal difference in observed behavior within this concentration range, further studies focused on selective oil permeation behavior at a single influent oil concentration of 200 mg/L.

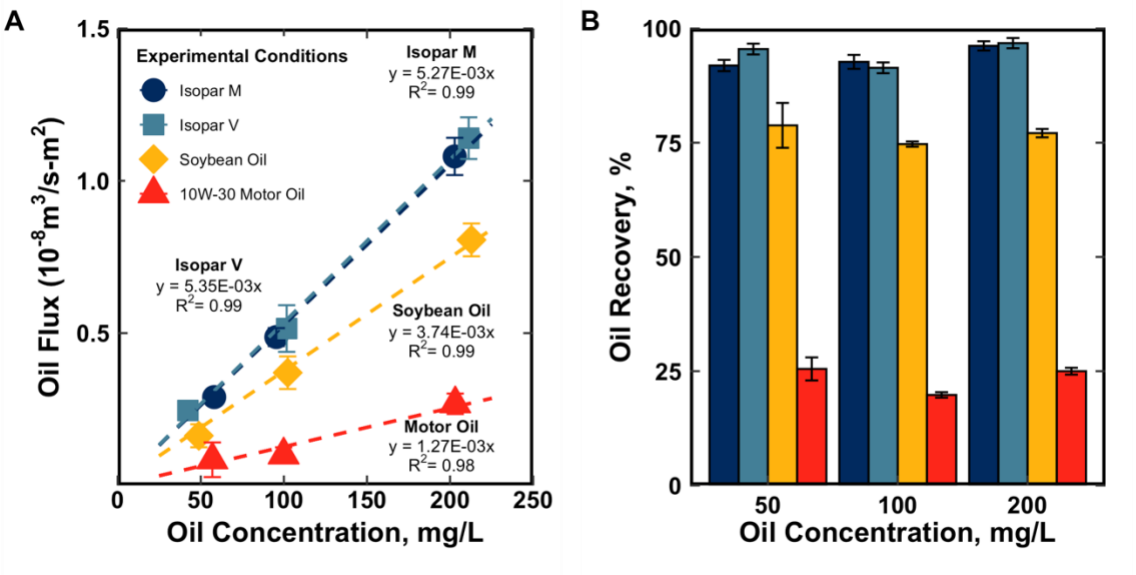

Figure 20: Influence of influent oil concentration on (A) oil flux and (B) oil recovery in a conditioned Membrane A at an influent flow rate of 3.8 L/min and a transmembrane pressure of 0.69 bar.

Influent Flow Rate Effect

Increasing influent flow rate has predominantly been shown to have an adverse effect on separation efficiency.[22,26] For example, Mercelat *et al.* observed a decrease in recovery with increasing influent flow rate for higher influent oil concentrations of 2% and 40% Isopar M within the same experimental system.[18] This decrease in permeation is attributable to the influent mass oil flow rate exceeding the maximum oil permeation. Within this study with much lower oil concentrations (*i.e.*, conditions not limited by membrane surface area), approach and coalescence are hypothesized to control mass transfer. As such, oil flux should increase linearly while oil recovery remains constant.

As anticipated, oil flux increased linearly with influent flow rate at a rate proportional to the increase in influent oil mass flow rate for Isopar M and Isopar V (**Figure 21A**). Consequently, oil recovery was relatively constant across the influent flow rates examined for the low viscosity oils (*i.e.*, Isopar M and Isopar V) (**Figure 21B**). These

results suggest the potential for selective oil permeation to serve as a high-throughput, modular treatment approach for oil recovery of lower viscosity oils. However, oil flux did not increase linearly with increased influent flow rate and influent oil mass for either Soybean Oil or Motor Oil. The slight increase observed in oil flux and oil recovery at 7.6 and 9.5 L/m for Motor Oil is attributed to declining performance in Membrane B not fully removing oil from the recycled water stream. However, in general, oil recovery declined with increasing influent flow rate.

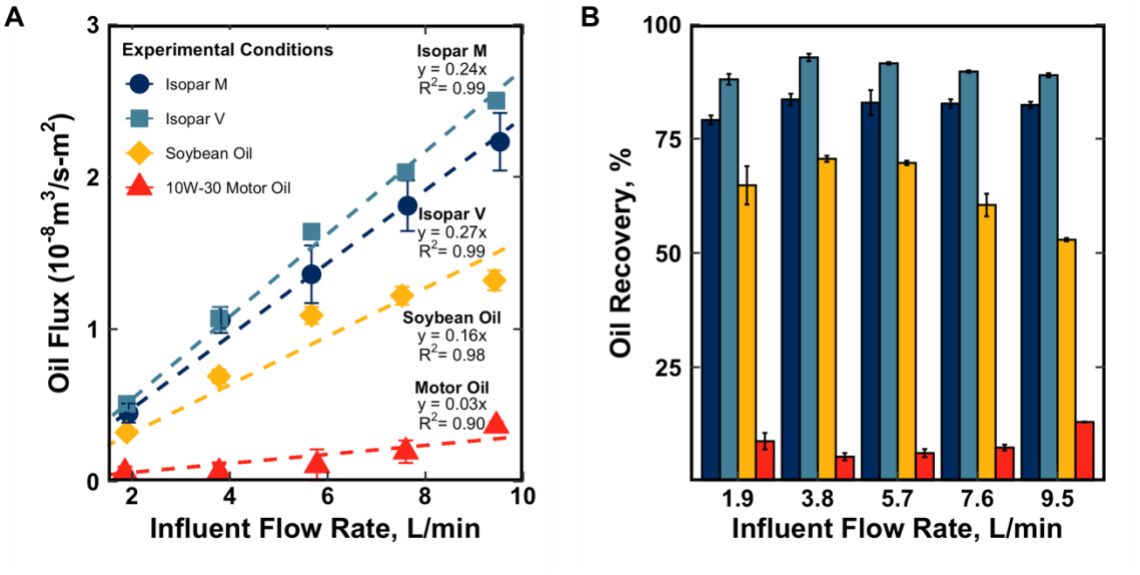

Figure 21: The effect of influent flow rate on (A) oil flux and (B) oil recovery in a conditioned Membrane A for experiments conducted with a transmembrane pressure of 1.4 bar and an influent oil concentration of 200 mg/L.

Deviation from the hypothesis that approach and coalescence limit mass transfer for oil-disperse solutions highlights how mechanistic competition may vary with respect to viscosity. For the lower viscosity oils (*i.e.*, Isopar M and Isopar V), approach and coalescence are still the dominant mechanisms with a five-fold increase in the influent oil mass flow rate. For example, a strong linear relationship was observed between oil flux

and influent oil mass flow rate (**Figure 22**) over a range of Isopar M concentrations and influent fluid flow rates. This result supports the dominance of approach and coalescence, as the same influent oil mass flow rate achieved in two different ways (*i.e.*, concentration variation and influent flow rate variation) achieves the same experimental outcomes.

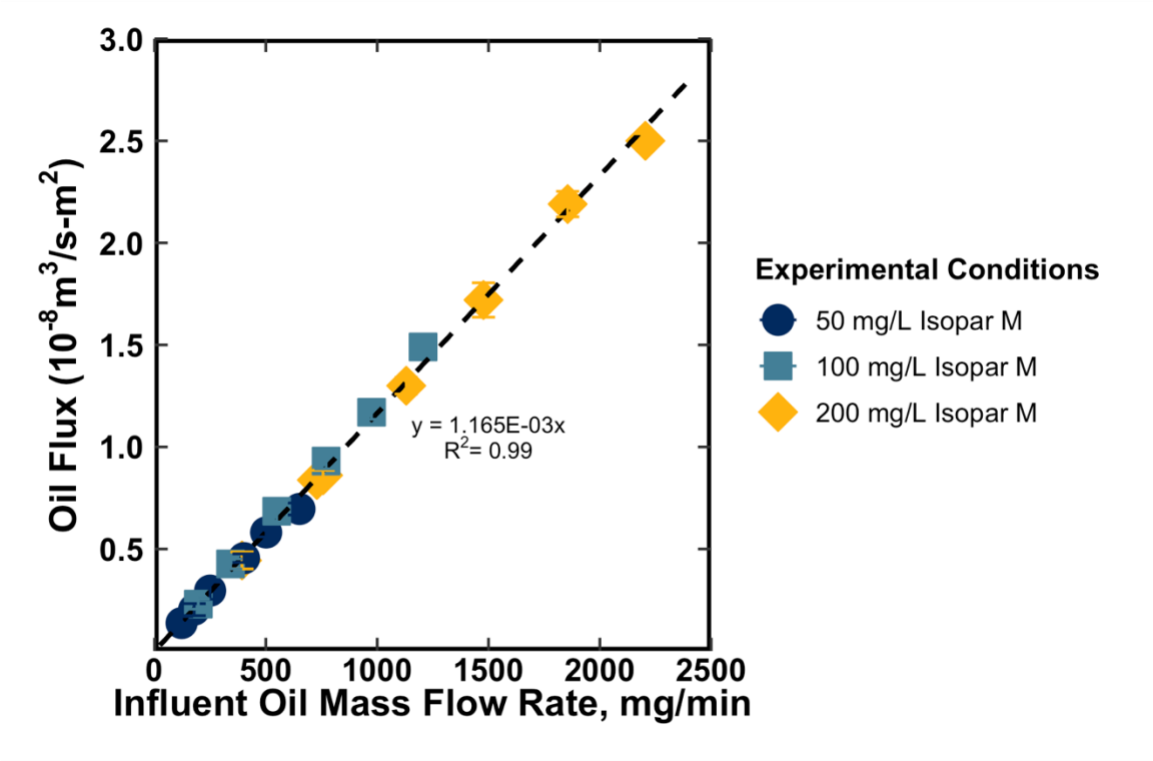

Figure 22: The observed relationship between influent oil mass flow rate and oil flux in Membrane A at a transmembrane pressure of approximately 1.38 bar. Oil concentrations ranging from approximately 44 mg/L to 207 mg/L with influent fluid flow rates of 1.9 L/min to 11.4 L/min.

However, for the higher viscosity oils (*i.e.*, Soybean Oil and Motor Oil), permeation and release instead of approach and coalescence are limiting oil recovery as the influent oil mass flow rate increases. Though other explanations for this might be possible, our conclusion based on this evidence is that oil recovery was limited by permeation and

release and not by approach and coalescence as the influent oil mass flow rate increased. This is a reasonable conclusion since the oil permeation capacity of the membrane decreases with increasing viscosity based on the Blake-Kozeny equation (**Equation 11**). Thus, for higher viscosity oils, lower influent flow rates and higher transmembrane pressures may produce superior oil recoveries.

Effect of Transmembrane Pressure

Studies investigating the relationship between oil flux and recovery and transmembrane pressure for oil-disperse solutions have not been consistent within the literature.[22,23,28] Magdich first observed an inverse relationship between oil flux and transmembrane pressure for 5% dodecane-water emulsions, but not for experiments using kerosene.[23] Mercelat *et al.* consistently observed a similar, inverse linear relationship between oil recovery and transmembrane pressure for oil-disperse solutions.[22] Mercelat *et al.* attributed this behavior to the permeation rate exceeding the coalescence rate, undermining the long-term stability of the oil film both on the membrane surface and potentially within the membrane pore.[18,22,183,184] However, Kong *et al.* found oil recovery increased with increasing transmembrane pressure for influent oil concentrations <1%.[28] Within the experimental conditions examined in this study (i.e., oil-disperse solutions), coalescence is hypothesized to be the operative mechanism. As such, oil recovery is anticipated to decline linearly with increasing transmembrane pressure.[22]

Experimental results in this study deviated from both the literature and our hypothesis. While oil recovery generally decreased with increasing transmembrane pressure (**Figure 23**), behavior inverted for the lowest transmembrane pressures. An inversion in oil recovery at transmembrane pressures between approximately 0.3 and 0.7 bar created a maxima for each oil.

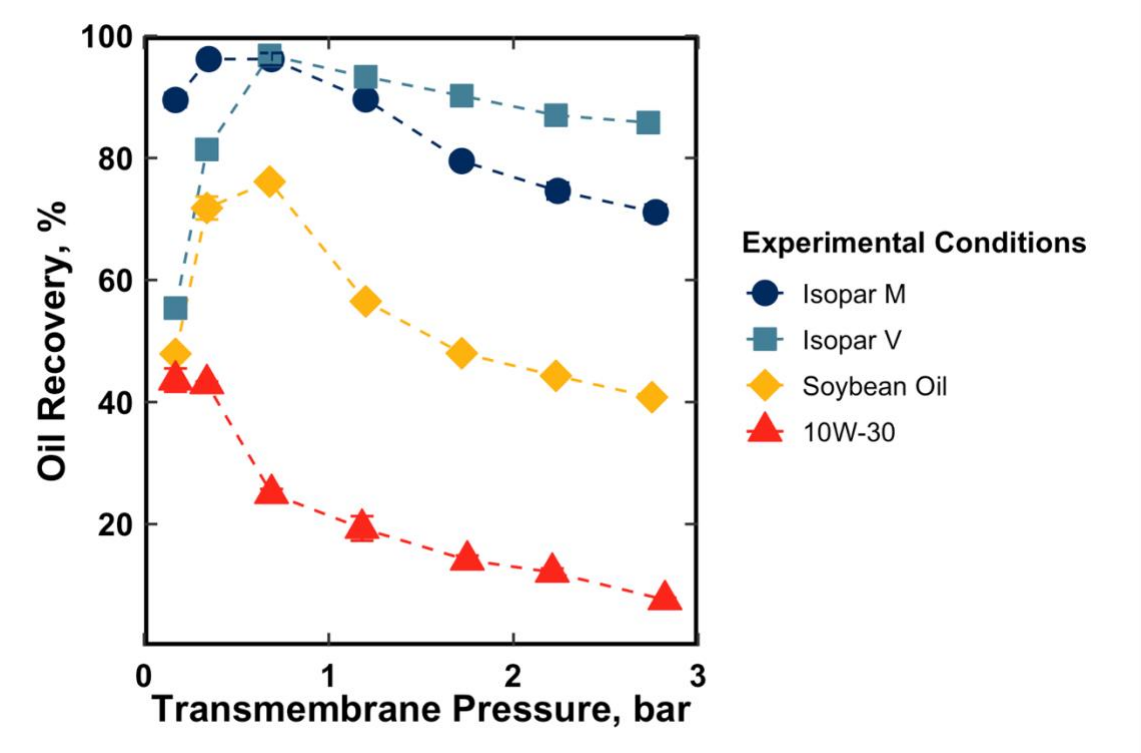

Figure 23: The influence of transmembrane pressure on oil recovery at influent oil concentrations of 200 mg/L at an influent flow rate of 3.8 L/min in Membrane A. Lines are for visual clarity only.

While this behavior has not been previously reported in the selective oil permeation literature, it is still consistent with our mechanistic understanding of the process and may be consistent with described deviations between the work of Magdich, Mercelat *et al.*, and Kong *et al.*[22,23,28] First, above the optimum transmembrane pressure, the experimental results are consistent with approach and coalescence controlling oil recovery and flux. At the optimum transmembrane pressure, the rate of approach and coalescence may be well-paired with the permeation rates, allowing for maximization of both the wetted surface area of the membrane and oil flux. Below the optimum transmembrane pressure, permeation and release control oil flux, as oil flux (particularly for viscous oils) may be limited by a

lack of necessary driving force to force the oil through the membrane pores and the hollow fibers. This hypothesis is supported by the linear relationship between oil recovery and inverse viscosity (as outlined in the Blake-Kozeny equation in **Equation 11**) that is only observed below the optimum transmembrane pressure (**Figure 24**). A return to an Ergun-style relationship (as outlined in **Equation 11**) is consistent with permeation controlled mass transfer, as Mercelat *et al.* demonstrated for oil flux in pure oil or oil-continuous solutions.[22] Thus, differences in the literature for the reported relationship between transmembrane pressure and oil flux are likely due to the variability of competition between coalescence and permeation at different transmembrane pressures for oil-disperse solutions.

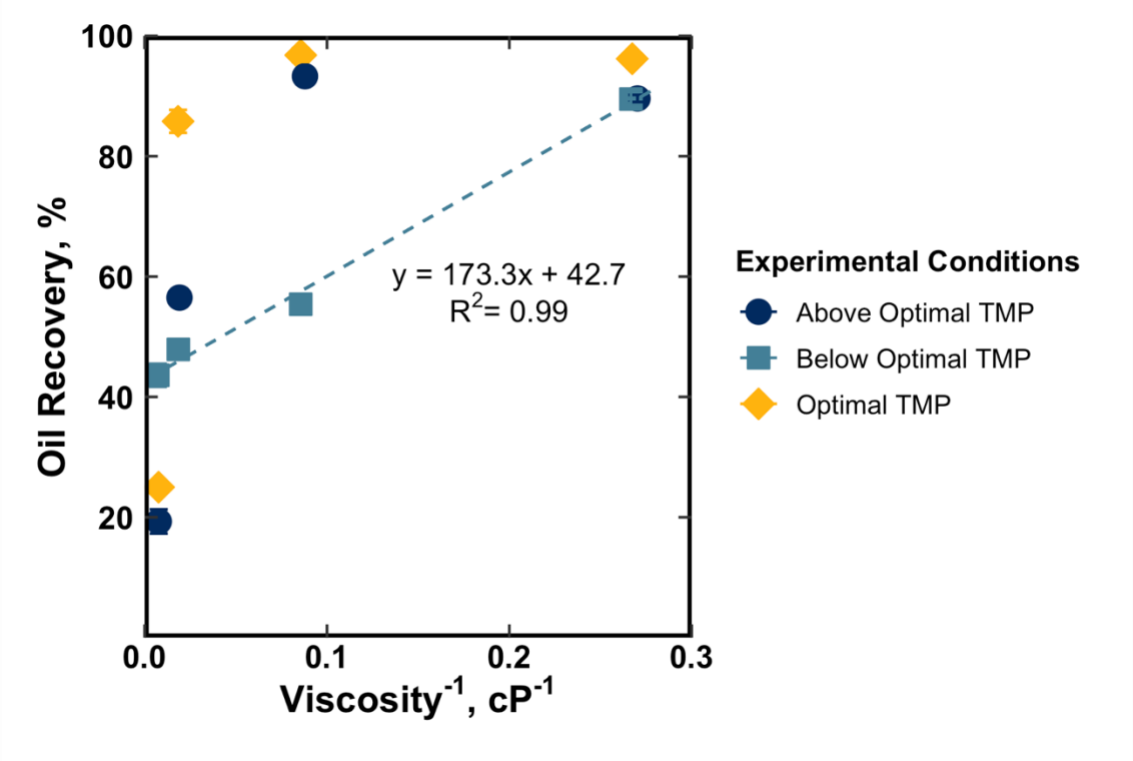

Figure 24: The relationship between viscosity and oil recovery above the optimum (P_T = 1.2 bar), at the optimum (P_T = 0.7 bar), and below the optimum (P_T = 0.2 bar). All data from Membrane A and an influent oil concentration of 200 mg/L and influent flow rate of 3.8 L/m.

Mass Transfer Modeling

Application of the Mercelat *et al.* model to the present dataset results in poor prediction of the data, particularly for data outside the ranges of the previous study (**Figure 25)**. As shown in **Table 6**, this study examined much lower oil concentrations over a broader range of influent flow rates and oil viscosities to evaluate the relevance of selective oil permeation to produced water treatment. In particular, the model predicts the change in oil flux with respect to the change in influent flow rate (*i.e.*, velocity) particularly poorly. This poor fit is likely due to inaccurate scaling of the oil concentration (C_{oil}) and shell-side velocity (v) to match the linear increase in mass flow rate caused by increasing the shell-side flow rate (See **Equation 12** and **Figure 22**). However, prediction of this behavior is particularly important within the present study as we have demonstrated the potential for selective oil permeation to serve as a modular, high-throughput method for oil-water separations in produced water treatment. As such, the influent oil mass flow rate was exchanged for this inlet oil concentration within the proposed model.

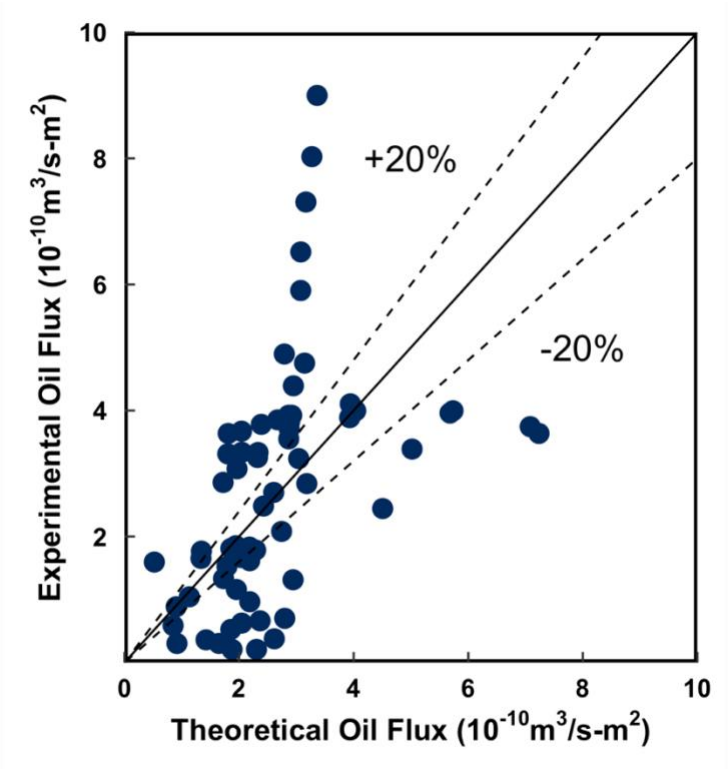

Figure 25: Performance of original mass transfer model for experimental results presented in this chapter.

Nonlinear regression of conditioned data from this dissertation ($C_{oil} \leq 200$ mg/L) and Mercelat *et al.* results in the following equation:

$$\frac{a_e}{a_t} = \frac{9.53\times10^{5}\cdot m_{oil}\cdot {P_T}^{-1.344}\cdot \mu^{1.046}\cdot v^{0.123}}{1 + 1.16\times10^{10}\cdot m_{oil}\cdot {P_T}^{-1.529}\cdot \mu^{1.893}\cdot v^{0.577}} \quad (15)$$

Where m_{oil} is the influent mass flow rate of oil (mg/s), P_T is the transmembrane pressure (Pa), μ is the viscosity (Pa-s), and *v'* is the volume averaged velocity (m/s) as derived by Mahmud *et al.* for a Liqui-Cel Extra Flow module as follows:

$$v' = \frac{Q_{shell}}{2\pi h}\cdot\frac{1}{r_{out}-r_{in}}\log\left(\frac{r_{mod}}{r_{ct}}\right) \quad (16)$$

Where Q_{shell} is the shell-side water flow rate (m^3/s), h is the length of the hollow fiber module capsule (*i.e.*, half of the total length due to the existence of the baffle) (m), r_{mod} is the inner radius of the membrane module (m), r_{ct} is the outer radius of the center tube of the membrane module.[182] The velocity (v, m/s) within the module is then defined as:

$$v = \frac{v'}{void\ fraction} \tag{17}$$

Application of the model (**Equation 15**) generally allows for the prediction of the oil flux of the present experimental data within 20% (**Figure 26**). The proposed model also generally allows for the prediction of Mercelat *et al.* data acquired in the same experimental system for oil concentrations less than 5%.[22] However, the model provides worse agreement for influent oil concentrations greater than 5%. This may be due to inherent changes in mechanistic competition between oil-disperse and oil-continuous solutions. Furthermore, additional work is necessary to understand mechanistic interactions within the transitional zone (5 to 10%).

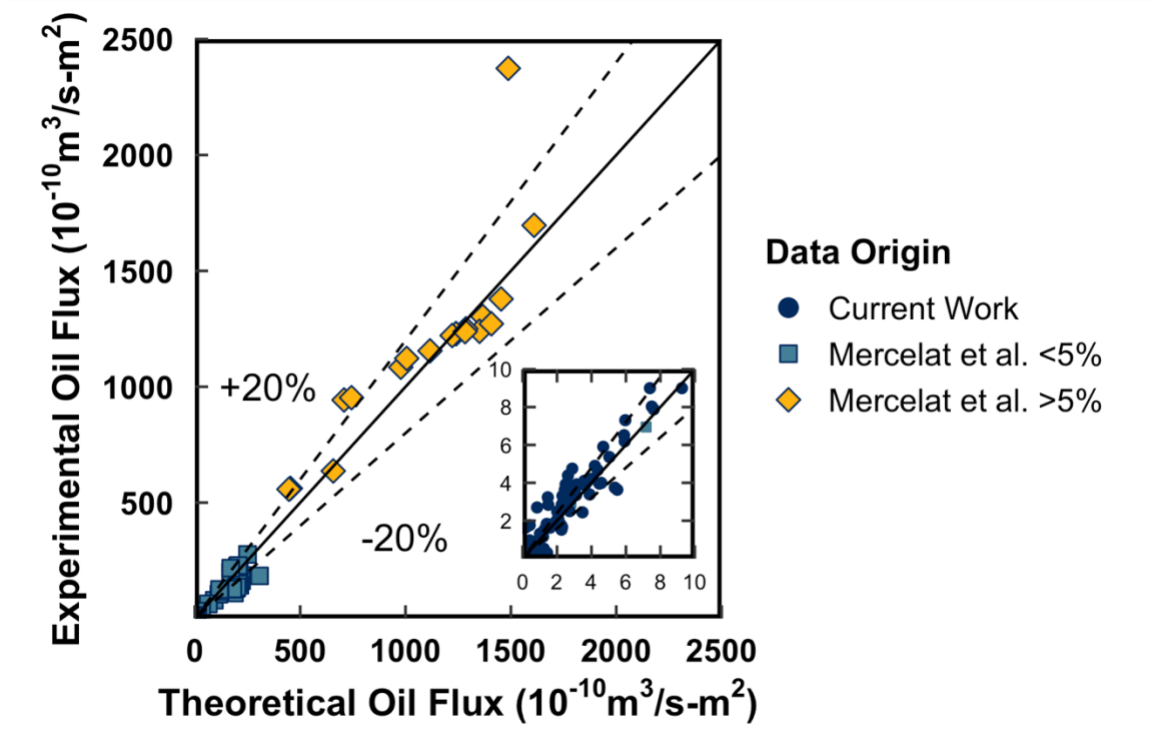

Figure 26: Prediction of oil recovery from **Equation 15** of data detailed in **Table A1** and from Mercelat *et al.* [22] Distinction between Mercelat *et al.* data above and below 5% is to note the difference between the oil-disperse region (blue squares) below the observed transition zone within their work and the oil-continuous region (yellow diamonds).

IMPLICATIONS AND APPLICATIONS

Experimental results presented throughout this chapter provide a strong foundation for understanding the opportunity space for selective permeation. First, this study demonstrated the potential for selective oil permeation to achieve high oil recoveries for low-viscosity oils for low influent oil concentrations. These results confirm the ability of selective oil permeation to achieve high oil recoveries from oil-in-water emulsions with low oil concentrations (< 1%).[22,23,28]

Second, within the oil concentration range examined, new relationships were observed between operating parameters (*e.g.,* transmembrane pressure, influent flow rate) and solution properties (*e.g.,* influent oil concentration, viscosity). For the low oil concentrations examined, influent flow rate had minimal impact on oil recovery for the low viscosity oils examined (*i.e.,* Isopar M, Isopar V). These results deviate from the literature and support our hypothesis that selective oil permeation is particularly well-suited to oil recovery from oil-in-water emulsions with low oil concentrations. Furthermore, for conditioned membranes (*i.e.,* both those soaked in oil for several days prior to first use, or those used for an extended time without pre-conditioning), mechanistic competition between coalescence and permeation resulted in optimum recoveries at low transmembrane pressures. These results may resolve conflicting trends in the literature for the relationship between oil recovery and transmembrane pressure for oil-disperse solutions. The observation of elevated oil recoveries at low transmembrane pressures presents the pragmatic opportunity for higher efficiency removal with lower required energy input. Ultimately, these results support the applicability of selective oil permeation as a modular, high-throughput secondary or tertiary oil-water separation process for low viscosity oils.

While the results presented in this chapter are broadly consistent with our mechanistic understanding of selective oil permeation, they also suggest the economic limitations of removing high-viscosity oils using selective oil permeation. A case study demonstrating the effects of this trend by estimating the required surface area necessary to achieve 90% removal is shown in **Figure 27**. The seemingly exponential increase in predicted surface area (particularly for elevated viscosities at high transmembrane pressures) may indicate economic limitations for the recovery of high viscosity oils using selective oil permeation. The elevated required surface areas also emphasize the importance of operating at low transmembrane pressures for oil-disperse solutions. Similar

limitations may exist over a broader range of oil concentrations. Future work assessing the technoeconomics of selective oil permeation is necessary to understand the opportunity space for this promising technology.

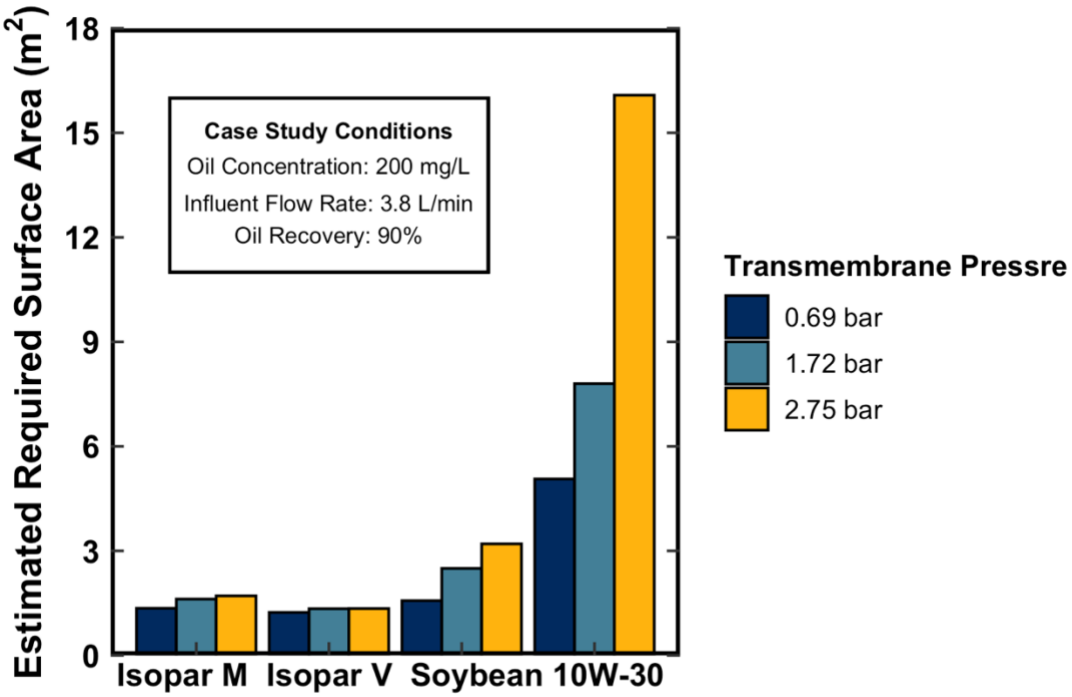

Figure 27: Results from case study showing the predicted required membrane surface area to achieve 90% oil recovery at 200 mg/L influent oil concentrations and an influent flow rate of 3.8 L/min based on experimental oil flux at corresponding conditions.

Finally, the study emphasized the importance of membrane conditioning and temporal variability in selective oil permeation. Observation of substantial improvements in oil recovery with respect to time supports the fundamental benefits (*e.g.*, minimization of viscous oil fouling at the membrane surface) of selective oil permeation over traditional membrane-based oil-water separations. Future research could help elucidate the fundamental changes occurring at the membrane surface to improve process performance.

These and other experimental results presented throughout the study ultimately support selective oil permeation as a promising secondary or tertiary oil-water separation approach that may be particularly well suited for both complex wastewaters and treatment scenarios (*e.g.,* petroleum wastewaters, metalworking wastewaters, food processing wastewaters). Furthermore, these results are promising for the application of selective oil permeation to oil spill cleanup, as the technology can address a wide variety of oil concentrations and achieve effluent concentrations that meet regulatory standards.

ACKNOWLEDGEMENTS

This project was funded by the Kuwait Foundation for the Advancement of Sciences under project code CN17-45EV-01. This material is based upon work supported by the National Science Foundation Graduate Research Fellowship under Grant No. DGE 2137420. I would also like to acknowledge JR Campos and Jarett Spinhirne for their technical support throughout this work.

Chapter 5: Effects of Water Quality on Selective Oil Permeation Performance

ABSTRACT

Selective oil permeation differs from traditional membrane-based oil-water separations by permeating oil through the membrane pores while retaining water. This approach has two main benefits: minimization of viscous fouling and the creation of a high-quality oil permeate stream. While many researchers have investigated the effects of operating conditions (*e.g.,* transmembrane pressure, flow rate) and solution characteristics (*e.g.,* oil concentration, oil characteristics) on process performance (*e.g.,* oil flux, oil recovery, permeate quality), few have systematically investigated the effects of water quality on process performance. Further, some of these studies have resulted in water breakthrough, undermining one of the main benefits of selective oil permeation. This study focuses on elucidating the effects of common water quality parameters (*e.g.*, pH, salinity, surfactant concentration) on selective oil permeation performance. Through this set of experiments, statistically significant relationships were observed between all water quality parameters examined (*i.e.,* pH, salinity, anionic surfactant concentration, nonionic surfactant concentration, and cationic surfactant concentration) and oil recovery. These initial water quality results indicate the potential for oil recovery from waters with varying water quality as well as the potential for process optimization through water quality parameter adjustment.

INTRODUCTION

Selective oil permeation is a membrane-based oil-water separations approach that permeates oil (instead of water) through a hydrophobic membrane.[19,20,22,23,26,28,158] Selective oil permeation provides two main advantages over traditional membrane-based oil-water separations. First, selective oil permeation generates a high-quality oil permeate stream, which may allow for resource recovery of valuable oils. Second, by exploiting the preferential oil wetting of the membrane surface, selective oil permeation minimizes viscous fouling of the membrane surface. Researchers have investigated the process using numerous insoluble oils to determine the relationship between operating parameters (*e.g.*, transmembrane pressure, flow rate), solution characteristics (*e.g.*, oil concentration, oil characteristics), and process performance (*e.g.*, oil flux, oil recovery, permeate quality).[19,20,22,23,26] These studies have also developed our mechanistic understanding of the process where oil flux is controlled by the approach and coalescence of the oil droplet on the membrane surface, permeation of the oil through the membrane surface, and release of the oil from the permeate side of the membrane (**Figure 2**).[22–24,27,28] However, few studies have studied the influence of water quality on selective oil permeation performance.

Understanding the impact of water quality on process performance is crucial to understanding both the opportunity space for selective oil permeation and mechanistic competition within the process. First, many oily wastewaters (*e.g.*, produced water, metalworking fluids) may contain high total dissolved solids concentrations as well as chemical additives (*e.g.*, surfactants, biocides, friction reducers, stabilizers).[2,33] Second, coalescence is often the dominant mechanisms for oil-disperse solutions.[22] The tendency of dispersed droplets to recombine (*i.e.*, emulsion instability) can be influenced by approach (or flocculation) involving interception, diffusion, and inertial impaction as well as coalescence (*i.e.*, deformation, film formation, and thin film rupture).[23,159,162–167]

Emulsion stability has been shown to be influenced by mechanical and electrical factors including viscosity, dispersed phase concentration, temperature, pH, emulsifier or surfactant concentration, interfacial tension, salt concentration, and phase density differences.[23,161,185,186] A summary of the factors considered in the study are shown in **Table 10**. For example, higher interfacial tension emulsions tend have lower emulsion stability due to a reduction in interfacial energy; the reduction in interfacial energy drives a reduction in interfacial area and thus increased deformability of the droplet.[58,159] Increased mechanical stability of the interfacial film theoretically allows for droplets to resist rupture.[23] From an electrostatics perspective, electrostatic repulsion between emulsion droplets dictates how closely two droplets or a droplet and a surface may approach.[23] For example, a reduction in the repulsive forces (*e.g.,* reducing the negative charge of oil droplets within the system, increasing the positive charge of the membrane surface, etc.) would theoretically favor coalescence within selective oil permeation.[23] However, despite the potential for emulsion stability to influence selective oil permeation performance, limited work has examined process performance through this lens.

Table 10: Hypothesized relationships between various factors impacting coalescence rates and their anticipated or observed effect on selective oil permeation performance.

An increase in…	**Coalescence Rate**	**Oil Recovery**	**Relevant Parameters**
Interfacial Tension	↑	↑	Salinity, Surfactants
Zeta Potential	↓	↓	pH, Surfactants, Salinity
Continuous Phase Viscosity	↓	↓	Salinity

Previous investigations of water quality effects in selective oil permeation have often followed expectations for the previously outlined mechanisms.[19,20,23,25,26,158] In particular, many studies have found surfactants and emulsifiers (*e.g.*, sodium dodecyl sulfate (SDS),[23,25] Pet Mix #9,[23] Alkylbenzene Sulfonic Acid (ABSA),[23] Triton-X,[23] bis(2-ethylhexyl)-phosphate,[26] ECA 5025,[19] Igepal CO 610,[19] and SPAN 80[19,20]) to be detrimental to selective oil permeation performance. Early work by Ueyama *et al.* observed a precipitous decline in oil flux with increasing the anionic surfactant (SDS) concentration (resulting in interfacial tensions between 4 mN/m and 16 mN/m) in kerosene emulsions. Ueyama *et al.* attributed this change in macroscopic performance to surfactant adsorption to the membrane surface which would prevent oil drops from adhering to the membrane surface.[25] Tirmizi *et al.* noted a decline in both oil flux and permeate quality within increasing surfactant (ECA 5025) concentrations (0 to 30 g/L) in tetradecane emulsions. Similarly, Ezzati *et al.* found that low emulsifier content produced the optimal performance via Taguchi experimental design and analysis of variance (ANOVA).[20] The decline was attributed to an increasingly stable emulsion forming a concentrated emulsion layer at the

membrane surface, depleting the oil phase at the membrane surface.[19] Broadly, results for the addition of anionic and nonionic surfactants are consistent with the hypothesized importance of coalescence rates on oil recovery in selective oil permeation. However, to the author's knowledge, no studies have examined the influence of cationic surfactants on selective oil permeation performance. Magdich observed enhanced performance in a polypropylene X-20 membrane coated with a cationic polymer (N(β-aminoethyl)-γ-aminopropyltrimethoxysilane).[23] While these results are promising, further work is necessary to evaluate the potential for cationic surfactants to enhance process performance.

The literature contains limited experiments with either pH variation or high salt concentrations. Magdich observed higher oil recovery for low pH solutions (pH = 2.4) than high pH (pH = 10.1) solutions with 10% influent oil and 1% ABSA. This behavior was attributed to decreased oil removal with increasing emulsion stability (*i.e.*, a more negative zeta potential), causing a decrease in coalescence rates within the membrane system. Magdich then hypothesized that the addition of 0.1 M KCl to a 10% ABSA emulsion would also increase oil recovery by reducing emulsion stability. Yet, the addition of KCl resulted in passage of water (instead of oil) through the membrane surface.[23] These results ultimately led Magdich to deem that selective oil permeation was impractical for solutions with surfactants or low oil concentrations.[23] However, the lack of isolation of these variables (*i.e.*, elevated surfactant concentration, salinity, low oil concentration) convolutes conclusions drawn from this study, particularly in the context of studies that have successfully recovered oil from low oil concentrations[22,28] or real, saline waters.[157]

Finally, studies with real wastewater may provide additional insight into the role of water quality. Seibert observed successful oil recovery from concentrated saline non-flocculated lysed algae in a microporous polypropylene membrane.[157] In contrast, Leiknes *et al.* observed water breakthrough in a microporous polyethylene membrane when

recovering oil from industrial cutting fluids (pH = 2, 4, 6, and 8) with high emulsifying agent concentrations (~20–30%).[158] Interestingly, water permeation decreased with decreasing pH.[158] Leiknes *et al.* attributed water breakthrough to the high concentrations of emulsifiers rendering the initially oil-wetted membrane hydrophilic.[158] Clearly, the conflicting nature of the results limits our ability to understand opportunities or limitations imposed by water quality. Further work is necessary to understand the role of water quality both fundamentally and within complex matrices.

Overall, the literature offers insight into the often-detrimental effects of anionic and nonionic surfactants, particularly when used in high concentrations. Yet, the effects of pH, salinity, and cationic surfactants have not been investigated in the literature. Since these parameters have been demonstrated to impact steps of coalescence (*e.g.,* deformation, film formation, and thin film rupture),[185] varying these parameters may impact oil recovery and flux in selective oil permeation. Thus, this study investigates common water quality parameters (*i.e.,* pH, salinity, surfactant concentration) to understand how water quality characteristics common to industrial wastewaters impact process performance. Through this study, we characterize the impact of parameters known to influence coalescence rates on oil recovery, identify opportunities for process optimization via water quality adjustment, and ultimately expand our understanding of the opportunity space for selective oil permeation.

METHODS

Solution Characteristics

Isopar M served as a synthetic oil throughout the experiments. Density (0.78 g/cm^3 at 25 degrees Celsius), oil viscosity (3.5 cP at 25 degrees Celsius), and interfacial tension were measured in triplicate using a Mettler Toledo DE40 Density Meter, NDJ-5S Digital

Rotational Viscometer, and a 70535 CSC-DuNouy Tensiometer. pH was adjusted through the addition of NaOH or HCl, respectively. Salinity was adjusted via the addition of NaCl. Finally, the effect of three surfactants (anionic surfactant: sodium dodecyl sulfate (SDS, MW = 288 g/mol), nonionic surfactant: polysorbate 80 (Tween 80, MW = 1,310 g/mol), and cationic surfactant: cetyltrimethyl ammonium bromide (CTAB, MW = 364 g/mol)) on macroscopic performance were investigated to understand the effects of anionic, cationic, and nonionic surfactants on macroscopic performance. Interfacial tensions of surfactant solutions are shown in **Figure 28**.

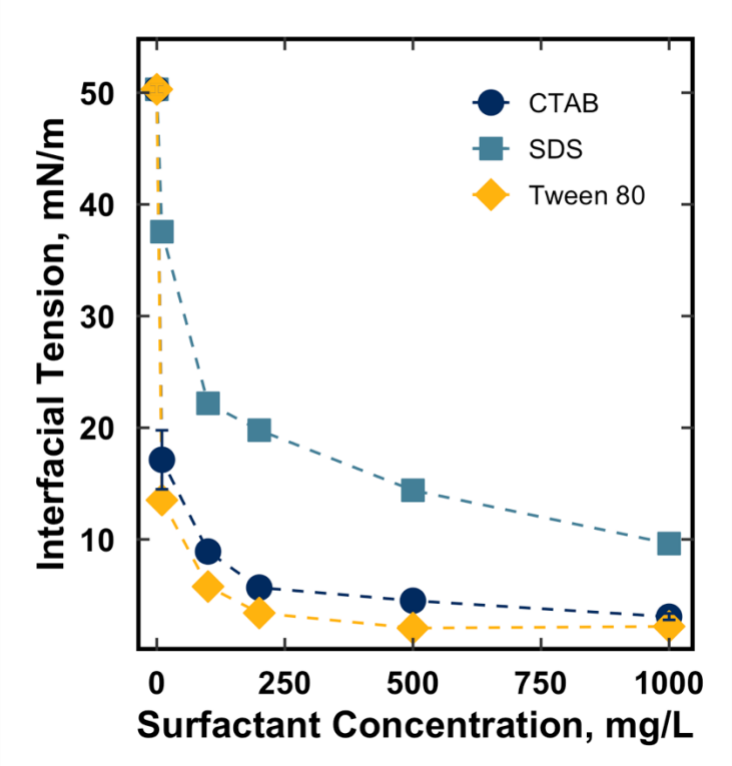

Figure 28: Relationship between interfacial tension and surfactant concentration for SDS (anionic), Tween 80 (nonionic), and CTAB (cationic).

Membrane System and Operating Procedure

The membrane contactors and experimental system used in this chapter has been previously described in **Chapter 3** and is shown in **Figure 29**. In brief, the process consists of two 3M^{TM} Liqui-Cel^{TM} Extra Flow Membrane Contactors (Membrane A and Membrane B) of varying size in series. A summary of membrane characteristics is provided in **Table 11**. All reported data in the following sections are from the primary membrane, Membrane A. Membrane A was sized to achieve oil recoveries <100% to allow for quantitative evaluation. In contrast, Membrane B , the guard membrane, was sized to attain 100% oil recovery to allow for system recycle by removing all oil from the water reservoir.[187]

Table 11: Hollow fiber membrane module specifications.

	Membrane A	**Membrane B**
Module dimensions (cm) [a]	6.4 x 20.3	10.2 x 71.1
Fiber outer diameter (μm) [a]	300	300
Fiber inner diameter (μm) [a]	220	220
Fiber wall thickness (μm) [a]	40	40
Pore size (μm) [a]	0.05	0.05
Porosity (%) [b]	40	40
Contact Angle (°) [c]	120	120
Membrane surface area (m^2) [a]	1.4	20

[a] Supplied by Manufacturer

[b] Mahmud *et al.* 2000

[c] Mercelat *et al.* 2021

In the experimental system, a peristaltic pump injected Isopar M into the suction of a high-shear pump. The high-shear pump generated the oil-water emulsion and moved the emulsion to the bottom shell-side port of Membrane A. Effluent water from the shell-side

of Membrane A then returned to the feed tank. The transmembrane pressure and influent flow rate for Membrane A were controlled via the variable speed drive on the high-shear pump and the valve downstream of Membrane A. Rosemount pressure transmitters monitored shell-side pressures. The tube-side pressure remained at atmospheric pressure. The transmembrane pressure was calculated by averaging the inlet and outlet shell-side pressure. An air diaphragm pump supplied water from the feed tank to Membrane B, which maintained the purity of the feed tank due to both its higher flow rate and larger surface area.

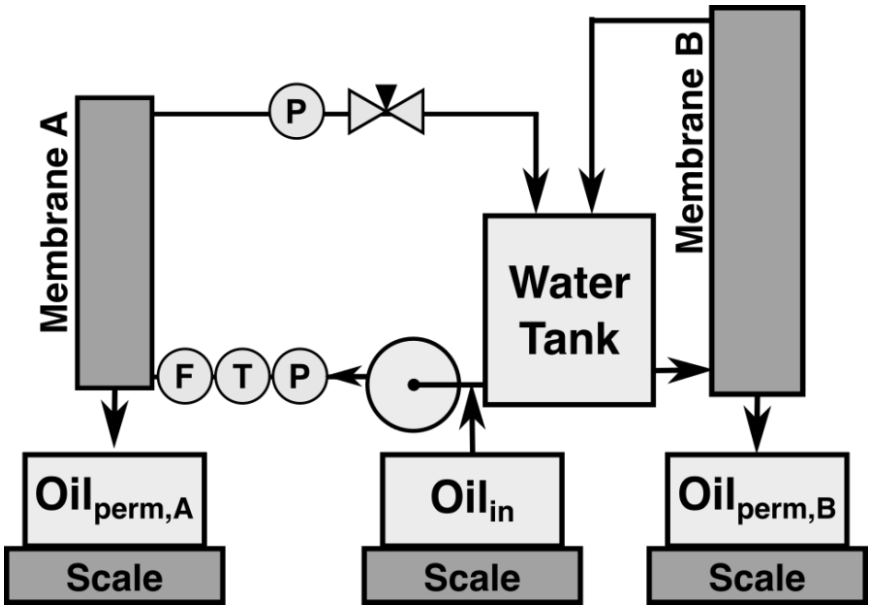

Figure 29: Process flow diagram of experimental apparatus. Membrane A (Dimensions: 6.4 cm x 20.3 cm, Surface Area: 1.4 m^2) serves as the primary membrane while Membrane B (Dimensions: 10.2 cm x 71.1 cm, Surface Area: 20 m^2) serves as the guard membrane. Abbreviations are as follows: pressure transmitter (P), temperature transmitter (T), flow transmitter (F), injected oil (Oil_{in}), oil permeate from Membrane A ($Oil_{perm,A}$), and oil permeate from Membrane B ($Oil_{perm,B}$).

Influent oil concentration, oil recovery, and oil flux were quantified gravimetrically via an Arlyn D-620T weigh scale (reported resolution of 1.0 gram) by monitoring all injected and permeated oil. The experimental system generally reached steady state within a few hours (< 4 hours). As noted in previous chapters, minimal relationship was observed between experimental duration and oil recovery once steady state was reached. Experiments ranged in duration from 8 to 69.5 hours but were generally 10 to 12 hours. Oil flux and oil recovery were calculated as a four-hour average as follows:

$$Oil\ Flux\ (\frac{m^3}{m^2-s}) = \frac{\dot{m}_{permeate}}{\rho_{oil} \times A_{membrane}} \quad (18)$$

$$Oil\ Recovery\ (\%) = \frac{\dot{m}_{permeate}}{\dot{m}_{injected}} \cdot 100\% \quad (19)$$

Where $\dot{m}_{permeate}$ was the mass flow of the permeate (g/s), $\dot{m}_{injected}$ was the mass flow of injected oil (g/s), ρ_{oil} was the density of the oil (g/cm^3), and $A_{membrane}$ was the surface area of the membrane (m^2). A DeltaV data acquisition system allowed for real-time data collection from all described instruments. The R programming environment was utilized for statistical analysis and to generate figures using the ggplot2.

Table 12 presents a summary of the conditions for the experiments investigating the impact of pH, salinity, and surfactants on selective oil permeation. Unless otherwise noted, experiments were conducted in quadruplicate. These experimental conditions were chosen to address gaps in the literature in ranges relevant to produced water (pH ≅ 4.3–10,[2] TDS ≅ < 500–400,000+ mg/L ,[188] Surfactants ≅ 500–1,800 mg/L[33]).

Table 12: Summary of experimental conditions examined during investigation. Abbreviations are as follows: All experiments conducted at oil concentrations of approximately 200 mg/L, transmembrane pressure of 0.69 bar, and influent flow rate of 3.8 L/min.

	Experimental Conditions
pH	pH = 4, 7, 10
Salinity	0, 5, 10, 30, and 50 g/L NaCl
Anionic Surfactant	0, 10, 100, and 1000 mg/L SDS
Nonionic Surfactant	0, 10, 100, and 1000 mg/L Tween 80
Cationic Surfactant	0, 10, 100, 200, 500, and 1000 mg/L CTAB
Salinity + Cationic Surfactant [a]	30 g/L NaCl with 10, 50, and 100 mg/L CTAB

[a] Each experiment examining salinity and cationic surfactant only conducted once.

RESULTS AND DISCUSSION

Oil recoveries ranged from 8.9–87.7% over the range of water quality parameters examined (**Table A2**). Crucially, no free water was observed in the permeate during the study. Broadly, these results indicate that, while oil recovery was feasible without water breakthrough at all conditions examined, there may be technoeconomic limitations to oil recovery via selective oil permeation for certain water quality characteristics.

Impact of pH

The isoelectric point of both polypropylene membranes and oil-in-water emulsions have been shown to vary with pH. [189,190] Stachurski and Michalek found *n*-alkanes to have a negative zeta potential due to the selective adsorption of OH^- ions creating excess negative charge at the oil-water interface. The zeta potential of the n-alkane decreased with decreasing pH (for $C_{16}H_{34}$ from approximately -85 mV at pH 10 to 0 mV at pH 3 at an ionic strength of 10^{-3} M NaCl) – indicating a decrease in pH resulting in a reduction in emulsion

stability for *n*-alkanes of similar size to those present in Isopar M.[190,191] Within the context of selective oil permeation, we hypothesize that, if emulsion stability increases with pH, then oil flux and recovery will decline with increasing pH. However, this effect may also be influenced by the impact of pH on the membrane surface, as the isoelectric point of polypropylene fibers also occurs at lower pH (~pH 5).[189] Thus, there may exist an optimum pH due to the interaction between the zeta potentials of both the membrane and the emulsion.

A statistically significant difference was observed between the neutral pH (pH 7) and either acidic (pH 4) and basic (pH 10) solutions, with the highest oil recovery and flux observed at pH 7 (**Table 13**). The observed decrease between pH 7 and pH 10 is consistent with our hypothesis that increased emulsion stability at higher pH will negatively impact oil recovery and flux. However, the decrease in oil flux and recovery between pH 7 and pH 4 deviates from our hypothesized mechanistic relationship. While this could be due to fundamental mechanisms outside of our initial hypotheses, it is important to note that the experiments were not conducted on a new, unconditioned module. As such, residual effects from prior experiments may have altered the membrane surface, complicating our ability to directly interpret these results. Consequently, further research would be necessary to confirm the deviation from our hypothesis, particularly when considering Magdich's observation of higher oil recovery at lower pH (pH 2.4).[23] However, the observation of changes in oil recovery and flux with pH in this work may indicate the potential for optimization opportunities through zeta potential adjustment via water quality parameters like pH.

Table 13: Impact of pH on oil recovery and oil flux. All experiments conducted in Membrane A at an oil concentration of approximately 200 mg/L, transmembrane pressure of 0.69 bar, and influent flow rate of 3.8 L/min.

pH	Oil Recovery, %	Oil Flux, m^3/m^2-s
4	84.7% ± 2.1%	9.61E-09 ± 2.42E-10
7	89.7% ± 1.2%	1.02E-08 ± 2.25E-10
10	75.8% ± 1.6%	8.57E-09 ± 1.67E-10

Salinity Effects

The addition of salt has generally been shown to decrease the stability of oil-in-water emulsions in both surfactant-stabilized[192–194] and non-surfactant-stabilized emulsions.[195] Traditionally, this behavior has often attributed to electrical double layer compression. However, some studies have observed increased emulsion stability through the addition of salt to both oil-in-water and water-in-oil emulsions.[186,196] Mechanistically, an increase in salt concentration should suppress the electrical double layer which will reduce emulsion stability and increase oil recovery.

Experimental results observed in this study were not consistent with our hypothesis. Minimal differences were observed across the NaCl concentrations observed in this study (**Table 14**). There were statistically significant ($p < 0.05$) increase in oil recovery and flux between the baseline condition (0 g/L NaCl) and 10 and 30 g/L NaCl for both oil recovery and oil flux. However, these results did not produce a consistent trend, as the 50 g/L NaCl performance was comparable to that at 0 g/L NaCl. The lack of consistency in the observed trend could be due to divergence between the effect of salinity and viscosity on coalescence rates. The addition of NaCl increases the interfacial tension of the solution, which should result in an increase in the coalescence rate.[192–195] However, as the NaCl concentration increases, the continuous phase (*i.e.*, water) viscosity increases, resulting in a decrease in

coalescence rates.[197] Ultimately, the lack of strong trend between salinity and selective oil permeation performance within this range may support the application of selective oil permeation to produced water treatment (at least up to 50 g/L TDS).

Table 14: Impact of sodium chloride concentration on oil recovery and oil flux. All experiments conducted in Membrane A at an oil concentration of approximately 200 mg/L, transmembrane pressure of 0.69 bar, and influent flow rate of 3.8 L/min.

NaCl Concentration, g/L	Oil Recovery, %	Oil Flux, m^3/m^2-s
0	79.2% ± 1.3%	9.12E-09 ± 1.62E-10
5	82.1% ± 2.6%	9.38E-09 ± 2.30E-10
10	85.2% ± 0.6%	9.89E-09 ± 7.79E-11
30	83.5% ± 0.5%	9.68E-09 ± 1.17E-10
50	81.7% ± 1.0%	9.34E-09 ± 7.69E-11

Anionic Surfactant Effects

Anionic surfactants are hypothesized to impact both mechanical factors and electrostatic processes that increase emulsion stability and, consequently, reduce coalescence rates.[23,161] By lowering interfacial tension (**Figure 28**), it is anticipated that there would be an increase in interfacial energy and interfacial area – thereby increasing the emulsion stability.[58] This increase in the deformability of the oil droplet may decrease coalescence rates.[159] Similarly, application of the Young-Laplace equation to selective oil permeation would suggest that declining interfacial tension undermining the long-term stability of the oil film both on the membrane surface and potentially within the membrane pore.[18,22,183,184] Furthermore, the addition of negatively charged surfactant may increase the electrostatic repulsion between the negatively charged oil droplets and negatively charged membrane surface. Outside of the impact of surfactants on coalescence, surfactant

adsorption or accumulation at the membrane surface could further limit oil recovery by fouling the membrane surface.[23,25] Finally, above the critical micelle concentration, micelles could physically obstruct the membrane pore further decreasing oil recovery by restricting permeation.

The observed relationship between oil flux, oil recovery, and anionic surfactant concentration is consistent with the above hypothesized mechanisms.[23,25] Oil flux and oil recovery decreased with increasing SDS concentration (and declining interfacial tension (**Figure 28**)) as anticipated by the literature (**Figure 30**). For example, oil recovery decreased slightly between 0 mg/L, 10 mg/L, and 100 mg/L SDS. However, the decreases were not significant ($p > 0.05$). A statistically significant reduction in both oil flux and oil recovery was observed between the baseline condition and 1,000 mg/L SDS.

These results are consistent with the literature. Ueyama *et al.* initially attributed the decline in oil flux for SDS concentrations between approximately 750 and 2,200 mg/L to surfactant adsorption to the membrane surface.[25] Magdich observed a similar decline in performance between 50 and 500 mg/L SDS that was attributed to either the accumulation of surfactant at the membrane surface or increased emulsion stability reducing the rate of coalescence and attachment.[23] While the experimental results observed in this study broadly support the literature, the lack of water breakthrough observed suggests that the careful selection of both membrane (*e.g.*, small pore diameter, narrow pore size distribution, pore geometry, module geometry, etc.) and operating conditions (*e.g.*, low transmembrane pressure) may reduce the likelihood of water breakthrough in selective oil permeation.

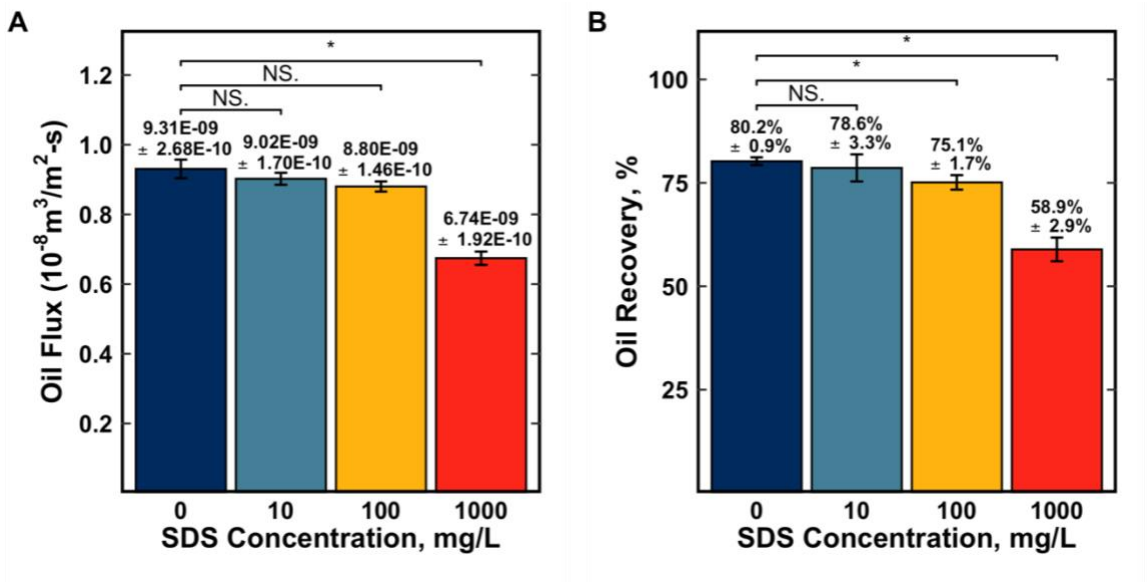

Figure 30: Impact of SDS on (A) oil flux and (B) oil recovery. All experiments conducted in Membrane A at an oil concentration of approximately 200 mg/L, transmembrane pressure of 0.69 bar, and influent flow rate of 3.8 L/min. Asterisk indicates statistical significance ($p < 0.05$) and NS indicates a lack of statistical significance ($p > 0.05$). Horizontal bars indicate the experimental conditions being compared for statistical significance.

Nonionic Surfactant Effects

Nonionic surfactants were hypothesized to follow a similar relationship with oil flux and oil recovery as anionic surfactants. Excluding increases in electrostatic repulsion, we hypothesize that the mechanisms outlined in the previous section detailing anionic surfactants would also be operative for nonionic surfactants. The literature also supports this conjecture. For example, Ezzati *et al.* determined via Taguchi and ANOVA methods that oil flux was optimal with lower concentrations of Span 80.[20] Magdich also observed a decrease in oil flux with a 1% solution of Triton X-102, which was attributed to the strong affinity between Triton X-102 and the polypropylene membrane surface.[23]

Within this study, oil recovery and flux generally decreased with increasing concentrations (and declining interfacial tension (**Figure 28**)) of Tween 80 (**Figure 31**). In

contrast to our expectations, a slight increase was observed in oil recovery and oil flux increased slightly between 0 mg/L and 10 mg/L. However, the increase in oil recovery was not statistically significant. As anticipated, there was a statistically significant decrease in both oil flux and oil recovery with increasing surfactant concentration between 0 mg/L and both 100 mg/L and 1,000 mg/L Tween 80.

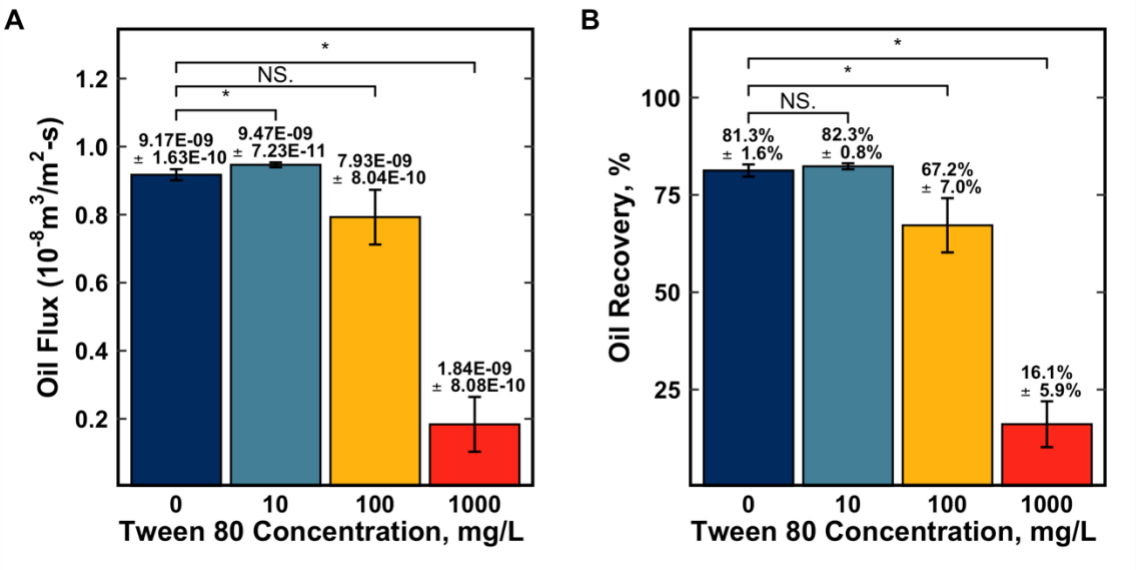

Figure 31: Impact of polysorbate 80 (Tween 80) on (A) oil flux and (B) oil recovery. All experiments conducted in Membrane A at an oil concentration of approximately 200 mg/L, transmembrane pressure of 0.69 bar, and influent flow rate of 3.8 L/min. Asterisk indicates statistical significance ($p < 0.05$) and NS indicates a lack of statistical significance ($p > 0.05$). Horizontal bars indicate the experimental conditions being compared for statistical significance.

Cationic Surfactant Effects

To the author's knowledge, the impact of cationic surfactant concentration on selective oil permeation performance has not been investigated in the literature. However, Magdich observed enhanced performance for Celgard polypropylene X-20 membrane

fibers (pore diameter 0.05 μm) that were coated with the cationic polymer N(β-aminoethyl)-γ-aminopropyltrimethoxysilane.[23] This behavior was hypothesized to be due to enhanced electrostatic interactions between negatively charged oil droplets and the positively charged fibers.[23] We hypothesize that similar phenomena may occur with the addition of cationic surfactants, wherein the negative zeta potential of the oil droplets would be reduced through the addition of cationic surfactant – thereby increasing attractive electrostatic interactions. A decrease in repulsive forces between the membrane surface and the emulsified oil droplets would then increase the rate of coalescence and ultimately increase oil recovery.

Within this study, increased cationic surfactant concentration (and declining interfacial tension (**Figure 28**)) resulted in an increase in both oil flux and oil recovery for CTAB concentrations less than 200 mg/L (**Figure 32**). While the difference between oil recovery and oil flux was not significant between the baseline condition and 10 mg/L CTAB, there was a significant difference between the baseline condition and 100 mg/L CTAB for both oil flux and oil recovery. The observed increase in oil recovery and oil flux is both consistent with our hypothesized importance of electrostatic interactions in the process and Magdich's original work with cationic coated membrane fibers. Furthermore, these results may ultimately support pursuing methods for exploiting electrostatic interactions within selective oil permeation (*e.g.,* chemical additives, membrane surface modification).

However, deviation from our hypothesized relationship between cationic surfactant concentration and selective oil permeation may highlight the need for more nuanced understanding of mechanistic competition between coalescence and permeation.[23,159,162–167] Within this study, a decline in both oil recovery and oil flux was observed for concentrations greater than or equal to 200 mg/L CTAB (**Figure 32**). Consequently, it

appears that there is an optimal amount of chemical addition that enhances attractive electrostatic interactions without resulting in the deleterious effects seen within the SDS and Tween 80 results (**Figure 30** and **Figure 31**, respectively). These results also highlight the potential for more nuanced mechanistic competition between steps of coalescence and permeation.[23,159,162–167]

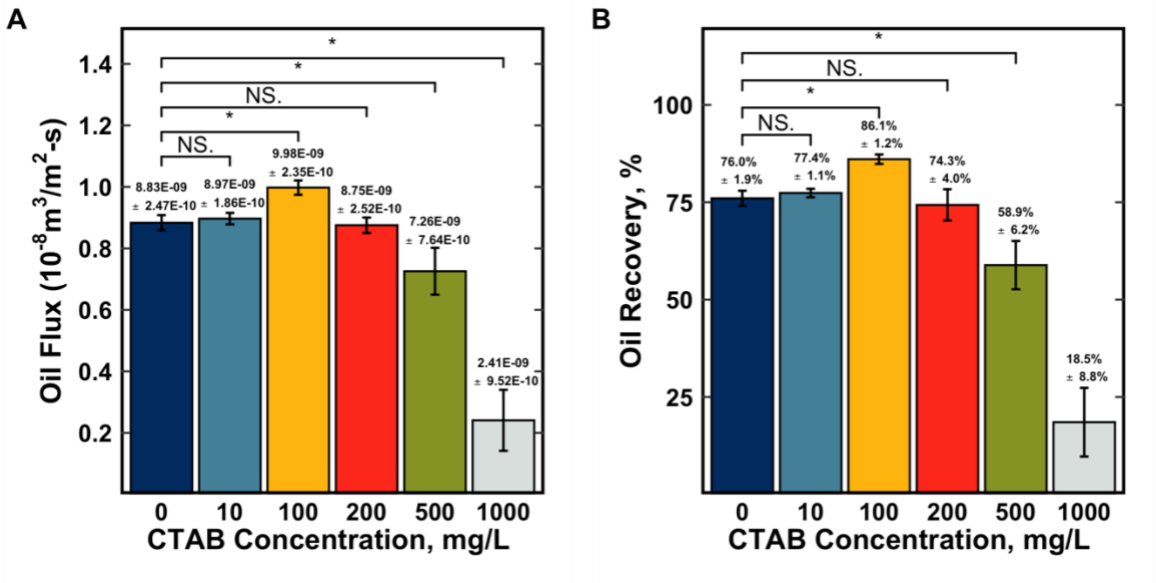

Figure 32: Impact of CTAB on (A) oil flux and (B) oil recovery. All experiments conducted in Membrane A at an oil concentration of approximately 200 mg/L, transmembrane pressure of 0.69 bar, and influent flow rate of 3.8 L/min. Asterisk indicates statistical significance ($p < 0.05$) and NS indicates a lack of statistical significance ($p > 0.05$). Horizontal bars indicate the experimental conditions being compared for statistical significance.

The identification of maxima throughout this study indicates the need to understand synergistic and antagonistic effects between multiple water quality parameters. While salt addition has generally been shown to decrease the stability of oil-in-water in both surfactant-stabilized[192–194] and non-surfactant-stabilized emulsions,[195] other researchers have shown an increase in emulsion stability with the addition of salt. [186,196] As such, we

initially hypothesized that the addition of salt to lower concentrations of a cationic surfactant would increase oil recovery in selective oil permeation. As such, additional experiments were conducted to examine the impact of cationic surfactant concentration in higher salinity solutions (30 g/L NaCl) (**Table 15**). While there was minimal difference between 0 and 10 mg/L CTAB, a substantial decline was observed for 50 mg/L and 100 mg/L CTAB. Deviation from our hypothesis ultimately highlight the need for additional research to characterize mechanisms to better predict the potential for synergistic and antagonistic affects for selective oil permeation.

Table 15: Experimental results suggesting antagonistic effects between salinity and CTAB concentrations. All experiments conducted in Membrane A at an oil concentration of approximately 200 mg/L, transmembrane pressure of 0.69 bar, and influent flow rate of 3.8 L/min.

CTAB, mg/L	Oil Recovery, %	Oil Flux, m^3/m^2-s
0	83.5% ± 0.5%	9.68E-09 ± 1.17E-10
10	84.1% ± 0.4%	9.77E-09 ± 3.30E-10
50	71.2% ± 0.4%	8.36E-09 ± 2.63E-10
100	40.4% ± 0.5%	4.64E-09 ± 2.85E-10

CONCLUSIONS

Experimental results presented in this chapter provide an initial dataset for understanding the impact of common water quality parameters on selective oil permeation. First, this study provided the first data observing the effects of pH, salinity, and cationic surfactants on selective oil permeation performance. Through this, we demonstrated the potential for selective oil permeation to recover oil (without water breakthrough) from oil-disperse solutions under various water quality conditions. Within our experimental system, statistically significant relationships were observed between oil flux and recovery, pH,

salinity, and surfactant concentration (**Table 16**). However, it should be noted that, bench-scale experiments on smaller, easily replaceable membranes without recycle could reduce the potential effects of water quality within the tank changing during the experiments and the potential effects of the changes in the membrane surface over time. Overall, confirmation of the impact of common water quality parameters on selective oil permeation is important for the eventual application of selective oil permeation to produced water treatment.

Table 16: Summary of one-way ANOVA results from experimental results presented in this chapter. Higher F-values indicate higher variability of the group mean variability. P_r values < 0.05 indicate the existence of a statistically significant relationship. Results of Tukey post-hoc tests are available in **Table A3**, **Table A4**, **Table A5**, **Table A6**, and **Table A7**.

	Oil Flux		**Oil Recovery**	
	F-Value	**p_r**	**F-Value**	**p_r**
pH	58.4	7.03E-06	74.3	2.53E-06
Salinity (NaCl)	17.49	1.61E-05	9.5	4.84E-04
Anionic Surfactant (SDS)	137.2	1.49E-09	67.1	9.07E-08
Nonionic Surfactant (Tween80)	153.3	7.85E-10	180.0	3.06E-10
Cationic Surfactant (CTAB)	100.8	1.62e-12	111.8	6.63e-13

Second, throughout the study, we hypothesized that altering emulsion stability by adjusting water quality parameters (pH, salinity, surfactant concentration) would influence coalescence rates – and ultimately impact oil flux and recovery. Experimental results for anionic, nonionic, and cationic surfactants were consistent with this mechanistic framework. Broadly, selective oil permeation performs better in solutions with lower surfactant concentrations (and thus higher interfacial tensions). Interestingly, a statistically

significant increase in oil recovery with certain concentrations of cationic surfactant may offer methods for enhancing process performance. However, further microscopic characterization of both the membrane and the emulsion could elucidate the mechanisms of enhanced electrostatic interactions within the process, assess synergistic and antagonistic effects, and determine the best process optimization methods.

Finally, statistically significant differences in oil recovery were observed for both pH and salinity. However, the observation of an optimum pH and salinity deviated from our initial hypotheses. These results are promising for the application of selective oil permeation to complex, high-salinity wastewaters like produced water. Furthermore, these results are encouraging for the application of selective oil permeation to oil spill cleanup, as the process is effective at salinities relevant to seawater over a broad range of oil concentrations.

ACKNOWLEDGEMENTS

This project was funded by the Kuwait Foundation for the Advancement of Sciences under project code CN17-45EV-01. This material is based upon work supported by the National Science Foundation Graduate Research Fellowship under Grant No. DGE 2137420. I would also like to thank Dr. Sergio Castellanos and SayedMorteza Malaekeh for their help with analysis. I would love to thank Laura Lee for her assistance in the laboratory. Finally, I would love to acknowledge JR Campos and Chris Sanders for their help at the Separations Research Program facility.

Chapter 6: Water Breakthrough during Selective Oil Permeation

ABSTRACT

Selective oil permeation differs from traditional membrane-based oil-water separations by permeating oil (instead of water) through the membrane pores. This approach has two main benefits: minimization of viscous fouling and creation of a high-quality oil permeate stream. However, multiple researchers have observed water permeation during selective oil permeation, undermining one of the main benefits of the selective oil permeation. Both Tirmizi *et al.* and Mercelat *et al.* have suggested that water breakthrough should be avoidable by applying a transmembrane pressure less than the critical entry pressure of water. This chapter builds on their work by investigating selective oil permeation through the lens of the Young-Laplace equation to provide a simple method of estimating critical entry pressure and permeate quality within selective oil permeation. However, the observed deviation between the experimental results and the theoretical estimates highlights the need for further research to resolve this issue. Ultimately, the experimental results may still be able to help future researchers and designers identify appropriate operating conditions and membrane properties to minimize the potential for water breakthrough.

INTRODUCTION

Selective oil permeation is a promising alternative to traditional membrane-based oil-water separations where oil (instead of water) is permeated through a hydrophobic membrane. [19,20,23,179,198] The process exploits the preferential oil wetting of the membrane to minimize viscous fouling[17,18] and generate a high-quality oil permeate.[19,20] Researchers have hypothesized that oil recovery is mechanistically controlled by the approach of the oil droplet to the membrane fiber, coalescence of an oil droplet at the oil film on the membrane surface, permeation of the oil through the membrane surface, and finally release of the oil from the permeate side of the membrane.[22–24,27,28] For oil-disperse solutions, coalescence, oil film formation, and oil film stability are crucial to process performance.[22] Studies have observed evidence of the importance of the oil film at the membrane surface through the extended operation of the membrane with oil recoveries over 95% for over two weeks, often with recovery improving over time.[18,22,157]

While permeating oil through the hydrophobic membrane limits the typical viscous fouling experienced by comparable hydrophilic systems, the process is susceptible to water fouling (*e.g.*, blocking or filling) of the membrane pore, which reduces the efficacy of the process.[22] Furthermore, water may pass through the membrane surface and contaminate the pure oil permeate at elevated transmembrane pressures. Both Tirmizi *et al.* and Mercelat *et al.* have suggested that the Young-Laplace equation may underly water breakthrough in selective oil permeation.[19,22] In particular, Mercelat *et al.* noted that the permeation of oil through the hydrophobic membrane surface requires the application of a transmembrane pressure between the critical entry pressure of the oil (*i.e.*, the applied pressure or pressure differential needed for the oil to enter the membrane pore) and the critical entry pressure of the water. If the transmembrane pressure is below the critical entry pressure of the oil, no separation will occur. Conversely, if the applied transmembrane

pressure is above the critical entry pressure of water, water may contaminate the oil permeate.[22]

Four studies have observed water breakthrough during selective oil permeation. Ezzati *et al.* observed that water content in the permeate increases with transmembrane pressure, residence time, temperature, and emulsifier content in a PTFE membrane with a mean pore size of 0.45 μm.[20] Similarly, Tirmizi *et al.* observed an increase in water content in the permeate with increasing surfactant concentration in both ceramic and polypropylene membranes with mean pore sizes of 0.02, 0.1, and 0.2 μm. Tirmizi *et al.* also found that the observed relationship between measured breakthrough pressure, interfacial tension, and contact angle displayed a relationship consistent with the Young-Laplace equation for a hydrophobic polypropylene membrane (pore diameter of 0.2 μm).[19] Magdich unintentionally induced water breakthrough in a 10% ABSA emulsion with 0.1 M KCl.[23] Finally, Leiknes *et al.* almost exclusively observed water breakthrough when using high emulsifier contents at relatively elevated transmembrane pressures in microporous polyethylene membranes.[158] These four studies have provided a valuable basis for understanding methods to induce water breakthrough (*e.g.*, low interfacial tension, high transmembrane pressure, large diameter pores) as well the phenomena underlying it. However, it is necessary to further explore water permeation to fundamentally understand membrane properties and parameters that may optimize oil recovery and protect the process from water breakthrough.

The experimental study discussed in this chapter focuses on the 3M™ Liqui-Cel™ Extra Flow membrane contactor which was originally designed for liquid-liquid extraction and for immobilizing a hydrocarbon interface within the pore.[199–205] This work predicts the critical entry pressure of water via the Young-Laplace equation and then applies an approach developed by Nazzal *et al.* for oil breakthrough in hydrophilic membranes to

estimate water content in the oil permeate. These theoretical estimates are then compared to experimental results. Finally, this work expands on **Chapter 5** by evaluating the effect of interfacial tension, oil concentration, and transmembrane pressure on oil recovery.

THEORY

Critical Water Entry Pressure

This analysis focuses on water permeation from a water film as shown in **Figure 33**. As noted by both Tirmizi *et al.* and Mercelat *et al.*, the Young-Laplace equation (**Equation 20**) underlies water breakthrough during selective oil permeation.[19,22] Like viscous fouling of the hydrophilic membrane surface by oil, a water film may develop at the hydrophobic membrane surface and limit oil permeation, particularly for oil-water separations from oil-disperse solutions. In this scenario, the critical watery entry pressure (*i.e.*, the theoretical maximum transmembrane pressure for a selective oil permeation system) can be estimated via the Young-Laplace equation as follows:

$$\Delta P_{critical} = -\left(\frac{2\gamma \cos \theta_w}{r_{pore}}\right) \quad (20)$$

Where $\Delta P_{critical}$ is the critical entry pressure (mN/m^2), γ is the interfacial tension (mN/m), θ_w is the contact angle of the water at the solid membrane surface, and r_{pore} is the pore radius (m) as shown in **Figure 33**.[171,206]

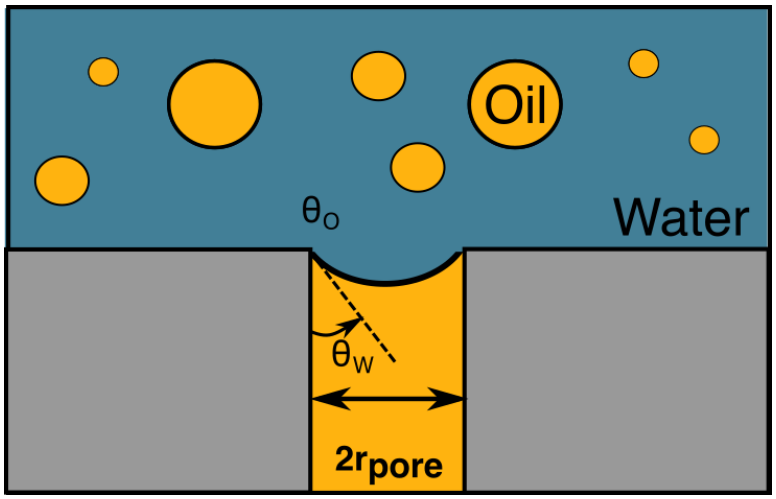

Figure 33: Diagram of water film permeation. Abbreviations and notations are as follows: θ_W is the contact angle of water, and θ_O is the contact angle of oil.

While the Young-Laplace equation serves as the basis for our model, many researchers have investigated scenarios that complicate the accurate prediction of critical entry pressures. For example, previous research investigating organic solvents (*e.g.*, ethanol, acetic acid) has noted that the Young-Laplace equation may prematurely predict permeation through the membrane surface.[171] Moreover, the Young-Laplace Equation's assumption of cylindrical capillaries limits its predictive capabilities for membranes with irregular pore shapes and pore size distributions. Many researchers have endeavored to address these discrepancies through various modifications of the Young-Laplace equation. For example, Purcell (and later Kim and Harriott) considered "doughnut" shaped pores.[171,207,208] Other modifications have included the addition of terms including geometry coefficients or structure angles as well as the utilization of a maximum pore radius within a distribution.[171,172,207] Furthermore, models developed by Nazzal *et al.* and Salama provide insight into more complex variants like water droplet (or droplets) becoming pinned at the membrane pore openings.[183,209,210] Salama also demonstrated how the

dynamics of water droplet pinning and permeation can further confound prediction of breakthrough.[209] Due to the wide variety of scenarios described in these variations on the Young-Laplace equation, it is necessary to experimentally confirm the accuracy of critical entry pressures calculated via any of these methods.

Water Content in Oil Permeate

This work expands on an approach developed by Nazzal *et al.* for oil breakthrough in hydrophilic membranes to estimate water content in the oil permeate for selective oil permeation. In this study, permeate quality is estimated by considering a mass balance around the membrane and the fraction of membrane surface for which the critical entry pressure is being exceeded (*i.e.*, the fraction of the membrane surface that is theoretically permeating water over oil). For each pore size distribution range (**Figure 9**), the critical entry pressure of a specific pore size ($\Delta P_{critical,i}$) within the distribution (r_i) can be calculated using **Equation 20**. For each pore size range, if $\Delta P_{critical,i}$ is greater than the applied transmembrane pressure, then no water breakthrough occurs. However, if $\Delta P_{critical,i}$ is less than the applied transmembrane pressure, we hypothesize that water flow through that specific pore size can be calculated using the Blake-Kozeny viscosity component of the Ergun equation as follows:

$$J_{water,i} = \frac{\Delta P_{applied} \times d_{pore,i}^2 \times \left(\frac{1-\varepsilon}{\varepsilon}\right)^{\frac{2}{3}} \times \varepsilon^3}{150 \times L \times \mu \times (1-\varepsilon)^2} \quad (21)$$

Where $J_{water,i}$ is the pure water flux (m^3/m^2-s), $d_{pore,i}$ is the specific pore diameter (m), ε is the porosity of the membrane, L is the membrane wall thickness (m), and μ is the water viscosity (Pa-s). Then, by considering the fraction of the membrane occupied by pores of this specific size, the water flow rate can then be calculated as follows:

$$Q_{water,i} = J_{water,i} \times A \times \chi_i \tag{22}$$

Where $Q_{i,water}$ is the water flow rate (m^3/s), A is the membrane area (m^2), and χ_i is the fraction of the membrane surface area occupied by the specific pore size that is theoretically permeating water over oil. The summation of these water flow rates ($Q_{i,water}$) over the full pore size distribution of the model provides an estimate of the total potential water flow rate into the permeate. However, particularly for oil-continuous solutions, it is necessary to verify that the quantity of water that theoretically could permeate through the membrane does not exceed the inlet water flow rate to the membrane module.

The permeated water (Q_{water}) can then be compared to the theoretical oil flux through the membrane. Mercelat *et al.* described oil flux as a fraction of pure oil flux that is related to the fractional wetted surface area of the membrane (a_e/a_t) itself as follows:

$$J_{O/W} = J_{Oil} \cdot \frac{a_e}{a_t} \tag{23}$$

Where $J_{o/w}$ is the oil flux from oil-water mixtures (m^3/m^2-s) and J_{oil} is the pure oil flux (m^3/m^2-s).[22] Pure oil flux (J_{oil}) can be described using a variant of **Equation 21**. However, $J_{o/w}$ must be reconsidered as the average pore size of the pores within the membrane for which water breakthrough does not occur (*i.e.*, $\Delta P_{critical,i} > \Delta P$). The fractional effective membrane surface area (a_e/a_t) is hypothesized to be linked to the actual surface area of the oil film on the fibers. The following model can then be used to predict the wetted surface area of the membrane by considering the competition between coalescence and eventual permeation of an oil droplet in the context of saturation:

$$\frac{a_e}{a_t} = \frac{1.65\times10^{12}\cdot C_{oil}\cdot\mu\cdot {P_T}^{-1.6}\cdot v^{0.3}}{1 + 2.66\times10^{15}\cdot C_{oil}\cdot\mu^{1.1}\cdot {P_T}^{-2.1}\cdot v^{0.4}} \tag{24}$$

Where C_{oil} is the volume fraction of oil and the liquid velocity, v (m/s), is defined as $v = \frac{Q_{shell}}{\frac{\pi}{4} d_{mod}^2}$. Oil flux can then be converted to the oil flow rate using the membrane surface area.

$$Q_{oil} = J_{o/w} \times A \times (1 - \sum \chi_{i,water-wet}) \quad (25)$$

Finally, a simple mass balance can be applied to calculate oil content of the permeate:

$$Permeate\ Quality\ (\%) = \left(1 - \frac{Q_{water}}{Q_{water}+Q_{oil}}\right) \times 100 \quad (26)$$

EXPERIMENTAL METHODS

Solution Characteristics

This study utilized three solutions with varying concentrations of Isopropyl Alcohol (IPA) in Millipore water to yield interfacial tensions ranging from approximately 10 to 50 mN/m. The interfacial tension of the oil-water system was characterized via the pendant drop method using a precision goniometer (**Figure 34**). The viscosity of IPA-water solutions is shown in **Table 17**.[211] The viscosity and density of the oil were characterized via an NDJ-5S Digital Rotational Viscometer and a DE40 Density Meter, respectively. Isopar M was determined to have a density of 0.78 g/cm^3 and a viscosity of 3.5 cP at 25 degrees Celsius. Permeate quality was analyzed for water-in-oil content via coulometric Karl Fischer titration using a Mettler Toledo C20 Coulometric Karl Fischer Titrator using Hydranal^{TM} Coulomat Oil.

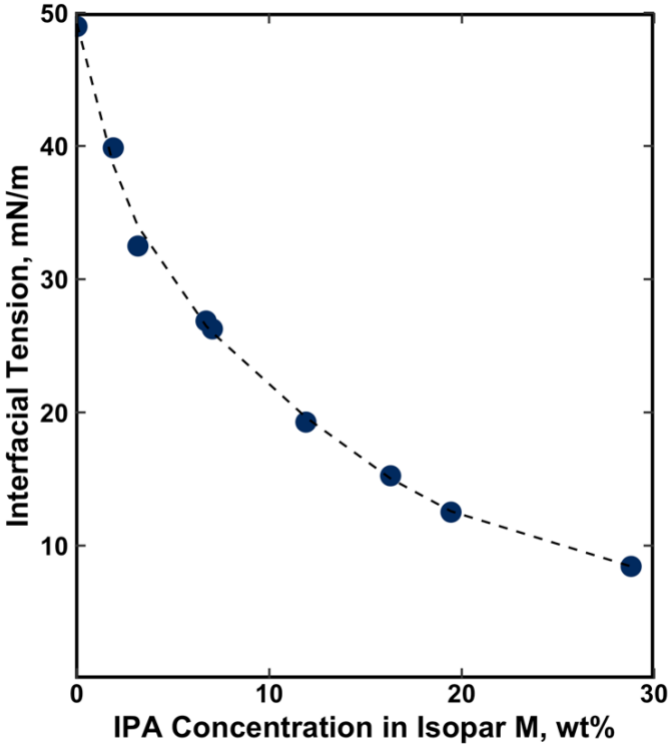

Figure 34: Interfacial tension in a distilled water-IPA-Isopar M system at 23°C provided by Jarett Spinhirne.

Table 17: Viscosity of Isopropyl Alcohol-Water Mixtures at 25°C.[211]

Isopropyl Alcohol, wt%	Viscosity, cP
0	0.90
10	1.35
20	1.84
30	2.23

Experimental Approach

All experiments were conducted using the membrane system as shown in **Figure 35**. Two hollow fiber membranes (3M™ Liqui-Cel™ Extra Flow Membrane Contactors) of varying size and surface area were utilized to separate oil-water mixtures. The membranes contained X50 fibers, which have a reported contact angle of 120°, porosity of 40%, nominal pore diameter of 0.047 μm, and a thickness of 40 μm.[22,182] All reported

permeate quality and oil recovery data were taken from the primary membrane, Membrane A (Diameter: 6.4 cm, Length: 20.3 cm, Surface Area: 1.4 m^2). Membrane A was designed to achieve less than 100% oil recovery to enable quantitative evaluation. In contrast, the guard membrane, Membrane B (Diameter: 10.2 cm, Length: 71.1 cm, Surface Area: 20 m^2), was sized to achieve 100% oil recovery to allow for recycle of the system for continuous operation by removing all of the oil not captured by Membrane A.[187]

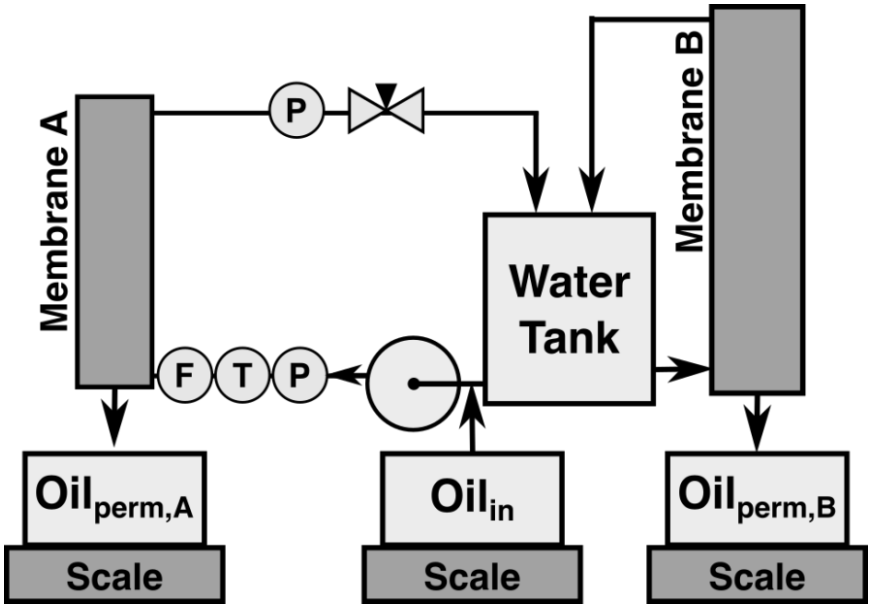

Figure 35: Process flow diagram of experimental apparatus. Membrane A (Dimensions: 6.4 cm x 20.3 cm, Surface Area: 1.4 m^2) serves as the primary membrane while Membrane B (Dimensions: 10.2 cm x 71.1 cm, Surface Area: 20 m^2) serves as the guard membrane. Abbreviations are as follows: pressure transmitter (P), temperature transmitter (T), flow transmitter (F), injected oil (Oil_{in}), oil permeate from Membrane A ($Oil_{perm,A}$), and oil permeate from Membrane B ($Oil_{perm,B}$).

A known quantity of Isopar M was injected via peristaltic pump into the influent water stream upstream of a high-shear pump to generate the oil-water emulsion. The water flow rate and transmembrane pressure of Membrane A were adjusted using either the

variable speed drive on the high shear pump or the needle valve downstream of Membrane A. Shell-side pressures were monitored continuously via Rosemount pressure transmitters. The emulsion entered Membrane A through the bottom shell-side port. Oil permeated through the hollow fibers.

Injected and permeated oil were quantified gravimetrically via an Arlyn D-620T weigh scale (reported resolution of 1.0 gram). The experimental system generally reached steady state within a few hours. As noted in previous chapters, minimal relationship was observed between experimental duration and oil recovery once steady state was reached. Experiments ranged in duration from 9.5 to 105 hours but were generally approximately 12 to 24 hours. Oil flux and oil recovery in Membrane A were calculated as a four-hour average as follows:

$$Oil\ Flux\ (\frac{m^3}{m^2-s}) = \frac{\dot{m}_{permeate}}{\rho_{oil} \times A_{membrane}} \quad (27)$$

$$Oil\ Recovery\ (\%) = \frac{\dot{m}_{permeate}}{\dot{m}_{injected}} \cdot 100\% \quad (28)$$

Where $\dot{m}_{permeate}$ was the mass flow of the permeate (g/s), $\dot{m}_{injected}$ was the mass flow of injected oil (g/s), ρ_{oil} was the density of the oil (g/cm^3), and $A_{membrane}$ was the surface area of the membrane (m^2). All instruments were connected to a DeltaV data acquisition system for real-time data collection. A summary of the experiments examining water breakthrough in selective oil permeation is presented in **Table 18**.

Table 18: Summary of experimental conditions examined during investigation. All experiments conducted at an influent flow rate of 3.8 L/min in Membrane A using Isopar M. Abbreviations are as follows: Influent Oil Concentration ($C_{oil,in}$), Isopropyl Alcohol (IPA), and Transmembrane Pressure (TMP).

Varied Parameters	**IPA (wt%)**	**$C_{oil,in}$ (mg/L)**	**$\Delta P/P_{critical,nominal}$[1]**
IPA%	0, 10, 20, 30	275	TMP = 1.4 bar
TMP and C_{oil}[2]	0, 5, 25	50, 500	0.01, 0.05, 0.1, 0.2, 0.3, 0.4, 0.5, 0.6, 0.7, 0.8, 0.9, 1.0

[1] $\Delta P/P_{critical,nominal}$ used when achievable within the design limitations of the membrane (TMP_{max} = ~4.2 bar).[187] Similarly, operation was limited at low transmembrane pressures by the experimental system due to the differential pressure across the membrane module. $P_{critical,nominal}$ corresponds to the critical entry pressure calculated using **Equation 20** for the nominal pore diameter (0.047 μm).

[2] For experiments of $\Delta P/P_{critical,nominal}$ greater than 0.5 only oil concentrations of 500 mg/L were used.

RESULTS AND DISCUSSION

Theoretical Critical Pressure of Water

Membranes with high hydrophobicity, low surface energy, small mean pore size, and a narrow pore size distribution should have elevated liquid entry pressures.[212] When paired with conducive operating conditions (*e.g.*, higher interfacial tension, lower transmembrane pressure), consideration of these parameters should limit the potential for water breakthrough.

The ability of the membrane to reject the non-wetting phase decreases with increasing membrane pore diameter (**Figure 36**).[171] As the membrane contains a range of pore diameters, we hypothesize that operational transmembrane pressures cannot exceed the critical entry pressure calculated for the maximum pore diameter. For example, this analysis indicates that water breakthrough for this particular membrane system is likely to begin at transmembrane pressures between approximately 1.7 and 8.3 bar for interfacial

tensions ranging from 10 to 50 mN/m when considering the maximum reported pore diameter.[22]

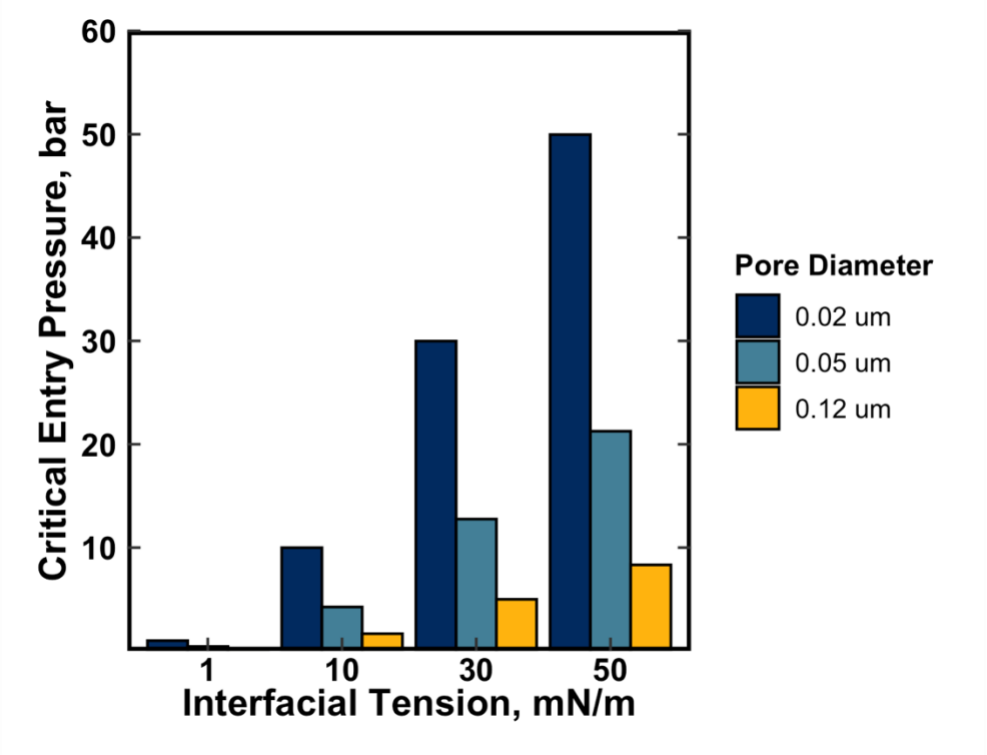

Figure 36: Estimated critical entry pressures using **Equation 20**.

As predicted by the Young-Laplace equation, critical entry pressures decrease with decreasing interfacial tension (**Figure 36**). This relationship is consistent with water breakthrough in the selective oil permeation literature. Tirmizi *et al.* observed increased water content in the permeate with increasing surfactant concentration and decreasing interfacial tension (28 ppm, 30 ppm, and 4.1% for 0, 0.5, and 20 kg/m^3 ECA 5025 in $C_{14}H_{30}$).[19] However, less systematic studies have also presented evidence of this phenomenon. For example, Magdich observed water breakthrough in solutions containing 1% PetMix#9 and 1% ABSA.[23] Leiknes *et al.* noted that selective oil permeation behaved as a UF membrane when in the presence of cutting fluids with higher emulsifier contents

(~20–30%).[158] Unpublished work in the same experimental system used in this work at the Separations Research Program at the University of Texas at Austin noted water breakthrough at elevated transmembrane pressures (> 2 bar) for emulsions with low interfacial tensions (< 2 mN/m). From these studies, it is evident that water breakthrough occurs in selective oil permeation for low interfacial tension systems when non-conducive transmembrane pressures are applied.

Permeate quality was then predicted for interfacial tensions ranging from 1 mN/m to 50 mN/m (**Figure 37**). Like Nazzal *et al.,* breakthrough will be considered in the context of the applied transmembrane pressure (ΔP) to the critical entry pressure of the nominal pore size diameter ($P_{critical,nominal}$) in the term $\Delta P/P_{critical,nominal}$. **Figure 37A** shows the sudden step change we would anticipate for all interfacial tensions measured at a $\Delta P/P_{critical,nominal}$ of approximately 0.4. The outlined method predicts water breakthrough at a $\Delta P/P_{critical,nominal}$ of 0.4 instead of 1 due to predicted breakthrough in pores larger than the nominal (> 0.047 μm). Consequently, it should be noted that the predicted step change at $\Delta P/P_{critical,nominal}$ of approximately 0.4 is a function of the pore size distribution of the specific membrane examined in this study. As the $\Delta P/P_{critical,nominal}$ approaches unity, the predicted oil content in the permeate declines precipitously for the 500 mg/L influent oil concentration case shown in **Figure 37A**. However, we anticipate that this behavior would be less stark for oil-continuous solutions, as the quantity of oil permeating the membrane would be substantially higher.

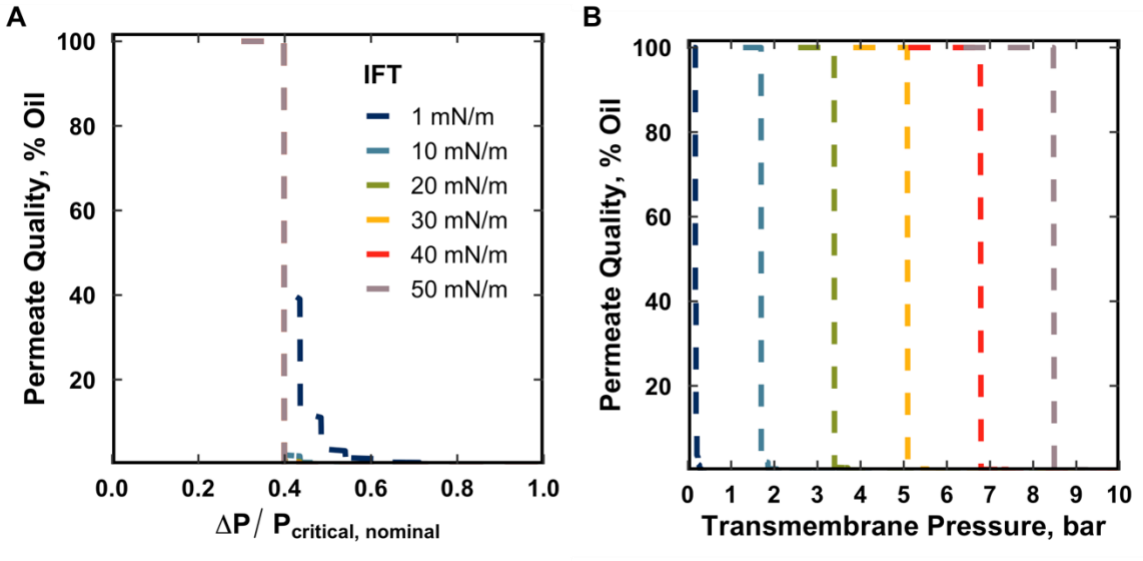

Figure 37: Example of predicted permeate water quality at a variety of interfacial tensions at influent oil concentration of 500 mg/L. Abbreviations are as follows: Interfacial Tension (IFT).

Figure 37B expands on **Figure 37A** by showing the predicted water quality in terms of applied transmembrane pressures instead of $\Delta P/P_{critical,nominal}$. The sudden step change in predictions of water content in the oil permeate prediction is consistent with observations by Tirmizi *et al.* for water content in the permeate with decreasing interfacial tension.[19] Through these theoretical results, we can begin to understand how the upper limit for applied transmembrane pressure in selective oil permeation may vary based on both membrane (*e.g.*, nominal pore size, width of pore size distribution) and solution characteristics (*e.g.*, interfacial tension). These theoretical results were also utilized to direct experimentation for ratios of transmembrane pressure to critical entry pressure ($\Delta P/P_{critical,nominal}$).

Permeate Quality and Model Comparison

For the initial planned experimental conditions examined in this chapter ($\Delta P/P_{critical,nominal}$ = 0.01–0.5), no visible free water was observed in the oil permeate (**Figure 40**). Two experiments ($\Delta P/P_{critical,nominal}$ = 0.3 and 0.4 and 10 mN/m) exhibited water-in-oil concentrations greater than 100 mg/L H_2O. However, no visible free water was observed in either experiment. To combat this, the examined range of $\Delta P/P_{critical,nominal}$ was extended to $\Delta P/P_{critical,nominal}$ values up to 1.0 for oil concentrations of 500 mg/L. However, in only one experimental condition ($\Delta P/P_{critical,nominal}$ = 0.9 and 10 mN/m) within this extended set of experiments exhibited visible free water breakthrough, which corresponded to a water content in the oil permeate of approximately 2,400 mg/L H_2O. The observation of water permeation as $\Delta P/P_{critical,nominal}$ approached unity is consistent with water breakthrough in the nominal pore diameter, but not consistent with our outlined approach that considered the pore size distribution of the membrane.

While the experimental results demonstrate superior membrane performance than was anticipated by the Young-Laplace equation, it draws into question the validity of directly applying the Young-Laplace equation to estimate water breakthrough in the membrane used in this work. Multiple factors may contribute to this deviation. For example, returning to **Equation 20**, water breakthrough is a function of the size and distribution of membrane pore radii, the contact angle of the water, and the interfacial tension of the system. Changes in any of these parameters would substantially influence the validity of the model results. Furthermore, this experimental study focuses on a 3M™ Liqui-Cel™ Extra Flow membrane contactor which was originally designed for liquid-liquid extraction and for immobilizing a hydrocarbon interface within the pore.[199–205] Additionally, these microporous membranes do not have distinct pore channels, which

undermines many of the geometric assumptions present in **Equation 20**. While this study used the Young-Laplace equation to provide a simple method of estimating water breakthrough, the experimental results suggest that it may be necessary to use more complex models such as those proposed by Nazzal *et al.* or Purcell. Validation of the critical entry pressure at the bench-scale may then allow for enhanced prediction and protection of permeate quality.

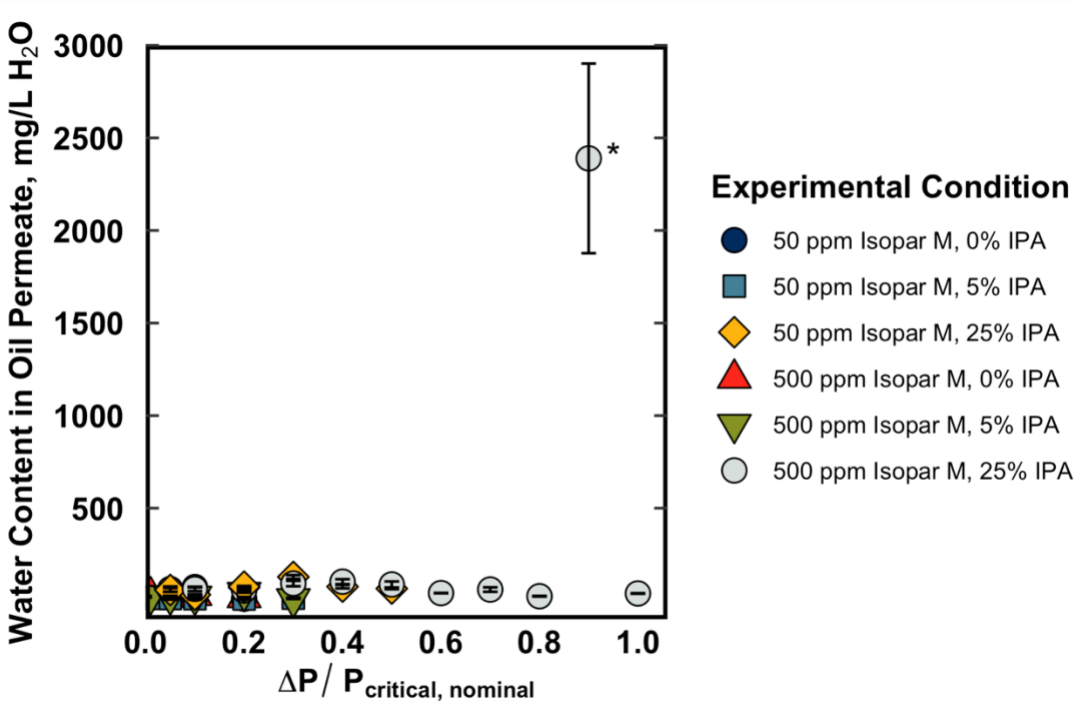

Figure 38: Deviation between influent and effluent permeate quality for experimental conditions examined. Free water only observed in experiment noted with asterisk in figure.

Finally, other phenomena contribute to water breakthrough in selective oil permeation. For example, mechanical failures in certain components within the membrane system (*e.g.*, gaskets) could have allowed for water to bypass the membrane. This likely

occurred in one failed experiment in which water breakthrough was observed in Membrane B (Membrane A: C_{oil} = 500 mg/L, P_T = 3.4 bar, Q = 3.8 L/min, IFT = 10 mN/m) when the transmembrane pressure in the Membrane B module averaged only approximately 0.4 bar. The lack of relationship between our estimates and actual results in Membrane A or Membrane B indicates that, while the Young Laplace equation may underly this phenomenon, geometric complications and other phenomenon may influence water breakthrough in our system. However, the Young-Laplace equation may still be able to provide a conservative estimate for the maximum transmembrane pressure for selective oil permeation when designing systems using 3M™ Liqui-Cel™ Extra Flow membrane contactors.

Oil Recovery

For oil-disperse solutions, approach and coalescence are often the operative mechanisms controlling mass transfer (See **Chapter 4**).[22] Yet, coalescence rates (*i.e.*, emulsions stability) are impacted by both interfacial tension and continuous phase viscosity (See **Chapter 5**). For example, lowering the interfacial tension is anticipated to increase the interfacial energy and interfacial area, thereby increasing the emulsion stability.[58] An increase in the deformability of the oil droplet may decrease coalescence rates ultimately reducing oil recovery and flux.[159] Similarly, increasing the viscosity of the continuous phase (**Table 17**), may slow continuous-phase film draining during coalescence, thereby decreasing the rate of coalescence. Again, we hypothesize that decreasing the rate of coalescence would reduce oil recovery and flux in selective oil permeation.

Experimental trends observed in this study were consistent with the hypothesized understanding of mechanistic competition in selective oil permeation. As anticipated, oil recovery decreased with decreasing interfacial tension, increasing continuous-phase

viscosity, and increasing transmembrane pressure for the oil-disperse solutions examined in this work (**Figure 39**). For example, at an influent concentration of 275 mg/L and transmembrane pressure of 1.4 bar, oil recoveries decreased from 33.2% to 3.8% when the IPA concentration was increased from 0 wt% IPA to 30 wt% IPA. These experimental results are consistent with those shown in **Chapter 5** and in the literature, as Magdich and Tirmizi *et al.* also observed a decrease in oil flux with decreasing interfacial tension.[19,23]

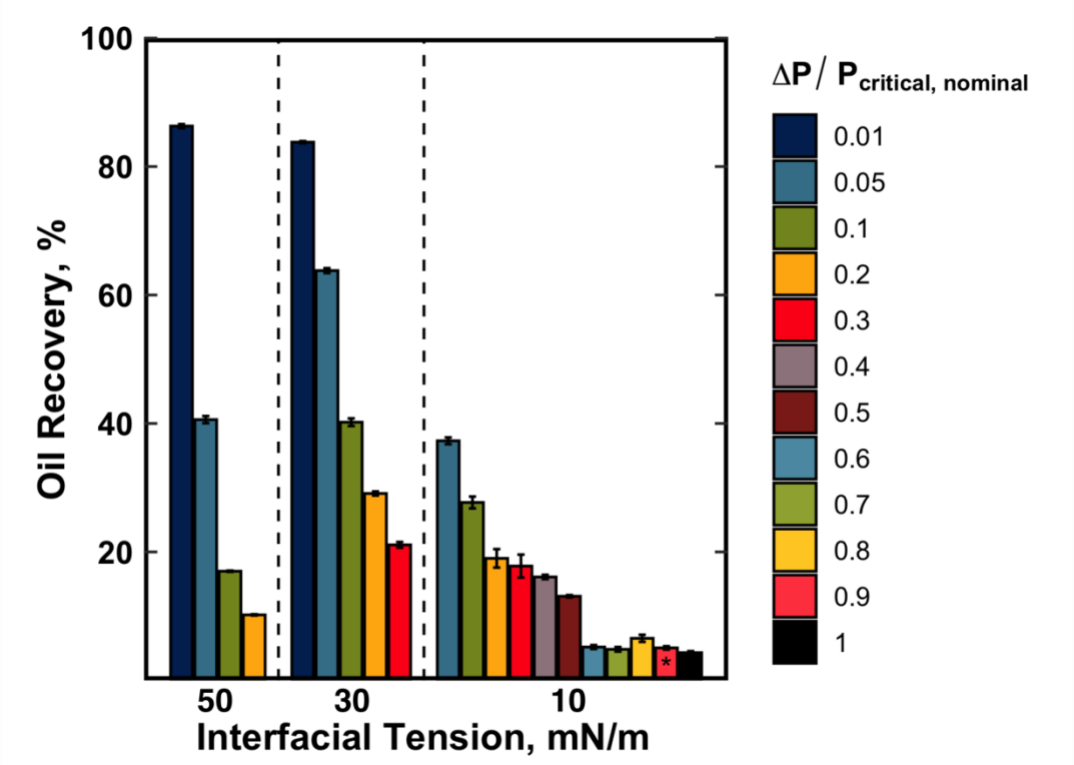

Figure 39: Relationship between oil recovery and $\Delta P/P_{critical}$. All data from Membrane A at an influent oil concentration of 500 mg/L and an influent flow rate of 3.8 L/min. Similar trends were observed for influent oil concentrations of 50 mg/L as shown in **Table A8**. Asterisk notes experiment that experienced visible water breakthrough.

Furthermore, competition between coalescence and permeation is hypothesized to create an inverse relationship between oil recovery and transmembrane pressure for oil-disperse solutions.[22] This phenomenon has been attributed to the Young-Laplace equation and the permeation rate exceeding the coalescence rate, undermining the long-term stability of the oil film both on the membrane surface and potentially within the membrane pore.[18,22] Consequently, a decrease in interfacial tension may also increase the likelihood of water droplets blocking the pore openings and, consequently, reducing both the fractional wetted surface area of the membrane as well as the membrane's permeation capability. We hypothesize that pore blockage would be exacerbated as $\Delta P / P_{critical,nominal}$ approached unity. This hypothesis is supported by the relatively consistent relationship between $\Delta P / P_{critical,nominal}$ and oil recovery across all experimental conditions examined (**Figure 40**). However, it should be noted that for oil-disperse solutions the behavior observed in **Figure 40** further highlights the necessity of operating selective oil permeation systems at a low transmembrane pressure as it both increases the oil recovery and reduces the likelihood of water breakthrough.

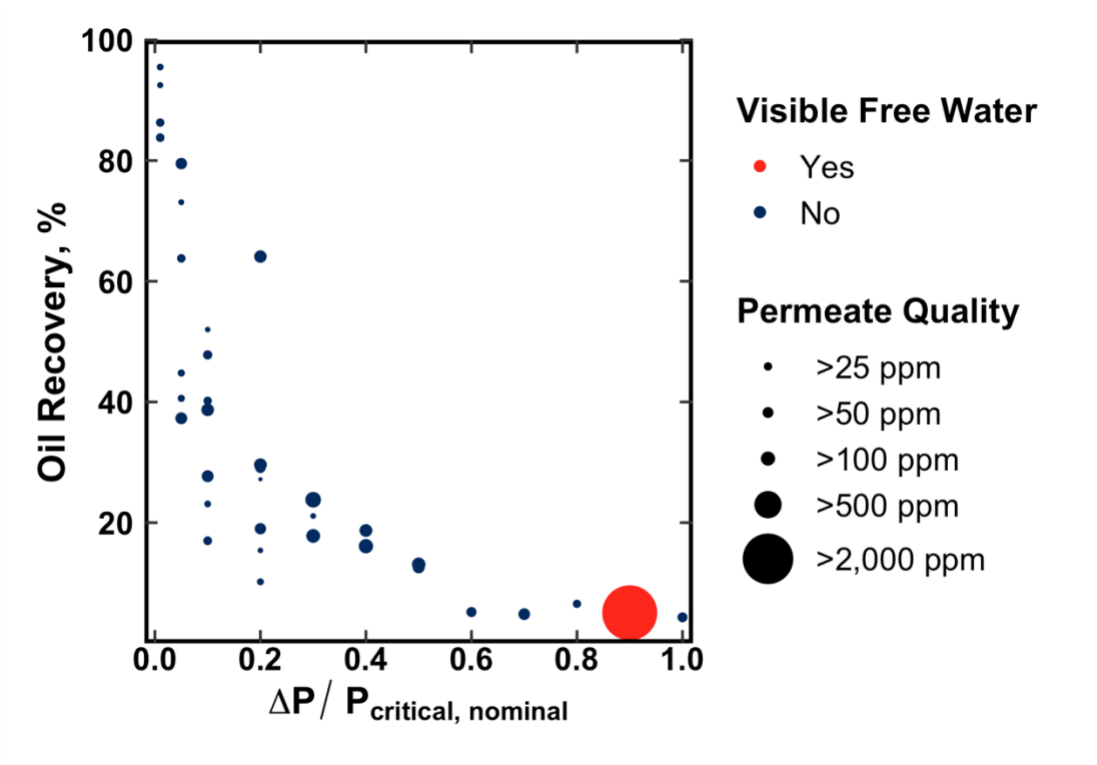

Figure 40: The relationship between permeate quality, oil recovery, and $\Delta P / P_{critical,nominal}$ over experimental conditions examined in Membrane A. Visible free water noted in red. Karl Fischer Titration results with water content in permeate (*i.e.,* permeate quality) are presented in **Table A8**.

CONCLUSION

As research continues to pursue novel oil-water separation methods that alter and exploit surface wetting to improve efficiency, it is necessary to consider how the dynamic nature of oil coalescence and oil films at the membrane surface may influence process performance (*i.e.*, oil recovery, oil flux, permeate quality). Competition between interfacial and transport phenomena may influence the attachment of water droplets and the formation of films. Similarly, the dynamic and complicated nature of mechanisms associated with oil-droplet coalescence may influence the formation and long-term stability of oil (and water) films at the membrane surface. Ultimately, additional work is necessary to

understand the complex and dynamic nature of competitive permeation of oil over water. Thus, this study simply offers a first approximation of addressing the goal of characterizing the competitive permeation of oil and water during selective oil permeation. However, the lack of agreement between the Young-Laplace equation and experimental results suggests that additional research is required to resolve this outstanding question in the literature.

The experimental results presented in this study indicate relationships between solution characteristics, operating conditions, and process performance. As anticipated, oil recovery and flux declined precipitously with increasing transmembrane pressure for oil-disperse solutions. Further, oil recovery decreased with decreasing interfacial tension. Importantly, water breakthrough was least likely in oil-disperse solutions at the conditions most favorable to high oil recovery (*i.e.*, low transmembrane pressure). This result reinforces the potential for selective oil permeation to be an efficient recovery technique for high-quality oil permeate from oil-disperse solutions. It also invites the question of using selective oil permeation to remove trace, non-dissolved water in oils via selective oil permeation. However, further research would be necessary to investigate the efficacy of oil-continuous solutions and the relationships between interfacial tension, permeate quality, and oil recovery.

Ultimately, this study suggests that water breakthrough is avoidable through thoughtful selection of membrane characteristics and operating conditions – specifically within solutions with low oil concentrations ($\leq$ 500 mg/L). Luckily, these conditions are also often those (*e.g.*, low transmembrane pressure) that maximize oil recovery. The lack of tradeoff between permeate quality and oil recovery for oil-disperse solutions highlights the applicability of selective oil permeation as a secondary or tertiary oil-water separation process.

ACKNOWLEDGEMENTS

This project was funded by the Kuwait Foundation for the Advancement of Sciences under project code CN17-45EV-01. This material is based upon work supported by the National Science Foundation Graduate Research Fellowship under Grant No. DGE 2137420. I would like to acknowledge Dr. Aurore Mercelat for an illuminating conversation that helped inspire this work. I would also like to thank You A. Wu, Marshall Allen, and Dr. Zak Page for their assistance in the analytical work. Finally, I would love to acknowledge JR Campos and Chris Sanders for their help at the Separations Research Program facility.

Chapter 7: Oil Recovery from Produced Water via Selective Oil Permeation

Carolyn M. Cooper[1], You Wu[1], Sarah Alshawish[2], Abdalrahman Alsulaili[2], Lynn E. Katz[1], Kerry A. Kinney[1], and A. Frank Seibert[1]

[1] The University of Texas at Austin, Austin, Texas, USA
[2] Kuwait University, Safat, Kuwait.

Previously published in the Conference Proceedings of the 2022 American Institute of Chemical Engineers Annual Meeting

ABSTRACT

High-efficiency oil-water separations are crucial to the success of treatment trains for the beneficial reuse of industrial wastewaters like produced water. While traditional membrane-based separations can achieve low minimum droplet removal and high oil removals, they often experience rapid viscous fouling of the membrane surface. Selective oil permeation is a promising alternate membrane-based approach in which oil permeates through the membrane surface instead of water. The process differs from traditional membrane-based oil-water separations by generating a high-quality oil permeate stream and minimizing viscous fouling by exploiting the preferential wetting of the membrane surface. Our previous research has observed encouraging results with synthetic oil-water emulsions over a range of operating parameters and solution characteristics. These studies have provided mechanistic insight and a fundamental understanding of the process. Yet, few studies have investigated selective oil permeation utilizing real industrial wastewaters. In this study, we apply the fundamental insights that we have gained using model systems to understand and optimize system performance with produced water. In doing so, we enhance our understanding of the opportunity space for selective oil permeation.

INTRODUCTION

Complications associated with the interplay between produced water quality,[1,2] quantity,[30] and treatment[2,54] have been discussed in numerous studies.[35,36] In the United States, these factors have resulted in the reuse of approximately 8% of produced water outside the oil and gas industry, versus the subsurface reinjection of approximately 90% of produced water.[30] Researchers have concluded that fit-for-purpose treatment that thoughtfully considers both water quality and end-use specific risks is necessary to increase the beneficial reuse of produced water. Further, to mitigate toxicity concerns in higher-order reuse (*e.g.*, streamflow augmentation, municipal reuse), advanced treatment processes (*e.g.*, advanced oxidation processes, membranes) may be required, often without confirmation that the toxicity has been reduced.[35,36] Moreover, advanced treatment often requires high-efficiency pretreatment to mitigate fouling and achieve high levels of efficacy.

Nearly all produced water management requires oil-water separations. Primary oil-water separation methods (*e.g.*, API separators) traditionally encompass gravity separation of free oil ($\geq$ 150 μm). Secondary oil-water separation approaches (*e.g.*, dissolved air filtration, hydrocyclones) target dispersed oil (> 50 μm) using chemical or centrifugal methods. Tertiary oil-water separation methods (*e.g.*, media filtration) remove emulsified oils ($\leq$ 50 μm) via either adsorption or filtration.[4,6] Researchers have also explored the application of membranes, where water permeates through the membrane, to remove emulsified oils. However, as with many membrane-based approaches, membrane-based oil-water separations often suffer from oil fouling, particularly with produced water.[110,114]

Selective oil permeation is a promising membrane-based oil-water separations technology that permeates oil (instead of water) through a hydrophobic membrane.[19,20,22,23,26,28,158] Selective oil permeation provides inherent advantages over

traditional membrane-based oil-water separations by exploiting the preferential wetting of the membrane surface, minimizing viscous fouling, and generating a high-quality oil permeate stream. Researchers have investigated the process using various insoluble oils to determine the relationship between operating parameters, solution characteristics, and process performance.[19,20,22,23,26] These studies have also developed our mechanistic understanding of the process where oil flux is controlled by the approach and coalescence of the oil droplet on the membrane surface, permeation of the oil through the membrane surface, and release of the oil from the permeate side of the membrane.[22–24,27,28]

However, these fundamental studies have not addressed two factors key to produced water treatment. First, produced water, like many other wastewaters, contains relatively low oil concentrations (2–565 mg/L) that must be reduced to less than 10–35 mg/L for beneficial reuse.[2,54] Minimal work has investigated oil recovery via selective oil permeation at concentrations less than 1%.[22,28] Second, no studies have detailed the performance of selective oil permeation with real produced waters. Minimal work has investigated selective oil permeation performance using real wastewater. While Seibert presented successful oil recovery performance data from concentrated non-flocculated lysed algae in a microporous polypropylene membrane,[157] Leiknes *et al.* observed water breakthrough in a microporous polyethylene membrane when recovering oil from industrial cutting fluids with high emulsifying agent concentrations (~20–30%).[158] Thus, further work is necessary to understand the applicability of selective oil permeation to produced water treatment.

This study will investigate the efficacy of selective oil permeation separations in produced water by characterizing the produced water, investigating the efficacy of selective oil permeation over a range of operating conditions, and providing a comparison of these results to the literature and an existing mass transfer model. Through this, we will

provide an enhanced understanding of the broader applicability of selective oil permeation to the treatment of produced water.

THEORY

Mercelat *et al.* proposed the following model for oil flux in selective oil permeation. The model views oil flux as a fraction of pure oil flux due to changes in the wetted surface area of the membrane:

$$J_{O/W} = J_{Oil} \cdot \frac{a_e}{a_t} \tag{29}$$

Where $J_{o/w}$ is oil flux from oil-water mixtures (m^3/m^2-s), J_{oil} is the pure oil flux (m^3/m^2-s), and a_e/a_t is the fractional effective membrane surface area fraction. Pure oil flux (J_{oil}) can then be described by the Blake-Kozeny viscosity component of the Ergun equation:

$$J_{Oil} = \frac{P_T \times d_{pore}^2 \times \left(\frac{1-\varepsilon}{\varepsilon}\right)^{\frac{2}{3}} \times \varepsilon^3}{150 \times L \times \mu \times (1-\varepsilon)^2} \tag{30}$$

Where J_{oil} is the pure oil flux (m^3/m^2-s), P_T is the applied transmembrane pressure (Pa), d_{pore} is the average pore diameter (m), ε is the porosity of the membrane, L is the membrane wall thickness (m), and μ is the oil viscosity (Pa-s). The fractional effective membrane surface area is calculated via the following semi-empirical model:

$$\frac{a_e}{a_t} = \frac{1.65 \times 10^{12} \cdot C_{oil} \cdot \mu \cdot {P_T}^{-1.6} \cdot v^{0.3}}{1 + 2.66 \times 10^{15} \cdot C_{oil} \cdot \mu^{1.1} \cdot {P_T}^{-2.1} \cdot v^{0.4}} \tag{31}$$

Where C_{oil} is the volume fraction of oil and the liquid velocity, v (m/s), is defined as the flow rate divided by the cross-sectional area of the module.

METHODS

Solution Characteristics

This study utilized de-oiled produced water from the Eagle Ford Basin in the United States. TSS and TDS were measured via ASTM D5907–18. Inductively coupled plasma mass spectrometry (Thermo Scientific ICAP TQ ICP-MS) were used to characterize cations while anions were characterized via ion chromatography conducted at the Lower Colorado River Authority Lab. Total petroleum hydrocarbons (TPH) were quantified via the Texas natural Resource Conservation Commission TNRCC Method 1005 using gas chromatography with flame ionization detection on an Agilent 6890. TOC was quantified via a Shimadzu TOC-L.

Isopar M served as a synthetic oil throughout the experiments. An NDJ-5S Digital Rotational Viscometer and a Mettler Toledo DE40 Density Meter characterized oil viscosity (3.5 cP) and density (0.78 g/cm^3) at 25 degrees Celsius, respectively. An inline JM Canty particle analyzer determined the emulsion droplet size distribution. The mean particle diameter was 5.7 μm. No free water was observed in the oil permeate during the study.

Membrane System and Operating Procedure

A process flow diagram of the experimental apparatus is shown in **Figure 41**. All reported recoveries in the following sections are from the primary microporous polypropylene hollow fiber membrane, Membrane A (3M™ Liqui-Cel™ Extra Flow Membrane Contactor: Diameter: 6.4 cm, Length: 20.3 cm, Surface Area: 1.4 m^2). The guard membrane, Membrane B (3M™ Liqui-Cel™ Extra Flow Membrane Contactor: Diameter: 10.2 cm, Length: 71.1 cm, Surface Area: 20 m^2) allowed for recycle of the system for continuous operation. Both Membrane A and Membrane B contained

commercially available X50 fibers, which have a reported porosity of 40%, a thickness of 40 μm, pore diameter of 0.05 μm, and a water contact angle of 120°.[22] Membrane A was pre-conditioned to wet the membrane pores and initialize the oil-wetted surface area by flowing pure Isopar M through the membrane for 24 hours.

A peristaltic pump injected a known mass of Isopar M into the suction of a high-shear pump. The high-shear pump generated the oil-water emulsion and moved the emulsion to the bottom shell-side port of the primary membrane, Membrane A. Effluent water from the shell-side of Membrane A returned to the feed tank. Membrane B received water from the feed tank and maintained the purity of the feed tank.

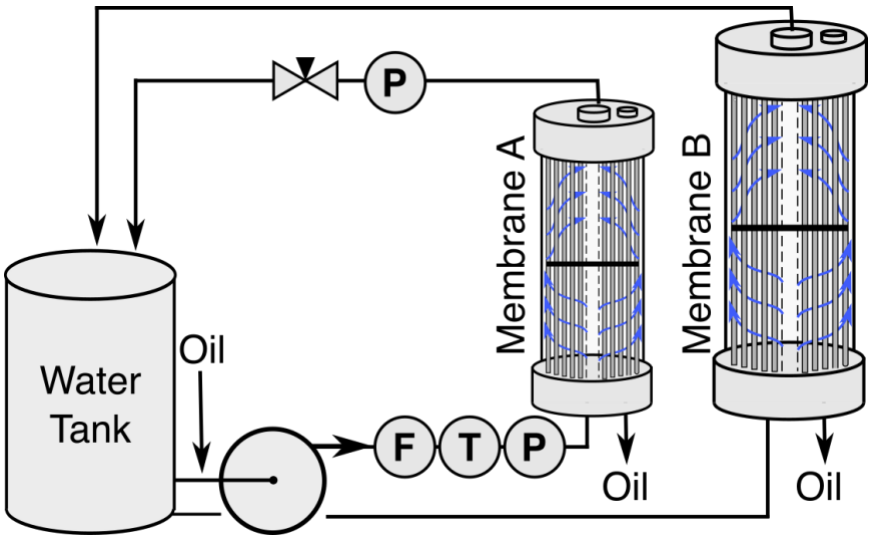

Figure 41: Process flow diagram of experimental apparatus. Membrane A (Dimensions: 6.4 cm x 20.3 cm, Surface Area: 1.4 m^2) serves as the primary membrane while Membrane B (Dimensions: 10.2 cm x 71.1 cm, Surface Area: 20 m^2) serves as the guard membrane. Abbreviations are as follows: pressure transmitter (P), temperature transmitter (T), and flow transmitter (F).

The transmembrane pressure and influent flow rate for Membrane A were controlled via the variable speed drive on the high-shear pump and the valve downstream of Membrane A. Shell-side pressures were monitored via a transmitter while tube-side pressure remained at atmospheric pressure. The transmembrane pressure was calculated by averaging the inlet and outlet shell-side pressure. Influent oil concentration, oil recovery, and oil flux were quantified gravimetrically via scale by monitoring all injected and permeated oil. Oil flux and oil recovery were calculated as a four-hour average as follows:

$$Oil\ Flux\ (\frac{m^3}{m^2-s}) = \frac{\dot{m}_{permeate}}{\rho_{oil} \times A_{membrane}} \quad (32)$$

$$Oil\ Recovery\ (\%) = \frac{\dot{m}_{permeate}}{\dot{m}_{injected}} \cdot 100\% \quad (33)$$

Where $\dot{m}_{permeate}$ was the mass flow of the permeate (g/s), $\dot{m}_{injected}$ was the mass flow of injected oil (g/s), ρ_{oil} was the density of the oil (g/cm^3), and $A_{membrane}$ was the surface area of the membrane (m^2). A DeltaV data acquisition system allowed for real-time data collection from all described instruments. The R programming environment was utilized for statistical analysis and to generate figures.

RESULTS AND DISCUSSION

Produced Water Characterization

Measured raw produced water characteristics are presented in **Table 19**. The produced water characteristics are consistent with ranges observed in the literature.[1,2]

Table 19: Raw produced water characteristics. All units in mg/L unless otherwise noted.

Variable	Value	Variable	Value	Variable	Value
pH	6.9	Alkalinity	137 mg/L as $CaCO_3$	SO_4^{2-}	167
Conductivity	72 mS/cm	Na^+	12,442	F^-	<1
TDS	47,192	K^+	120	NO_2^-	<1
TSS	250	Mg^{2+}	227	NO_3^-	<1
Turbidity	334 NTU	Ca^{2+}	7,488	PO_4^{3-}	<0.1
TPH	17	Cl^-	30,500		
TOC	67	Br^-	174		

Selective Oil Permeation Process Performance

Oil recoveries of 74.3% to 99.9% were observed over sixteen experimental conditions. Some experiments achieved effluent oil concentrations of less than 1.0 mg/L, indicating the potential for selective oil permeation to regulatory requirements for beneficial reuse. Exemplar pre- and post-treatment pictures are shown in **Figure 42A**. Much of the visual difference between the raw produced water and Membrane A feed was achieved by the membrane system within minutes of circulating the produced water within the system. A summary of the experimental results is provided in **Table A9**.

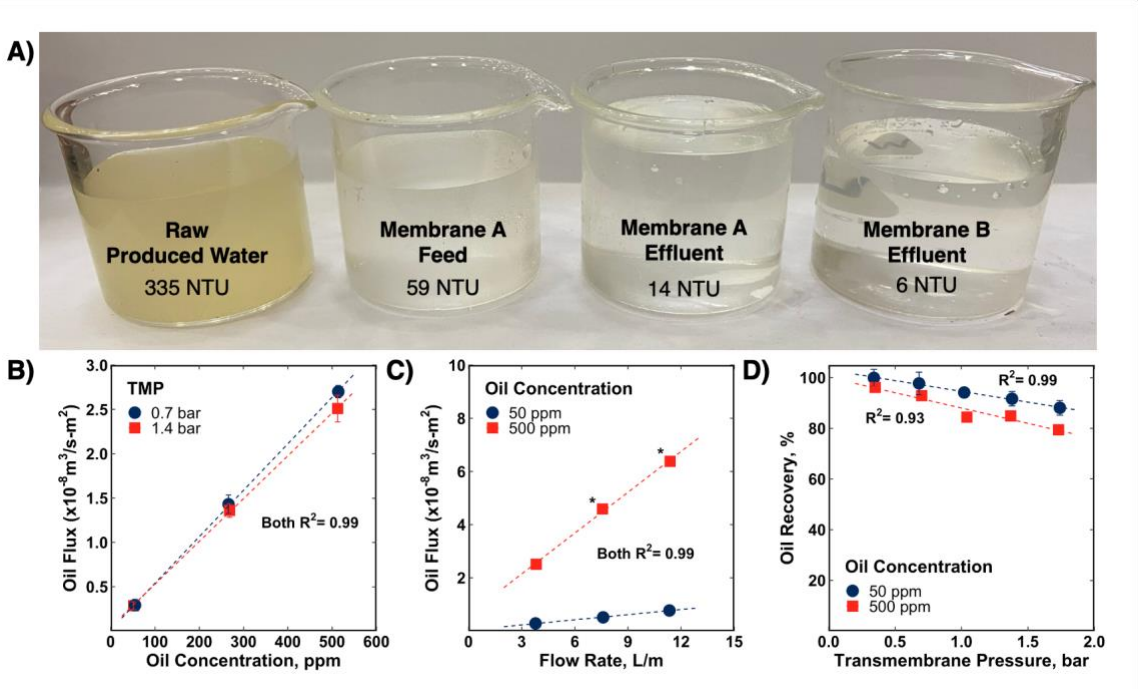

Figure 42: (A) Visual changes in produced water throughout the process at an influent Isopar M concentration of 500 ppm, transmembrane pressure of 0.7 bar, and influent flow rate of 3.8 L/m. (B) The effect of oil concentration on oil flux. Experiments conducted at 3.8 L/min in Membrane A. (C) The effect of influent flow rate on oil flux. Experiments conducted at a transmembrane pressure of 0.7 bar in Membrane A. Asterisks note experiments requiring two hour averaging due to system limitations. (D) The effect of transmembrane pressure on oil recovery. Experiments conducted at a flow rate of 3.8 L/min in Membrane A.

Effect of Oil Concentration

Oil flux exhibited a linear relationship (R^2 = 0.99 for 0.7 and 1.4 bar) with influent concentration in this study (**Figure 42B**). Kong *et al.* first observed this linear relationship between oil flux and oil concentration for oil concentrations less than 1 wt.%.[28] Mercelat *et al.* later expanded on this work and found a saturation-style relationship between oil flux and oil concentrations ranging from 200 ppm to 100%.[22] Within the oil-disperse region, a

linear relationship was observed between oil concentration and oil flux. This behavior was attributed to coalescence (instead of permeation) limiting oil flux.[22]

Oil recoveries decreased slightly at 0.7 bar (97.8% ± 4.4% at 50 ppm to 92.9% ± 1.0% at 500 ppm) and more substantially at 1.4 bar (91.7% ± 2.8% at 50 ppm to 84.9% ± 0.7% at 500 ppm) with increasing oil concentration. The decrease in oil recovery with increasing influent oil mass flow rate is also consistent with the proposed saturation-style model, where permeation becomes limiting as the oil film approaches to the maximum wetted surface area.[22]

Effect of Influent Flow Rate

A linear relationship (R^2=0.99) was observed between oil flux and influent flow rate for 50 ppm and 500 ppm (**Figure 42C**). Oil recovery decreased slightly for both 50 ppm (91.7% ± 2.9% at 3.8 L/m to 86.4% ± 2.0% at 11.4 L/m) and 500 ppm (84.9% ± 0.7% at 3.8 L/m to 74.3% ± 1.0% at 11.4 L/m). This result may indicate that the influent oil mass exceeds the wetted surface area of the membrane, transferring the dominant mechanism from coalescence to permeation as the influent oil mass flow rate increases. However, the relatively constant oil recovery may offer a pragmatic opportunity for selective oil permeation to serve as a high-throughput, modular treatment process.

Effect of Transmembrane Pressure

Previous researchers evaluating oil flux and recovery in oil-continuous solutions have observed relationships between oil flux and transmembrane pressure that are consistent with the Ergun equation.[19,22,23] Similarly, Kong *et al.* found oil recovery increased with increasing transmembrane pressure for influent oil concentrations <1%.[28] In contrast, this study observed an inverse relationship between transmembrane pressure

and oil recovery (**Figure 42B and Figure 42D**). Magdich noted similar behavior for a 5% dodecane-water mixture, but not for experiments using a higher viscosity oil.[23] Mercelat *et al.* also observed this behavior for influent Isopar M concentrations of 2%. Mercelat *et al.* attributed the behavior to the rate of permeation surpassing the rate of coalescence and reducing the wetted surface area fraction (a_e/a_t) of the membrane.[22]

Increased oil recovery at lower applied transmembrane pressures offers two key advantages. First, elevated oil recovery at lower applied transmembrane pressure reduces the required energy input for the process. Second, water breakthrough is hypothesized to occur when the applied transmembrane pressure exceeds the critical entry pressure of the water. Thus, the operation of selective oil permeation systems at lower transmembrane pressures reduces the likelihood of water breaking through into the permeate while increasing oil recoveries.

Performance and Model Comparison

Application of the existing mass transfer model to the expanded data indicated potential discrepancies (**Figure 43**). These discrepancies may be due to applying the initial model outside of the original parameter ranges.[22] For example, the model performs poorly for influent flow rates greater than 3.8 L/m, which may be due to the exponents associated with concentration and velocity in the original model not correctly scaling with 7.6 and 11.4 L/m. Ultimately, further research is necessary to expand the original mass transfer model to adequately predict oil flux over a broader set of operating and water quality conditions.

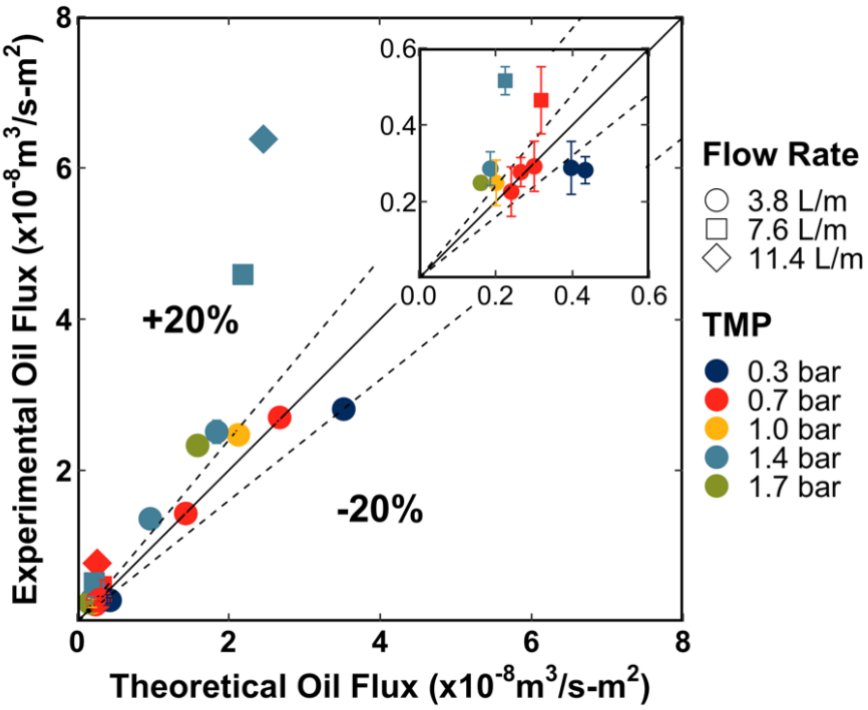

Figure 43: Parity plot between theoretical and experimental oil flux.

CONCLUSIONS

This study demonstrated the potential for selective oil permeation to achieve high oil recoveries (>90%) in oil-water separations with produced water without evidence of free water in the pure oil permeate. These oil recoveries may allow selective oil permeation to achieve oil concentrations required for beneficial reuse.

This study examined some of the lowest influent oil concentrations in the literature. Successful oil recovery within this concentration range demonstrates the potential for selective oil permeation to serve as a secondary or tertiary oil-water separation process. Within the examined experimental conditions, selective oil permeation process performance corresponded with competition between the hypothesized mechanisms: approach and coalescence, permeation, and release.[22] Crucially, the dominance of approach

and coalescence offers advantages. For example, high oil recoveries at low transmembrane pressures also minimizes the likelihood of water breakthrough and reduces required energy throughput. The minimal relationship between oil recovery and influent flow rate suggests selective oil permeation could serve as a high-throughput, modular process at certain oil concentrations. Finally, the experimental data generally exceeded the theoretical expectations of the original model.

Broadly, these results indicate the potential for selective oil permeation to serve as a secondary or tertiary oil-water separation process for produced water treatment. While this study presents promising results for selective oil permeation, future fundamental studies are necessary to elucidate the effects of produced water on membrane fouling and the longevity of the membrane.

ACKNOWLEDGEMENTS

This project was funded by the Kuwait Foundation for the Advancement of Sciences under project code CN17-45EV-01. This material is based upon work supported by the National Science Foundation Graduate Research Fellowship under Grant No. DGE 2137420. I would also like to thank Benjamin Kienzle for his analytical support. Finally, I would love to acknowledge Chris Sanders for his help at the Separations Research Program facility and assistance acquiring the produced water.

Chapter 8: Conclusions and Recommendations

CONCLUSIONS

This dissertation investigated how operative mechanisms impact selective oil permeation performance (*i.e.*, oil flux, oil recovery, oil permeate quality) through varying oil characteristics (*e.g.*, viscosity), solution characteristics (*e.g.*, interfacial tension, pH, salinity), and operating conditions (*e.g.*, transmembrane pressure, influent flow rate) for oil concentrations less than 500 mg/L. The set of studies furthers our understanding of the selective oil permeation process and its opportunity space.

While prior work had predominantly focused on oil concentrations greater than 1%, **Chapter 4** demonstrated that selective oil permeation can achieve elevated oil removals (>90%) at much lower oil concentrations. Successful recovery of oil at concentrations less than 1% without macroscopic evidence of membrane fouling resolves conflicting conclusions within the literature about the applicability of the process within this lower concentration range. Furthermore, the study identified the presence of optimal and suboptimal operating ranges induced by mechanistic competition between approach, coalescence, permeation, and release. Careful consideration of these optimal and suboptimal conditions may explain existing discrepancies within the selective oil permeation literature surrounding the relationship between transmembrane pressure and oil recovery as well as influent flow rate and oil recovery for oil-disperse solutions. Finally, the study emphasized the importance of membrane conditioning and temporal variability in selective oil permeation. Observation of substantial improvements in oil recovery with respect to time supports the fundamental benefits (*e.g.*, minimization of viscous oil fouling at the membrane surface) of selective oil permeation over traditional membrane-based oil-

water separations. These experimental results ultimately support selective oil permeation as a secondary or tertiary oil-water separation approach.

Chapter 5 demonstrated the potential for selective oil permeation to recover oil (without water breakthrough) from oil-disperse solutions under various water quality conditions relevant to produced water. Each water quality parameter examined (pH, salinity, and surfactant concentrations) was observed to have a statistically significant effect on oil flux and oil recovery. Additionally, the relationships between the individual water quality parameters and process performance were broadly consistent with the proposed mechanistic framework, highlighting the dominance of coalescence for oil-disperse solutions and the importance of emulsion stability. Furthermore, results presented in **Chapter 5** provide preliminary support for enhancing process performance via water quality adjustment. Ultimately, these findings broaden our mechanistic understanding of the process and the potential opportunity space for selective permeation, particularly for produced water treatment and oil-spill cleanup.

Chapter 6 investigated selective oil permeation through the lens of the Young-Laplace equation. Previous researchers had identified operating conditions that induced water breakthrough (*e.g.,* low interfacial tension of the influent produced water, high transmembrane pressure), but the results from these previous experiments provided limited guidance for avoiding water breakthrough. While there was ultimately neither agreement nor correlation between the theoretical expectations and experimental results in **Chapter 6**, the Young-Laplace equation may still provide a conservative method of estimating the maximum applied transmembrane pressure. Ultimately, the lack of water breakthrough observed for nearly all experimental conditions in **Chapters 5** and **6** is promising for the application of selective oil permeation to industrial wastewaters like produced water.

Key factors identified in **Chapters 4, 5,** and **6** were combined through experiments using real produced water in **Chapter 7**. The observed relationships between operating parameters and solution characteristics observed in **Chapter 7** were consistent with results for comparable solution characteristics (*e.g.*, oil concentration, water quality) and operating conditions (*e.g.*, transmembrane pressure, influent flow rate) in **Chapters 4** and **5**. Furthermore, as anticipated from results presented in **Chapter 6**, no water breakthrough was observed during experiments with real produced water. These results indicate that selective oil permeation has the potential to meet regulatory requirements for the beneficial reuse of produced water.

FUTURE WORK

While this dissertation has furthered our understanding of selective oil permeation, there is still a lack of understanding surrounding membrane fouling and membrane longevity for the process. Addressing these remaining gaps in the literature will help to better define the opportunity space for how selective oil permeation can best contribute to the circular water economy. The following projects may aid in achieving these goals.

Membrane Fouling

Membrane fouling is one of the main challenges for the application of membrane-based treatment approaches. Yet, no studies have systematically evaluated fouling within selective oil permeation. Many studies have noted that surfactant adsorption at the membrane surface appears to result in oil flux decline.[19,20,23,25] Similar interactions between the membrane surface and solution may have reduced oil flux in the experiments reported in **Chapter 5**. Furthermore, biological fouling appeared to limit the life of the membrane module (due to factors including low oil recovery and high shell-side differential pressures)

throughout this work. Similarly, changes in salinity were sometimes observed to cause declines in membrane performance**.** Application of bench-scale experiments and conventional membrane characterization techniques (*e.g.,* contact angle, scanning electron microscopy, atomic force microscopy) would likely be able to substantially advance our understanding of how common contaminants might be impacting the membrane morphology and performance during long-term, pilot-scale experimentation. Additional research is also necessary to expand on existing cleaning methods (**Table A11** and **Table A12**) to determine effective methods of cleaning and restoring performance to membrane modules in selective oil permeation.

Membrane Surface Modification

Researchers have investigated selective oil permeation using a variety of membrane materials (*e.g.,* polypropylene,[19,22,23,26,157] polyethylene,[158] ceramic,[19] polyvinylidene fluoride,[28] poly(tetrafluoroethylene)[20,24,25]). Membrane modification is one method researchers have used to provide enhanced process performance. For example, within traditional membrane-based oil-water separations, researchers have investigated the addition of hydrophilic additives, surface modifications, and creation of novel materials that exploit surface properties like wettability.[124–138] Within the selective oil permeation literature, Magdich observed improvements in membrane performance by coating Celgard polypropylene X-20 membrane fibers (pore diameter 0.05 μm) with the cationic polymer N(β-aminoethyl)-γ-aminopropyltrimethoxysilane.[23] These results indicate the potential to use smart, tailored membrane design to enhance selective oil permeation process performance.

Direct Observation of Selective Oil Permeation

Much of the mechanistic understanding of the selective oil permeation process relies on the hypothesized existence of an oil film at the membrane surface following coalescence. Mercelat *et al.* hypothesized that the development of an oil film aids in coalescence, supports permeation, and ultimately controls macroscopic performance.[22] As such, the development and expansion of the oil film may aid in oil recovery, while destabilization and reduction in the oil film can reduce long-term oil flux. Within this current work, membrane performance was observed to improve over the course of 127 days of operation (**Chapter 4)**. Further, membrane performance increased when membrane pre-conditioning methods were applied (**Chapter 4**). Throughout these studies, researchers have touted the wetting of the membrane surface as paramount to process performance. Yet, no microscopic characterization work has been conducted to validate the existence of the hypothesized oil film or confirm oil film characteristics and operating parameters that influence the growth or reduction in the oil film during selective oil permeation. Bench-scale experimentation that paired direct observation techniques with conventional membrane characterization techniques could likely confirm our mechanistic understanding of selective oil permeation.

Integrated Treatment Trains

Researchers have hypothesized that achieving the circular water economy for complex industrial wastewater will require the development of autonomous, precise, resilient, intensified, electrified, modular treatment trains.[34] Throughout this dissertation, we have demonstrated the ability for selective oil permeation to achieve many of these goals. Furthermore, **Chapter 7** demonstrated the potential for selective oil permeation to treat produced water and achieve regulatory effluent oil and grease requirements. Yet,

many membrane-based treatment processes often benefit from their integration into more complex treatment train designs to achieve synergistic effects. Thus, integration of selective oil permeation into a produced water treatment train (**Figure 44**) could provide an interesting avenue for further investigation.

Figure 44: Example of an integrated process treatment train using selective oil permeation for the beneficial reuse of produced water. Abbreviations are as follows: Total Oil and Grease (TOG), Total Suspended Solids (TSS), Total Dissolved Solids (TDS), and Total Organic Carbon (TOC). Dashed line indicates breakdown of larger organic compounds via advanced oxidation to generate assimilable organic carbon.

Technoeconomic Analysis

Finally, while this dissertation has demonstrated the technical potential for selective oil permeation, it is necessary to evaluate the economic viability of selective oil permeation. Evaluation of the technoeconomics will enable a better understanding of the research necessary for the technology to reach pipe parity with comparable oil-water separations approaches.

Appendix

SUPPLEMENTARY TABLES

Table A1: Summary of Chapter 4 experimental results. Abbreviations are as follows: Influent Oil Concentration (C_{oil}), Transmembrane Pressure (TMP), and Influent Flow Rate (Q).

C_{oil}, mg/L	TMP, bar	Q, L/min	Oil Recovery, %	Oil Flux, m^3/m^2-s
Isopar M – Unconditioned Membrane				
201.0	2.8	3.7	22.9	2.52E-09
193.9	0.7	3.8	72.6	7.98E-09
196.0	0.4	3.8	87.4	9.53E-09
196.0	0.2	3.8	90.2	9.80E-09
195.6	1.4	1.9	38.1	2.03E-09
196.9	1.4	3.8	54.3	5.97E-09
200.7	1.4	5.7	58.3	9.75E-09
208.7	1.4	7.6	63.1	1.46E-08
198.7	1.4	9.5	61.7	1.73E-08
Isopar M – Unconditioned Membrane after 67 Days of Operation				
191.3	2.8	3.8	65.2	6.96E-09
201.5	0.70	3.7	89.3	1.00E-08
200.9	0.3	4.2	92.8	1.05E-08
200.3	0.2	3.7	86.1	9.53E-09
194.5	2.2	3.8	66.8	7.39E-09
193.8	1.7	3.8	70.0	7.67E-09
192.8	1.2	3.8	74.7	8.21E-09
206.9	1.4	1.9	77.5	4.44E-09
199.3	1.4	3.8	78.2	8.61E-09
198.3	1.4	5.7	78.6	1.30E-08
194.4	1.4	7.6	78.6	1.72E-08

195.3	1.4	9.5	79.5	2.19E-08
Isopar M – Unconditioned Membrane after 127 Days of Operation				
200.1	2.8	3.9	71.1	7.94E-09
202.9	2.2	3.8	74.6	8.54E-09
204.3	1.7	3.8	79.5	9.04E-09
204.5	1.2	3.8	89.6	1.03E-08
202.8	0.7	3.8	96.2	1.08E-08
206.4	0.4	3.7	96.2	1.10E-08
205.6	0.2	3.7	89.5	1.04E-08
Isopar M – 7 Day Isopar M Soak Conditioned Membrane				
201.6	2.8	3.8	68.1	7.71E-09
202.1	0.7	3.7	93.2	1.05E-08
201.5	0.4	3.8	97.4	1.09E-08
200.6	0.2	3.8	97.9	1.08E-08
199.5	2.3	3.8	70.2	7.90E-09
199.5	1.7	3.8	77.7	8.16E-09
201.6	1.2	3.8	85.1	9.53E-09
188.9	1.4	1.9	75.4	3.83E-09
205.4	1.4	3.8	78.9	9.24E-09
192.8	1.4	5.7	78.7	1.28E-08
197.7	1.4	7.6	76.2	1.69E-08
194.9	1.4	9.5	73.4	2.01E-08
Isopar M – 14 Day Isopar M Conditioned Membrane				
210.1	2.7	3.8	77.1	9.20E-09
208.1	0.7	3.8	95.4	1.11E-08
203.3	0.3	3.9	96.6	1.11E-08
208.6	0.2	3.8	89.0	1.01E-08
209.2	2.2	3.8	79.0	9.27E-09

206.4	1.7	3.8	80.5	9.26E-09
206.4	1.2	3.8	84.8	9.86E-09
206.9	1.4	1.9	79.1	4.49E-09
224.4	1.4	3.8	83.6	1.06E-08
191.3	1.4	5.7	82.9	1.36E-08
193.1	1.4	7.6	82.7	1.81E-08
192.9	1.4	9.5	82.4	2.23E-08
Isopar M – Concentration Variation				
58.1	0.7	3.7	91.9	2.90E-09
95.5	0.7	3.7	92.7	4.87E-09
202.8	0.7	3.8	96.2	1.08E-08
Isopar V – Concentration Variation				
42.3	0.7	3.7	95.5	2.46E-09
101.7	0.7	3.8	91.4	5.15E-09
211.2	0.7	3.7	96.8	1.14E-08
Soybean Oil – Concentration Variation				
46.8	0.7	3.8	78.8	1.63E-09
102.3	0.7	3.8	74.7	3.70E-09
212.9	0.7	3.8	77.1	8.06E-09
Motor Oil 10W30 – Concentration Variation				
57.0	0.7	3.8	25.5	8.42E-10
99.9	0.7	3.8	19.8	1.00E-09
203.1	0.7	3.8	25.0	2.68E-09
Isopar M – Flow Rate Variation				
206.9	1.36	1.9	79.1	4.49E-09
224.4	1.40	3.8	83.6	1.06E-08
191.3	1.38	5.7	82.9	1.36E-08
193.1	1.38	7.6	82.7	1.81E-08

192.9	1.39	9.5	82.4	2.23E-08
Isopar M – Mass Flow Rate Variation				
206.9	1.36	1.9	77.5	4.44E-09
199.3	1.38	3.8	78.2	8.61E-09
198.3	1.38	5.7	78.6	1.30E-08
194.4	1.38	7.6	78.6	1.72E-08
195.3	1.38	9.5	79.5	2.19E-08
193.4	1.37	11.4	76.8	2.50E-08
191.9	1.37	3.8	78.0	8.38E-09
64.0	1.38	1.9	76.2	1.37E-09
46.9	1.38	3.8	79.0	2.03E-09
43.8	1.38	5.7	79.2	2.96E-09
52.9	1.38	7.6	78.1	4.55E-09
52.8	1.37	9.5	78.5	5.81E-09
57.1	1.38	11.4	81.1	6.96E-09
103.6	1.37	1.9	80.5	2.30E-09
89.9	1.37	3.8	83.9	4.27E-09
96.3	1.37	5.7	83.9	6.85E-09
101.4	1.37	7.6	82.0	9.31E-09
102.6	1.38	9.5	82.7	1.17E-08
105.8	1.38	11.4	83.8	1.49E-08
Isopar V – Flow Rate Variation				
208.4	1.37	1.9	88.00	5.09E-09
209.0	1.38	3.8	92.80	1.07E-08
213.4	1.38	5.7	91.50	1.64E-08
200.5	1.37	7.6	89.70	2.03E-08
200.5	1.38	9.5	88.90	2.50E-08
Soybean Oil – Flow Rate Variation				

195.5	1.38	1.9	64.8	3.22E-09
200.4	1.38	3.8	70.6	6.90E-09
212.4	1.38	5.7	69.7	1.09E-08
202.4	1.39	7.6	60.5	1.22E-08
202.2	1.39	9.5	52.9	1.32E-08
Motor Oil 10W30 – Flow Rate Variation				
204.3	1.4	1.9	8.80	5.79E-10
209.0	1.4	3.7	5.40	5.80E-10
214.8	1.4	5.8	6.20	1.05E-09
215.1	1.4	7.6	7.40	1.95E-09
210.2	1.4	9.5	13.00	3.65E-09
Isopar M – TMP Variation				
200.1	2.8	3.9	71.1	7.94E-09
202.9	2.2	3.8	74.6	8.54E-09
204.3	1.7	3.8	79.5	9.04E-09
204.5	1.2	3.8	89.6	1.03E-08
202.8	0.7	3.8	96.2	1.08E-08
206.4	0.4	3.7	96.2	1.10E-08
205.6	0.2	3.7	89.5	1.04E-08
Isopar V – TMP Variation				
210.4	2.7	3.8	85.8	1.01E-08
211.2	2.2	3.8	87.0	1.02E-08
212.6	1.7	3.7	90.2	1.05E-08
210.8	1.2	3.8	93.3	1.09E-08
211.9	0.7	3.7	96.8	1.14E-08
212.6	0.3	3.8	81.4	9.41E-09
213.3	0.2	3.8	55.4	6.79E-09
Soybean Oil – TMP Variation				

214.8	0.2	3.7	47.9	4.91E-09
214.1	0.3	3.7	71.8	7.50E-09
217.0	0.7	3.7	76.1	7.89E-09
214.4	1.2	3.7	56.5	5.78E-09
209.8	1.7	3.8	48.0	4.96E-09
214.4	2.2	3.8	44.3	4.63E-09
211.9	2.8	3.8	40.8	4.24E-09
Motor Oil 10W30 – TMP Variation				
202.0	0.3	3.8	43.0	4.59E-09
203.1	0.7	3.8	25.0	2.68E-09
190.4	0.2	3.8	43.6	4.43E-09
212.6	1.2	3.7	19.3	1.84E-09
200.7	1.8	3.9	14.1	1.74E-09
198.6	2.2	4.0	12.1	1.46E-09
200.7	2.8	3.9	7.6	8.44E-10

Table A2: Summary of experimental data from Chapter 5. All experiments conducted at an influent oil concentration of approximately 200 mg/L, influent flow rate of 3.8 L/min, and TMP of 0.7 bar. Flux values are displayed in m^3/m^2-s. Recovery values are displayed in % oil recovery.

	Flux	**Recovery**	**Flux**	**Recovery**	**Flux**	**Recovery**	**Flux**	**Recovery**
pH								
	Observation 1		**Observation 2**		**Observation 3**		**Observation 4**	
4	9.37E-09	82.3	9.60E-09	83.8	9.54E-09	86.6	9.94E-09	86.2
7	1.02E-08	91.2	1.00E-08	88.9	1.01E-08	88.7	1.05E-08	90.0
10	8.81E-09	77.2	8.53E-09	76.1	8.53E-09	73.6	8.42E-09	76.3
Salinity (mg/L NaCl)								
0	9.32E-09	78.2	8.94E-09	78.5	9.05E-09	81.2	9.16E-09	78.9
5	9.05E-09	78.4	9.49E-09	82.5	9.56E-09	83.0	9.44E-09	84.5
10	9.89E-09	84.4	1.00E-08	85.0	9.84E-09	85.7	9.83E-09	85.7
30	9.60E-09	83.0	9.55E-09	83.3	9.77E-09	83.5	9.78E-09	84.2

50	9.43E-09	80.7	9.28E-09	81.7	9.28E-09	81.2	9.38E-04	83.1
Anionic Surfactant (Sodium Dodecyl Sulfate, SDS) (mg/L SDS)								
0	9.51E-09	79.0	9.28E-09	80.0	9.50E-09	81.2	8.94E-09	80.6
10	9.27E-09	83.28	8.99E-09	78.2	8.94E-09	75.88	8.89E-09	77.08
100	8.60E-09	72.67	8.83E-09	75.92	8.83E-09	76.66	8.95E-09	75.19
1,000	6.50E-09	54.95	6.90E-09	60.46	6.90E-09	61.50	6.68E-09	58.73
Cationic Surfactant (Cetyltrimethyl Ammonium Bromide, CTAB) (mg/L CTAB)								
0	8.56E-09	73.88	8.71E-09	75.25	8.94E-09	76.49	9.12E-09	78.45
10	9.22E-09	77.45	8.94E-09	76.8	8.77E-09	78.9	8.94E-09	76.39
100	9.66E-09	85.19	9.95E-09	85.08	1.02E-08	87.74	1.01E-08	86.21
200	8.54E-09	74.53	8.54E-09	71.24	9.05E-09	77.20	8.88E-09	74.29
500	8.32E-09	67.86	7.18E-09	57.20	7.02E-09	56.90	6.51E-09	53.50
1,000	1.98E-09	15.23	3.74E-09	29.76	1.42E-09	8.89	2.49E-09	20.28
Nonionic Surfactant (Polysorbate 80, Tween 80) (mg/L Tween 80)								
0	9.37E-09	83.52	9.11E-09	80.09	9.22E-09	80.26	8.99E-09	81.23
10	9.55E-09	82.42	9.44E-09	82.36	9.49E-09	83.25	9.38E-09	81.34
100	8.99E-09	76.4	8.07E-09	68.51	7.53E-09	63.26	7.13E-09	60.59
1,000	3.00E-09	24.95	1.64E-09	13.31	1.13E-09	13.22	1.58E-09	12.92

Table A3: Adjusted P-values from Tukey post-hoc analysis for pH. Values less than 0.05 indicate statistically significant difference between experimental conditions.

	Oil Flux	**Oil Recovery**
pH 7 – pH 4	0.0114	0.0049
pH 10 – pH 4	0.0002	0.0001
pH 10 – pH 7	0.0000	0.0000

Table A4: Adjusted P-values from Tukey post-hoc analysis for NaCl concentration. Values less than 0.05 indicate statistically significant difference between experimental conditions.

	Oil Flux	**Oil Recovery**
5,000 mg/L NaCl – 0 mg/L NaCl	0.1182	0.0797
10,000 mg/L NaCl – 0 mg/L NaCl	0.0000	0.0003
30,000 mg/L NaCl – 0 mg/L NaCl	0.0005	0.0056
50,000 mg/L NaCl – 0 mg/L NaCl	0.2384	0.1583
10,000 mg/L NaCl – 5,000 mg/L NaCl	0.0014	0.0547
30,000 mg/L NaCl – 5,000 mg/L NaCl	0.0786	0.6420
50,000 mg/L NaCl – 5,000 mg/L NaCl	0.9922	0.9943

30,000 mg/L NaCl –10,000 mg/L NaCl	0.2703	0.4916
50,000 mg/L NaCl – 10,000 mg/L NaCl	0.0006	0.0260
50,000 mg/L NaCl – 30,000 mg/L NaCl	0.0355	0.4161

Table A5: Adjusted P-values from Tukey post-hoc analysis for anionic surfactant. Values less than 0.05 indicate statistically significant difference between experimental conditions.

	Oil Flux	**Oil Recovery**
10 mg/L SDS – 0 mg/L SDS	0.2348	0.7799
100 mg/L SDS – 0 mg/L SDS	0.0169	0.0454
1,000 mg/L SDS – 0 mg/L SDS	0.0000	0.0000
100 mg/L SDS – 10 mg/L SDS	0.4288	0.2157
1,000 mg/L SDS – 10 mg/L SDS	0.0000	0.0000
1,000 mg/L SDS – 100 mg/L SDS	0.0000	0.0000

Table A6: Adjusted P-values from Tukey post-hoc analysis for nonionic surfactant. Values less than 0.05 indicate statistically significant difference between experimental conditions.

	Oil Flux	**Oil Recovery**
10 mg/L Tween 80 – 0 mg/L Tween 80	0.8876	0.9876
100 mg/L Tween 80 – 0 mg/L Tween 80	0.0437	0.0051
1,000 mg/L Tween 80 – 0 mg/L Tween 80	0.0000	0.0000
100 mg/L Tween 80 –10 mg/L Tween 80	0.0124	0.0029
1,000 mg/L Tween 80 –10 mg/L Tween 80	0.0000	0.0000
1,000 mg/L Tween 80 –100 mg/L Tween 80	0.0000	0.0000

Table A7: Adjusted P-values from Tukey post-hoc analysis for cationic surfactant. Values less than 0.05 indicate statistically significant difference between experimental conditions.

	Oil Flux	**Oil Recovery**
10 mg/L CTAB – 0 mg/L CTAB	0.9992	0.9981
100 mg/L CTAB – 0 mg/L CTAB	0.0743	0.0627
200 mg/L CTAB – 0 mg/L CTAB	0.9999	0.9947
500 mg/L CTAB – 0 mg/L CTAB	0.0076	0.0007
1,000 mg/L CTAB – 0 mg/L CTAB	0.0000	0.0000
100 mg/L CTAB –10 mg/L CTAB	0.1423	0.1365
200 mg/L CTAB – 10 mg/L CTAB	0.9928	0.9315

500 mg/L CTAB – 10 mg/L CTAB	0.0036	0.0003
1,000 mg/L CTAB – 10 mg/L CTAB	0.0000	0.0000
200 mg/L CTAB – 100 mg/L CTAB	0.0502	0.0221
500 mg/L CTAB – 100 mg/L CTAB	0.0000	0.0000
1,000 mg/L CTAB – 100 mg/L CTAB	0.0000	0.0000
500 mg/L CTAB – 200 mg/L CTAB	0.0116	0.0020
1,000 mg/L CTAB – 200 mg/L CTAB	0.0000	0.0000
1,000 mg/L CTAB – 500 mg/L CTAB	0.0000	0.0000

Table A8: Experimental data for Chapter 6. All experiments conducted at 3.8 L/min. Abbreviations are as follows: Oil Concentration (C_{oil}, mg/L), Transmembrane Pressure (ΔP, bar), Oil flux ($J_{o/w,}$ m^3/m^2-s), Isopropyl Alcohol Concentration (IPA, wt%)

C_{oil}	P_T/P_c	ΔP	Oil Recovery	$J_{o/w}$	Permeate Quality (mg/L H_2O)
Millipore Water (IFT ≅ 50 mN/m)					
50	0.01	0.21	95.5	2.31E-09	15.3
50	0.05	1.06	44.8	1.47E-09	17.3
50	0.1	2.13	23.1	7.92E-10	15.0
50	0.2	4.26	15.4	4.55E-10	10.8
500	0.01	0.21	86.3	2.50E-08	25.9
500	0.05	1.06	40.6	1.16E-08	17.2
500	0.1	2.13	17	4.86E-09	28.0
500	0.2	4.26	10.2	2.95E-09	16.0
Millipore Water with 5 wt.% IPA (IFT ≅ 30 mN/m)					
50	0.01	0.13	92.5	2.80E-09	12.7
50	0.05	0.64	73.1	2.20E-09	11.8
50	0.1	1.28	52.0	1.36E-09	10.9
50	0.2	2.55	27.2	9.06E-10	9.3
50	0.3	3.79	23.3	7.95E-10	13.6
500	0.01	0.13	83.8	2.34E-08	27.4

500	0.05	0.64	63.8	1.82E-08	26.0
500	0.1	1.28	40.2	1.17E-08	24.7
500	0.2	2.55	29.1	8.57E-09	45.7
500	0.3	3.73	21.1	5.96E-09	11.3
Millipore Water with 25 wt.% IPA (IFT ≅ 10 mN/m)					
50	0.05	0.21	79.5	2.15E-09	58.1
50	0.1	0.43	47.8	1.81E-09	32.5
50	0.2	0.85	29.6	1.36E-09	55.9
50	0.3	1.28	23.8	6.78E-10	128.6
50	0.4	1.70	18.7	4.53E-10	76.3
50	0.5	2.13	12.6	3.97E-10	65.8
500	0.05	0.21	37.3	1.09E-08	62.8
500	0.1	0.43	27.7	8.47E-09	73.7
500	0.2	0.85	19.0	5.71E-09	71.7
500	0.3	1.28	17.8	4.97E-09	93.1
500	0.4	1.70	16.1	4.64E-09	103.1
500	0.5	2.13	13.1	3.62E-09	87.80
500	0.6	2.49	5.2	1.48E-09	41.3
500	0.7	2.89	4.9	1.47E-09	60.5
500	0.8	3.45	5.8	1.71E-09	24.3
500	0.9	3.71	4.6	1.43E-09	2389.4
500	1.0	4.21	4.4	1.28E-09	39.3
Millipore Water with Varying IFT					
C_{in}	**IPA**	**ΔP**	**Oil Recovery**	**$J_{o/w}$**	**Permeate Quality (mg/L H_2O)**
275	0	1.37	33.2	5.26E-09	54.3
275	10	1.39	23.4	3.68E-09	49.5
275	20	1.38	5.4	9.05E-10	83.9

275	30	1.38	3.8	6.79E-10	49.0

Table A9: A summary of the experimental results for Chapter 7. Abbreviations are as follows: Inlet Oil Concentration (C_{oil}), Transmembrane Pressure (ΔP), and Inlet Flow Rate (Q).

C_{oil}, mg/L	**ΔP, bar**	**Q, L/min**	**Oil Recovery, %**	**Oil Flux, m^3/m^2-s**
51.8	1.4	3.8	91.7 (± 2.6)	2.86E-09 (± 4.38E-10)
50.5	1.4	7.6	87.5 (± 1.5)	5.15E-09 (± 3.65E-10)
52.9	1.4	11.4	86.4 (± 2.0)	7.72E-09 (± 4.45E-10)
49.3	0.4	3.8	96.0 (± 6.9)	2.77E-09 (± 7.35E-10)
48.6	0.7	3.8	92.7 (± 2.8)	2.77E-09 (± 3.79E-10)
46.9	1.0	3.8	93.1 (± 3.7)	2.49E-09 (± 5.93E-10)
51.4	1.7	3.8	85.8 (± 4.3)	2.49E-09 (± 1.70E-10)
266.0	0.7	3.8	94.4 (± 1.3)	1.43E-09 (± 1.04E-09)
268.3	1.4	3.8	86.7 (± 1.0)	1.36E-08 (± 7.71E-10)
501.3	0.4	3.8	96.2 (± 0.4)	2.81E-08 (± 1.31E-09)
513.8	0.7	3.8	92.9 (± 1.1)	2.70E-08 (± 6.96E-10)
505.4	1.0	3.8	84.9 (± 0.5)	2.47E-08 (± 3.36E-10)
508.2	1.7	3.8	79.4 (± 0.6)	2.33E-08 (± 7.85E-10)
512.4	1.4	3.8	84.9 (± 0.7)	2.51E-08 (± 1.51E-09)
499.3	1.4	7.6	79.7 (± 0.3)	4.59E-08 (± 2.60E-10)
498.5	1.4	11.4	74.3 (± 1.0)	6.37E-08 (± 7.78E-10)

Table A10: Characterization of Tap Water in Austin, TX from Mercelat *et al.*[22]

Parameter	
pH	9.6

Total Hardness (mg/L as $CaCO_3$)	87
Conductivity (μmhos/cm)	285
Total Alkalinity (mg/L as $CaCO_3$)	62
Phenol Alkalinity (mg/L as $CaCO_3$)	16
Total Organic Carbon (mg/L)	2.5
Turbidity (NTU)	0.06

Table A11: Mercelat's recommended chemical cleaning method for biological fouling.[18] Additional details regarding performance and procedure are detailed in the Mercelat dissertation.

Process Description	**Time (h)**
Recirculate isopropyl alcohol until permeation on tube side	0.5
Drain Contactor	
Recirculate 5% w/w NaOH Solution	2
Drain Contactor	
Recirculate 5% w/w Citric Acid Solution	2
Drain Contactor	
Rinse with water until inlet pH is equivalent to outlet pH	0.3
Dry with warm nitrogen flow from tube side to shell side	12
Integrity Test for Membrane	

Table A12: 3M™'s recommended chemical cleaning method for severe fouling.[213]

Process Description	**Time (h)**
Flush contactor once-through with clean water, filtered to 5-micron absolute, at ambient temperature	0.25
Drain Contactor	

Pressurize shell side of contactor with 50 vol% Isopropanol-water or ethanol-water solution, not exceeding max pressure rating. Allow alcohol solution to come out of both lumen ports, then cap off lumen ports and let contactor soak	1
Recirculate 2-6 wt.% caustic (NaOH or KOH) solution prepared with 5-micron (abs.) filtered water; suggested cleaning solution temperature 86-122°F (30-50°C)	1–4
Drain Contactor	
Recirculate 10 wt.% citric acid, or 1-6 wt.% nitric, phosphoric, hydrochloric, or mixed acid solution prepared with 5-micron (abs.) filtered water; suggested cleaning solution temperature ambient	1–2
Drain Contactor	
Flush contactor once-through with clean water, filtered to 5-micron absolute, at ambient temperature (until inlet pH is equal to the outlet pH)	
Drain Contactor	
Blow air or an inert gas through lumen side of contactor at maximum available flow rate without exceeding flow or pressure rating	0.25+
Dry contactor thoroughly using procedure described separately later in this guide. Warm gas would dry contactor much faster. Inert gas is preferred for drying. Clean and dry air could be used but air temperature should not exceed 122°F (50°C)	
Integrity Test	

Glossary

Table A13: Summary of abbreviations (Abbr.) used throughout the text.

Term	Abbr.	Term	Abbr.
Analysis of Variance	ANOVA	Microfiltration	MF
Alkylbenzene Sulfonic Acid	ABSA	Nanofiltration	NF
American Petroleum Institute	API	Reverse Osmosis	RO
Corrugated Plate Interceptor	CPI	Sodium Dodecyl Sulfate	SDS
Chemical Oxygen Demand	COD	Total Dissolved Solids	TDS
Cetyltrimethyl Ammonium Bromide	CTAB	Total Oil and Grease	TOG
Dissolved Air Flotation	DAF	Total Organic Carbon	TOC
Granular Activated Carbon	GAC	Total Petroleum Hydrocarbons	TPH
Hydrocarbon	HC	Total Suspended Solids	TSS
Interfacial Tension	IFT	Transmembrane Pressure	TMP
Isopropyl Alcohol	IPA	Ultrafiltration	UF

References

1. Benko, K. L. & Drewes, J. E. Produced water in the Western United States: Geographical distribution, occurrence, and composition. *Environ. Eng. Sci.* **25**, 239–246 (2008).

2. Fakhru'l-Razi, A. *et al.* Review of technologies for oil and gas produced water treatment. *J. Hazard. Mater.* **170**, 530–551 (2009).

3. Jiménez, S., Micó, M. M., Arnaldos, M., Medina, F. & Contreras, S. State of the art of produced water treatment. *Chemosphere* **192**, 186–208 (2018).

4. Pintor, A. M. A., Vilar, V. J. P., Botelho, C. M. S. & Boaventura, R. A. R. Oil and grease removal from wastewaters: Sorption treatment as an alternative to state-of-the-art technologies. A critical review. *Chem. Eng. J.* **297**, 229–255 (2016).

5. Jafarinejad, S. & Jiang, S. C. Current technologies and future directions for treating petroleum refineries and petrochemical plants (PRPP) wastewaters. *J. Environ. Chem. Eng.* **7**, 103326 (2019).

6. Judd, S. *et al.* The size and performance of offshore produced water oil-removal technologies for reinjection. *Sep. Purif. Technol.* (2014). doi:10.1016/j.seppur.2014.07.037

7. Sobolciak, P. *et al.* Materials and Technologies for the Tertiary Treatment of Produced Water Contaminated by Oil Impurities through Nonfibrous Deep-Bed Media : A Review. 1–26 (2020).

8. Tanudjaja, H. J., Hejase, C. A., Tarabara, V. V., Fane, A. G. & Chew, J. W. Membrane-based separation for oily wastewater: A practical perspective. *Water Research* **156**, (2019).

9. Tummons, E. N., Tarabara, V. V., Chew, J. W. & Fane, A. G. Behavior of oil droplets at the membrane surface during crossflow

microfiltration of oil-water emulsions. *J. Memb. Sci.* **500**, 211–224 (2016).

10. Masoudnia, K., Raisi, A., Aroujalian, A. & Fathizadeh, M. Treatment of Oily Wastewaters Using the Microfiltration Process: Effect of Operating Parameters and Membrane Fouling Study. *Sep. Sci. Technol.* **48**, 1544–1555 (2013).

11. Hu, B. & Scott, K. Microfiltration of water in oil emulsions and evaluation of fouling mechanism. *Chem. Eng. J.* **136**, 210–220 (2008).

12. Cao, D. Q., Iritani, E. & Katagiri, N. Properties of filter cake formed during dead-end microfiltration of O/W emulsion. *J. Chem. Eng. Japan* **46**, 593–600 (2013).

13. Xu, X., Li, J., Xu, N., Hou, Y. & Lin, J. Visualization of fouling and diffusion behaviors during hollow fiber microfiltration of oily wastewater by ultrasonic reflectometry and wavelet analysis. *J. Memb. Sci.* **341**, 195–202 (2009).

14. Yao, S., Costello, M., Fane, A. G. & Pope, J. M. Non-invasive observation of flow profiles and polarisation layers in hollow fibre membrane filtration modules using NMR micro-imaging. *J. Memb. Sci.* **99**, 207–216 (1995).

15. Salahi, A., Abbasi, M. & Mohammadi, T. Permeate flux decline during UF of oily wastewater: Experimental and modeling. *Desalination* **251**, (2010).

16. Lobo, A., Cambiella, Á., Benito, J. M., Pazos, C. & Coca, J. Ultrafiltration of oil-in-water emulsions with ceramic membranes: Influence of pH and crossflow velocity. *J. Memb. Sci.* **278**, 328–334 (2006).

17. Seibert, A. F. No Title. in *2011 Annual AIChE Conference* (2011).

18. Mercelat, A. Fundamental Study of Hydrophobic Microporous Membrane Contactors for the Recovery of Insoluble Oil from Oil-Water Mixtures. (The University of Texas at Austin, 2016).

19. Tirmizi, N. P., Raghuraman, B. & Wiencek, J. Demulsification of Water/Oil/Solid Emulsions by Hollow-Fiber Membranes. *AIChE J.* **42**, 1263–1276 (1996).

20. Ezzati, A., Gorouhi, E. & Mohammadi, T. Separation of water in oil emulsions using microfiltration. *Desalination* (2005). doi:10.1016/j.desal.2005.03.086

21. Kipp, P. B., Seibert, F. & Connelly, R. Non-Dispersive Process for Insoluble Oil Recovery from Aqueous Slurries. **2**, 31 (2013).

22. Mercelat, A. Y., Cooper, C. M., Kinney, K. A., Seibert, F. & Katz, L. E. Mechanisms for Direct Separation of Oil from Water with Hydrophobic Hollow Fiber Membrane Contactors. (2021). doi:10.1021/acsestengg.1c00055

23. Magdich, P. The Removal of Oil from Oil-Water Mixtures using Selective Oil Filtration. (The University of Minnesota, 1988).

24. Unno, H., Saka, H. & Akehata, T. Oil Separation From Oil-Water Mixture By A Porous Poly(Tetrafluoroethylene) (Ptfe) Membrane. *J. Chem. Eng. Japan* **19**, 281–286 (1986).

25. Ueyama, K., Fukuura, K. & Furusaki, S. Oil-phase permeation behavior of o/w emulsion through a porous polytetrafluoroethylene membrane. *J. Chem. Eng. Japan* **20**, 618–622 (1987).

26. Daiminger, U., Nitsch, W., Plucinski, P. & Hoffmann, S. Novel techniques for oil / water separation. **99**, 197–203 (1995).

27. Unno, H., Taguchi, K. & Akehata, T. Liquid permeation through (poly)-tetrafluoroethylene (ptfe) membrane. *J. Chem. Eng. Japan* **20**,

52–57 (1987).

28. Kong, J. & Li., K. Oil removal from oil-in-water emulsions using PVDF membranes. *Sep. Purif. Technol.* (1999). doi:10.1016/S1383-5866(98)00114-2

29. Hoek, E. M. V. *et al.* Produced Water. in *Oil & Gas Produced Water Management* 3 – 14 (Morgan & Claypool Publishers, 2021).

30. Veil, J. *U . S . Produced Water Volumes and Management Practices in 2017. US. Produced Water Management* (2020).

31. Al-Ghouti, M. A., Al-Kaabi, M. A., Ashfaq, M. Y. & Da'na, D. A. Produced water characteristics, treatment and reuse: A review. *J. Water Process Eng.* **28**, 222–239 (2019).

32. Jiang, W. *et al.* A Critical Review of Analytical Methods for Comprehensive Characterization of Produced Water. *Water* **13**, 183 (2021).

33. Stringfellow, W. T., Domen, J. K., Camarillo, M. K., Sandelin, W. L. & Borglin, S. Physical, chemical, and biological characteristics of compounds used in hydraulic fracturing. *J. Hazard. Mater.* **275**, 37–54 (2014).

34. Cath, T. *et al. Resource Extraction Sector Technology Roadmap*. (2021).

35. Cooper, C. M. *et al.* Oil and Gas Produced Water Reuse: Opportunities, Treatment Needs, and Challenges. *ACS ES&T Eng.* **2**, 347–366 (2022).

36. Conrad, C. L. *et al.* Fit-for-purpose treatment goals for produced waters in shale oil and gas fields. *Water Res.* **173**, (2020).

37. Hoek, E. M. V. *et al.* Produced Water Treatment Fundamentals. in *Oil*

& Gas Produced Water Management 25–31 (Morgan & Claypool Publishers, 2021). doi:10.2118/27177-ms

38. Klemz, A. C. *et al.* Oilfield produced water treatment by liquid-liquid extraction: A review. *J. Pet. Sci. Eng.* **199**, (2021).

39. Ferreira, A. R. *et al.* Feasibility study on produced water oxidation as a pretreatment at offshore platform. *Process Saf. Environ. Prot.* **160**, 255–264 (2022).

40. Liu, Y. *et al.* A review of treatment technologies for produced water in offshore oil and gas fields. *Sci. Total Environ.* **775**, 145485 (2021).

41. Rahman, A., Agrawal, S., Nawaz, T. & Pan, S. A Review of Algae-Based Produced Water Treatment for Biomass and Biofuel Production. 1–27 (2020).

42. Lusinier, N. *et al.* Biological treatments of oilfield produced water: A comprehensive review. *SPE J.* **24**, 2135–2147 (2019).

43. Camarillo, M. K. & Stringfellow, W. T. Biological treatment of oil and gas produced water: a review and meta-analysis. *Clean Technol. Environ. Policy* **20**, 1127–1146 (2018).

44. Al-Kaabi, M. A., Zouari, N., Da'na, D. A. & Al-Ghouti, M. A. Adsorptive batch and biological treatments of produced water: Recent progresses, challenges, and potentials. *J. Environ. Manage.* **290**, 112527 (2021).

45. Jain, P., Sharma, M., Dureja, P., Sarma, P. M. & Lal, B. Bioelectrochemical approaches for removal of sulfate, hydrocarbon and salinity from produced water. *Chemosphere* **166**, 96–108 (2017).

46. Passos da Motta, A. R. *et al.* Produced water treatment for oil removal by membrane separation process: review. *Eng. Sanit. e Ambient.* **18**, 15–26 (2013).

47. Adham, S., Hussain, A., Minier-Matar, J., Janson, A. & Sharma, R. Membrane applications and opportunities for water management in the oil & gas industry. *Desalination* **440**, 2–17 (2018).

48. Alzahrani, S. & Mohammad, A. W. Challenges and trends in membrane technology implementation for produced water treatment: A review. *J. Water Process Eng.* **4**, 107–133 (2014).

49. Munirasu, S., Haija, M. A. & Banat, F. Use of membrane technology for oil field and refinery produced water treatment - A review. *Process Saf. Environ. Prot.* **100**, 183–202 (2016).

50. Jepsen, K. L., Bram, M. V., Pedersen, S. & Yang, Z. Membrane fouling for produced water treatment: A review study from a process control perspective. *Water (Switzerland)* **10**, (2018).

51. Zoubeik, M., Ismail, M., Salama, A. & Henni, A. New Developments in Membrane Technologies Use in the Treatment of Produced Water: A Review. *Arab. J. Sci. Eng.* **43**, 2093–2118 (2018).

52. Samuel, O. *et al.* Oilfield-produced water treatment using conventional and membrane-based technologies for beneficial reuse: A critical review. *J. Environ. Manage.* **308**, 114556 (2022).

53. Zolghadr, E., Firouzjaei, M. D., Amouzandeh, G., LeClair, P. & Elliott, M. The Role of Membrane-Based Technologies in Environmental Treatment and Reuse of Produced Water. *Front. Environ. Sci.* **9**, 1–11 (2021).

54. Chang, H. *et al.* Potential and implemented membrane-based technologies for the treatment and reuse of flowback and produced water from shale gas and oil plays: A review. *Desalination* (2019). doi:10.1016/j.desal.2019.01.001

55. Dickhout, J. M. *et al.* Produced water treatment by membranes: A review from a colloidal perspective. *J. Colloid Interface Sci.* **487**, 523–

534 (2017).

56. Shaffer, D. L. *et al.* Desalination and reuse of high-salinity shale gas produced water: Drivers, technologies, and future directions. *Environ. Sci. Technol.* **47**, 9569–9583 (2013).

57. Subramani, A. & Jacangelo, J. G. Emerging desalination technologies for water treatment: A critical review. *Water Res.* **75**, 164–187 (2015).

58. Xie, W. *et al.* Solar-driven desalination and resource recovery of shale gas wastewater by on-site interfacial evaporation. *Chem. Eng. J.* **428**, 132624 (2022).

59. Yousef, R., Qiblawey, H. & El-Naas, M. H. Adsorption as a process for produced water treatment: A review. *Processes* **8**, 1–22 (2020).

60. Gul Zaman, H. *et al.* Produced water treatment with conventional adsorbents and MOF as an alternative: A review. *Materials (Basel).* **14**, 1–29 (2021).

61. Zhu, X., Tu, W., Wee, K. H. & Bai, R. Effective and low fouling oil/water separation by a novel hollow fiber membrane with both hydrophilic and oleophobic surface properties. *J. Memb. Sci.* **466**, 36–44 (2014).

62. Costa, T. C. *et al.* Evaluation of the technical and environmental feasibility of adsorption process to remove water soluble organics from produced water: A review. *J. Pet. Sci. Eng.* **208**, (2022).

63. Lin, L., Jiang, W., Chen, L., Xu, P. & Wang, H. Treatment of produced water with photocatalysis: Recent advances, affecting factors and future research prospects. *Catalysts* **10**, 1–18 (2020).

64. Coha, M., Farinelli, G., Tiraferri, A., Minella, M. & Vione, D. Advanced oxidation processes in the removal of organic substances from produced water: Potential, configurations, and research needs.

Chem. Eng. J. **414**, 128668 (2021).

65. dos Santos, E. V., Bezerra Rocha, J. H., de Araújo, D. M., de Moura, D. C. & Martínez-Huitle, C. A. Decontamination of produced water containing petroleum hydrocarbons by electrochemical methods: A minireview. *Environ. Sci. Pollut. Res.* **21**, 8432–8441 (2014).

66. Sun, Y. *et al.* A critical review of risks, characteristics, and treatment strategies for potentially toxic elements in wastewater from shale gas extraction. *Environ. Int.* **125**, 452–469 (2019).

67. Silva, T. L. S., Morales-Torres, S., Castro-Silva, S., Figueiredo, J. L. & Silva, A. M. T. An overview on exploration and environmental impact of unconventional gas sources and treatment options for produced water. *J. Environ. Manage.* **200**, 511–529 (2017).

68. Ghafoori, S. *et al.* New advancements, challenges, and future needs on treatment of oilfield produced water: A state-of-the-art review. *Sep. Purif. Technol.* **289**, 120652 (2022).

69. Nasiri, M., Jafari, I. & Parniankhoy, B. Oil and Gas Produced Water Management: A Review of Treatment Technologies, Challenges, and Opportunities. *Chem. Eng. Commun.* **204**, 990–1005 (2017).

70. Liden, T., Santos, I. C., Hildenbrand, Z. L. & Schug, K. A. Treatment modalities for the reuse of produced waste from oil and gas development. *Sci. Total Environ.* **643**, 107–118 (2018).

71. Liden, T., Clark, B. G., Hildenbrand, Z. L. & Schug, K. A. *Unconventional Oil and Gas Production: Waste Management and the Water Cycle*. *Environmental Issues Concerning Hydraulic Fracturing* **1**, (Elsevier Inc., 2017).

72. Igunnu, E. T. & Chen, G. Z. Produced water treatment technologies. *Int. J. Low-Carbon Technol.* **9**, 157–177 (2014).

73. Estrada, J. M. & Bhamidimarri, R. A review of the issues and treatment options for wastewater from shale gas extraction by hydraulic fracturing. *Fuel* **182**, 292–303 (2016).

74. Olajire, A. A. Recent advances on the treatment technology of oil and gas produced water for sustainable energy industry-mechanistic aspects and process chemistry perspectives. *Chem. Eng. J. Adv.* **4**, 100049 (2020).

75. Piccioli, M., Aanesen, S. V., Zhao, H., Dudek, M. & Øye, G. Gas Flotation of Petroleum Produced Water: A Review on Status, Fundamental Aspects, and Perspectives. *Energy and Fuels* (2020). doi:10.1021/acs.energyfuels.0c03262

76. Sobolčiak, P. *et al.* Some theoretical aspects of tertiary treatment of water/oil emulsions by adsorption and coalescence mechanisms: A review. *Water (Switzerland)* **13**, 1–26 (2021).

77. da Silva Almeida, F. B. P., Esquerre, K. P. S. O. R., Soletti, J. I. & De Farias Silva, C. E. Coalescence process to treat produced water: an updated overview and environmental outlook. *Environ. Sci. Pollut. Res.* **26**, 28668–28688 (2019).

78. Sjöblom, J. *et al.* Our current understanding of water-in-crude oil emulsions. Recent characterization techniques and high pressure performance. *Adv. Colloid Interface Sci.* **100**–**102**, 399–473 (2003).

79. Tellez, G. T., Nirmalakhandan, N. & Gardea-Torresdey, J. L. Performance evaluation of an activated sludge system for removing petroleum hydrocarbons from oilfield produced water. *Adv. Environ. Res.* (2002). doi:10.1016/S1093-0191(01)00073-9

80. Neff, J. M., Sauer, T. C. & Maciolek, N. *Composition, Fate and Effects of Produced Water Discharges to Nearshore Marine Waters*. *Produced Water* (1992). doi:10.1007/978-1-4615-2902-6_30

81. Zolfaghari, R., Fakhru'l-Razi, A., Abdullah, L. C., Elnashaie, S. S. E. H. & Pendashteh, A. Demulsification techniques of water-in-oil and oil-in-water emulsions in petroleum industry. *Sep. Purif. Technol.* **170**, 377–407 (2016).

82. Santander, M., Rodrigues, R. T. & Rubio, J. Modified jet flotation in oil (petroleum) emulsion/water separations. *Colloids Surfaces A Physicochem. Eng. Asp.* **375**, 237–244 (2011).

83. Ali, M. F. & Alqam, M. H. Role of asphaltenes, resins and other solids in the stabilization of water in oil emulsions and its effects on oil production in Saudi oil fields. *Fuel* **79**, 1309–1316 (2000).

84. Veil, J., Puder, M., Elcock, D. & Redweik, R. *A White Paper Describing Produced Water from Production of Crude Oil, Natural Gas, and Coal Bed Methane*. (2004).

85. Khan, N. A. *et al.* Volatile-organic molecular characterization of shale-oil produced water from the Permian Basin. *Chemosphere* **148**, 126–136 (2016).

86. Danforth, C. *et al.* An integrative method for identification and prioritization of constituents of concern in produced water from onshore oil and gas extraction. *Environ. Int.* **134**, 105280 (2020).

87. Rosenblum, J. *et al.* Temporal characterization of flowback and produced water quality from a hydraulically fractured oil and gas well. *Sci. Total Environ.* **596**–**597**, 369–377 (2017).

88. Rosenblum, J., Thurman, E. M., Ferrer, I., Aiken, G. & Linden, K. G. Organic Chemical Characterization and Mass Balance of a Hydraulically Fractured Well: From Fracturing Fluid to Produced Water over 405 Days. *Environ. Sci. Technol.* **51**, 14006–14015 (2017).

89. Oetjen, K. *et al.* Temporal characterization and statistical analysis of flowback and produced waters and their potential for reuse. *Sci. Total*

Environ. **619**–**620**, 654–664 (2018).

90. Orem, W. *et al.* Organic substances in produced and formation water from unconventional natural gas extraction in coal and shale. *Int. J. Coal Geol.* **126**, 20–31 (2014).

91. Blondes, M. S. *et al.* U.S. Geological Survey National Produced Waters Geochemical Database v2.3. (2019). doi:https://doi.org/10.5066/F7J964W8

92. Cambiella, A., Benito, J. M., Pazos, C. & Coca, J. Centrifugal separation efficiency in the treatment of waste emulsified oils. *Chem. Eng. Res. Des.* **84**, 69–76 (2006).

93. Sharifi, H. & Shaw, J. M. Secondary drop production in packed-bed coalescers. *Chem. Eng. Sci.* **51**, 4817–4826 (1996).

94. Han, Y. *et al.* A review of the recent advances in design of corrugated plate packs applied for oil–water separation. *J. Ind. Eng. Chem.* **53**, 37–50 (2017).

95. Frising, T., Noïk, C. & Dalmazzone, C. The liquid/liquid sedimentation process: From droplet coalescence to technologically enhanced water/oil emulsion gravity separators: A review. *J. Dispers. Sci. Technol.* **27**, 1035–1057 (2006).

96. Chapter 15 Liquid-Liquid Extraction. in *Perry's Handbook* (McGraw-Hill, 2019).

97. Azam, H., Hoagland, F. M., Cooper, J. E. & Sun, P. Fundamentals of Produced Water Treatment in the Oil and Gas Industry. 1–86 (2019).

98. Saththasivam, J., Loganathan, K. & Sarp, S. An overview of oil-water separation using gas flotation systems. *Chemosphere* **144**, 671–680 (2016).

99. Wahi, R., Chuah, L. A., Choong, T. S. Y., Ngaini, Z. & Nourouzi, M. M. Oil removal from aqueous state by natural fibrous sorbent: An overview. *Sep. Purif. Technol.* **113**, 51–63 (2013).

100. Singh, C. J., Mukhopadhyay, S. & Rengasamy, R. S. *Fibrous coalescence filtration in treating oily wastewater: A review*. *Journal of Industrial Textiles* **0**, (2021).

101. Mognon, J. L., Bicalho, I. C. & Ataíde, C. H. Mini-hydrocyclones application in the reduction of the total oil-grease (TOG) in a prepared sample of produced water. *Sep. Sci. Technol.* **51**, 370–379 (2016).

102. Ashaghi, K. S., Ebrahimi, M. & Czermak, P. Ceramic Ultra- and Nanofiltration Membranes for Oilfield Produced Water Treatment: A Mini Review. *Open Environ. Sci.* **1**, 1–8 (2008).

103. Landsman, M. R. *et al.* Water Treatment: Are Membranes the Panacea? *Annu. Rev. Chem. Biomol. Eng.* **11**, 559–585 (2020).

104. Mueller, J., Cen, Y. & Davis, R. H. Crossflow microfiltration of oily water. *J. Memb. Sci.* **129**, 221–235 (1997).

105. Chakrabarty, B., Ghoshal, A. K. & Purkait, M. K. Ultrafiltration of stable oil-in-water emulsion by polysulfone membrane. *J. Memb. Sci.* **325**, 427–437 (2008).

106. Ebrahimi, M. *et al.* Innovative ceramic hollow fiber membranes for recycling/reuse of oilfield produced water. *Desalin. Water Treat.* **55**, 3554–3567 (2015).

107. Hua, F. L. *et al.* Performance study of ceramic microfiltration membrane for oily wastewater treatment. *Chem. Eng. J.* **128**, 169–175 (2007).

108. Padaki, M. *et al.* Membrane technology enhancement in oil-water separation. A review. *Desalination* **357**, 197–207 (2015).

109. Huang, Q., Gomaa, H. G. & Hashem, N. Flux Characteristics of Oil Separation from O/W Emulsions using Highly Hydrophilic UF Membrane in Narrow Channel. *Sep. Sci. Technol.* **49**, 12–21 (2014).

110. Abbasi, M., Mirfendereski, M., Nikbakht, M., Golshenas, M. & Mohammadi, T. Performance study of mullite and mullite-alumina ceramic MF membranes for oily wastewaters treatment. *Desalination* **259**, 169–178 (2010).

111. Ahmad, T., Guria, C. & Mandal, A. Optimal synthesis and operation of low-cost polyvinyl chloride/bentonite ultrafiltration membranes for the purification of oilfield produced water. *J. Memb. Sci.* **564**, 859–877 (2018).

112. Bilstad, T. & Espedal, E. Membrane separation of produced water. *Water Sci. Technol.* **34**, 239–246 (1996).

113. Yong, C., Wu, O., Environmental, A. & Canada, G. Re-injecting Produced Water into Tight Oil Reservoirs. in *SPE Canadian Unconventional Resources Conference* 1–7 (2012).

114. Lee, J. M. & Frankiewicz, T. Treatment of produced water with an ultrafiltration (UF) membrane - A field trial. *SPE Annu. Tech. Conf. Proc.* (2005). doi:10.2118/95735-ms

115. Visvanathan, C., Svenstrup, P. & Ariyamethee, P. Volume reduction of produced water generated from natural gas production process using membrane technology. *Water Sci. Technol.* **41**, 117–123 (2000).

116. Ersahin, M. E. *et al.* Treatment of produced water originated from oil and gas production wells: a pilot study and cost analysis. *Environ. Sci. Pollut. Res.* **25**, 6398–6406 (2018).

117. Qiao, X., Zhang, Z., Yu, J. & Ye, X. Performance characteristics of a hybrid membrane pilot-scale plant for oilfield-produced wastewater. *Desalination* **225**, 113–122 (2008).

118. Subramani, A. *et al.* Recovery optimization of membrane processes for treatment of produced water with high silica content. *Desalin. Water Treat.* **36**, 297–309 (2011).

119. Weschenfelder, S. E., Borges, C. P. & Campos, J. C. Oilfield produced water treatment by ceramic membranes: Bench and pilot scale evaluation. *J. Memb. Sci.* **495**, 242–251 (2015).

120. Zsirai, T. *et al.* Ceramic membrane filtration of produced water: Impact of membrane module. *Sep. Purif. Technol.* **165**, 214–221 (2016).

121. Zsirai, T., Qiblawey, H., Buzatu, P., Al-Marri, M. & Judd, S. J. Cleaning of ceramic membranes for produced water filtration. *J. Pet. Sci. Eng.* **166**, 283–289 (2018).

122. Beery, M., Pflieger, C. & Weyd, M. Sustainable industrial wastewater reuse using ceramic nanofiltration: Results from two pilot projects in the oil and gas and the ceramics industries. *J. Water Reuse Desalin.* **10**, 462–474 (2020).

123. Dehghani, Y., Honarvar, B., Azdarpour, A. & Nabipour, M. Pilot-scale experiments on a hybrid membrane-electrocoagulation system to produced water treatment in a domestic oil reservoir. *Water Pract. Technol.* **16**, 210–225 (2021).

124. Shi, H. *et al.* A modified mussel-inspired method to fabricate TiO2 decorated superhydrophilic PVDF membrane for oil/water separation. *J. Memb. Sci.* **506**, 60–70 (2016).

125. Zhang, S. *et al.* Cupric Phosphate Nanosheets-Wrapped Inorganic Membranes with Superhydrophilic and Outstanding Anticrude Oil-Fouling Property for Oil/Water Separation. *ACS Nano* **12**, 795–803 (2018).

126. Ou, R., Wei, J., Jiang, L., Simon, G. P. & Wang, H. Robust

Thermoresponsive Polymer Composite Membrane with Switchable Superhydrophilicity and Superhydrophobicity for Efficient Oil-Water Separation. *Environ. Sci. Technol.* **50**, 906–914 (2016).

127. Prince, J. A. *et al.* Ultra-wetting graphene-based PES ultrafiltration membrane – A novel approach for successful oil-water separation. *Water Res.* **103**, 311–318 (2016).

128. Tseng, H. H., Wu, J. C., Lin, Y. C. & Zhuang, G. L. Superoleophilic and superhydrophobic carbon membranes for high quantity and quality separation of trace water-in-oil emulsions. *J. Memb. Sci.* **559**, 148–158 (2018).

129. Jamalludin, M. R. *et al.* Facile fabrication of superhydrophobic and superoleophilic green ceramic hollow fiber membrane derived from waste sugarcane bagasse ash for oil/water separation. *Arab. J. Chem.* **13**, 3558–3570 (2020).

130. Ma, W. *et al.* Durable superhydrophobic and superoleophilic electrospun nanofibrous membrane for oil-water emulsion separation. *J. Colloid Interface Sci.* **532**, 12–23 (2018).

131. Wei, C. *et al.* Fabrication of pH-Sensitive Superhydrophilic/Underwater Superoleophobic Poly(vinylidene fluoride)- graft -(SiO 2 Nanoparticles and PAMAM Dendrimers) Membranes for Oil–Water Separation . *ACS Appl. Mater. Interfaces* **12**, 19130–19139 (2020).

132. Wu, L., Zhang, J., Li, B. & Wang, A. Mechanical- and oil-durable superhydrophobic polyester materials for selective oil absorption and oil/water separation. *J. Colloid Interface Sci.* (2014). doi:10.1016/j.jcis.2013.09.028

133. Shang, Y. *et al.* An in situ polymerization approach for the synthesis of superhydrophobic and superoleophilic nanofibrous membranes for oil-water separation. *Nanoscale* **4**, 7847–7854 (2012).

134. Gu, J. *et al.* Robust preparation of superhydrophobic polymer/carbon nanotube hybrid membranes for highly effective removal of oils and separation of water-in-oil emulsions. *J. Mater. Chem. A* **2**, 15268–15272 (2014).

135. Tang, X. *et al.* In situ polymerized superhydrophobic and superoleophilic nanofibrous membranes for gravity driven oil-water separation. *Nanoscale* **5**, 11657–11664 (2013).

136. Qing, W. *et al.* Robust superhydrophobic-superoleophilic polytetrafluoroethylene nanofibrous membrane for oil/water separation. *J. Memb. Sci.* **540**, 354–361 (2017).

137. Gupta, R. K., Dunderdale, G. J., England, M. W. & Hozumi, A. Oil/water separation techniques: A review of recent progresses and future directions. *J. Mater. Chem. A* **5**, 16025–16058 (2017).

138. Huang, S., Ras, R. H. A. & Tian, X. Antifouling membranes for oily wastewater treatment: Interplay between wetting and membrane fouling. *Curr. Opin. Colloid Interface Sci.* **36**, 90–109 (2018).

139. Babayev, M., Du, H., Botlaguduru, V. S. V. & Kommalapati, R. R. Zwitterion-modified ultrafiltration membranes for Permian Basin produced water pretreatment. *Water (Switzerland)* **11**, 1–15 (2019).

140. Wandera, D., Wickramasinghe, S. R. & Husson, S. M. Modification and characterization of ultrafiltration membranes for treatment of produced water. *J. Memb. Sci.* **373**, 178–188 (2011).

141. Naderi, N., Hosseini, S. S. & Atassi, Y. Tailoring the Morphology and Performance of Polyacrylonitrile Ultrafiltration Membranes for Produced Water Treatment via Solvent Mixture Strategy. 1655–1665 (2022). doi:10.1002/ceat.202100638

142. Mahmodi, G. *et al.* Improving antifouling property of alumina microfiltration membranes by using atomic layer deposition technique

for produced water treatment. *Desalination* **523**, 115400 (2022).

143. Wandera, D., Himstedt, H. H., Marroquin, M., Wickramasinghe, S. R. & Husson, S. M. Modification of ultrafiltration membranes with block copolymer nanolayers for produced water treatment: The roles of polymer chain density and polymerization time on performance. *J. Memb. Sci.* **403**–**404**, 250–260 (2012).

144. Verma, V. K. & Subbiah, S. Fouling resistant sericin-coated polymeric microfiltration membrane. *J. Chem. Technol. Biotechnol.* **94**, 3637–3649 (2019).

145. Zhen, X. H., Yu, S. L., Wang, B. H. & Zheng, H. F. Flux enhancement during ultrafiltration of produced water using turbulence promoter. *J. Environ. Sci. (China)* **18**, 1077–1081 (2006).

146. Hemmati, M., Rekabdar, F., Gheshlaghi, A., Salahi, A. & Mohammadi, T. Effects of air sparging, cross flow velocity and pressure on permeation flux enhancement in industrial oily wastewater treatment using microfi ltration. *Desalin. Water Treat.* **39**, 33–40 (2012).

147. Silalahi, S. H. D. & Leiknes, T. High frequency back-pulsing for fouling development control in ceramic microfiltration for treatment of produced water. *Desalin. Water Treat.* **28**, 137–152 (2011).

148. Gao, Y. *et al.* A multivariate study of backpulsing for membrane fouling mitigation in produced water treatment. *J. Environ. Chem. Eng.* **9**, (2021).

149. Silalahi, S. H. D. & Leiknes, T. O. Cleaning strategies in ceramic microfiltration membranes fouled by oil and particulate matter in produced water. *Desalination* **236**, 160–169 (2009).

150. QIU, Y. ren, ZHONG, H. & ZHANG, Q. xiu. Treatment of stable oil/water emulsion by novel felt-metal supported PVA composite

hydrophilic membrane using cross flow ultrafiltration. *Trans. Nonferrous Met. Soc. China (English Ed.* **19**, 773–777 (2009).

151. Tong, T., Carlson, K. H., Robbins, C. A., Zhang, Z. & Du, X. Membrane-based treatment of shale oil and gas wastewater: The current state of knowledge. *Front. Environ. Sci. Eng.* **13**, 1–17 (2019).

152. Motta, A., Borges, C., Esquerre, K. & Kiperstok, A. Oil Produced Water treatment for oil removal by an integration of coalescer bed and microfiltration membrane processes. *J. Memb. Sci.* **469**, 371–378 (2014).

153. Abdel-Shafy, H. I., Mansour, M. S. M. & El-Toony, M. M. Integrated treatment for oil free petroleum produced water using novel resin composite followed by microfiltration. *Sep. Purif. Technol.* **234**, 116058 (2020).

154. Kiss, Z. L., Kovács, I., Veréb, G., Hodúr, C. & László, Z. Treatment of model oily produced water by combined pre-ozonation–microfiltration process. *Desalin. Water Treat.* **57**, 23225–23231 (2016).

155. Ferreira, A. D. da F. *et al.* Fouling mitigation in produced water treatment by conjugation of advanced oxidation process and microfiltration. *Environ. Sci. Pollut. Res.* **28**, 12803–12816 (2021).

156. Aryanti, N., Kusworo, T. D., Oktiawan, W. & Wardhani, D. H. Performance of ultrafiltration-ozone combined system for produced water treatment. *Period. Polytech. Chem. Eng.* **63**, 438–447 (2019).

157. Seibert, F. *et al.* Non-Dispersive Process for Insoluble Oil Recovery from Aqueous Slurries. **2**, 28 (2013).

158. Leiknes, T. & Semmens, M. J. Membrane filtration for preferential removal of emulsified oil from water. *Water Sci. Technol.* **41**, 101–108 (2000).

159. Hazlett, R. N. Fibrous bed coalescence of water: Steps in the Coalescence Process. *Ind. Eng. Chem. Fundam.* **8**, 625–632 (1969).

160. Landahl, H. D. & Herrmann, R. G. Sampling of liquid aerosols by wires, cylinders, and slides, and the efficiency of impaction of the droplets. *J. Colloid Sci.* **4**, 103–136 (1949).

161. Chen, Y., Narayan, S. & Dutcher, C. S. Phase-Dependent Surfactant Transport on the Microscale: Interfacial Tension and Droplet Coalescence. *Langmuir* **36**, 14904–14923 (2020).

162. Spielman, L. A. & Goren, S. L. Theory of Coalescence by Flow through Porous Media. *Ind. Eng. Chem. Fundam.* **11**, 66–72 (1972).

163. Spielman, L. A. & Goren, S. L. Experiments in Coalescence by Flow through Fibrous Mats. *Ind. Eng. Chem. Fundam.* **11**, 73–83 (1972).

164. Spielman, L. A. & Su, Y. P. Coalescence of Oil-in-Water Suspensions by Flow through Porous Media. *Ind. Eng. Chem. Fundam.* **16**, 272–282 (1977).

165. Andan, S., Hariharan, S. I. & Chase, G. G. Continuum model evaluation of the effect of saturation on coalescence filtration. *Sep. Sci. Technol.* **43**, 1955–1973 (2008).

166. Sherony, D. F. & Kintner, R. C. Coalescence of an Emulsion in a Fibrous Bed: Part I. Theory. *Can. J. Chem. Eng.* **49**, 314 – 320 (1971).

167. Sherony, D. F. & Kintner, R. C. Coalescence of an Emulsion in a Fibrous Bed: Part II. Experimental. *Can. J. Chem. Eng.* **49**, 321–325 (1971).

168. Sokolović, R. M. Š., Vulić, T. J. & Sokolović, S. M. Effect of bed length on steady-state coalescence of oil-in-water emulsion. *Sep. Purif. Technol.* **56**, 79–84 (2007).

169. Agarwal, S., Von Arnim, V., Stegmaier, T., Planck, H. & Agarwal, A. Role of surface wettability and roughness in emulsion separation. *Sep. Purif. Technol.* **107**, 19–25 (2013).

170. Camarillo, M. K., Domen, J. K. & Stringfellow, W. T. Physical-chemical evaluation of hydraulic fracturing chemicals in the context of produced water treatment. *J. Environ. Manage.* **183**, 164–174 (2016).

171. Kim, B. S. & Harriott, P. Critical entry pressure for liquids in hydrophobic membranes. *J. Colloid Interface Sci.* **115**, 1–8 (1987).

172. Morrow, N. R. Effects of Surface Roughness on Contact Angle With Special Reference To Petroleum Recovery. *J. Can. Pet. Technol.* **14**, 42–53 (1975).

173. Bazhenov, S. D., Bildyukevich, A. V. & Volkov, A. V. Gas-liquid hollow fiber membrane contactors for different applications. *Fibers* **6**, (2018).

174. Naseri, A., Nikazar, M. & Mousavi Dehghani, S. A. A correlation approach for prediction of crude oil viscosities. *J. Pet. Sci. Eng.* **47**, 163–174 (2005).

175. Hoffmann, S. & Nitsch, W. Membrane Coalescence for Phase Separation of Oil-in-Water Emulsions Stabilized by Surfactants and Dispersed into Smallest Droplets. *Chem. Eng. Technol.* **24**, 22–27 (2001).

176. Kawakatsu, T., Boom, R. M., Nabetani, H., Kikuchi, Y. & Nakajima, M. Emulsion breakdown: Mechanisms and development of multilayer membrane. *AIChE J.* **45**, 967–975 (1999).

177. Hlavacek, M. Break-up of oil-in-water emulsions induced by permeation through a microfiltration membrane. *J. Memb. Sci.* **102**, 1–7 (1995).

178. Hong, A., Fane, A. G. & Burford, R. Factors affecting membrane coalescence of stable oil-in-water emulsions. *J. Memb. Sci.* **222**, 19–39 (2003).

179. Konishi, M. *et al.* The separation of oil from an oil-water-bacteria mixture using a hydrophobic tubular membrane. *Biochem. Eng. J.* (2005). doi:10.1016/j.bej.2004.11.012

180. Scott, K., Jachuck, R. J. & Hall, D. Crossflow microfiltration of water-in-oil emulsions using corrugated membranes. *Sep. Purif. Technol.* **22**–**23**, 431–441 (2001).

181. Kukizaki, M. & Goto, M. Demulsification of water-in-oil emulsions by permeation through Shirasu-porous-glass (SPG) membranes. *J. Memb. Sci.* (2008). doi:10.1016/j.memsci.2008.05.029

182. Mahmud, H., Kumar, A., Narbaitz, R. M. & Matsuura, T. A study of mass transfer in the membrane air-stripping process using microporous polypropylene hollow fibers. *J. Memb. Sci.* (2000). doi:10.1016/S0376-7388(00)00381-1

183. Nazzal, F. F. & Wiesner, M. R. Microfiltration of emulsions. *Water Environ. Res.* **68**, 1187–1191 (1996).

184. Cumming, I. W., Holdich, R. G. & Smith, I. D. The rejection of oil by microfiltration of a stabilised kerosene/water emulsion. *J. Memb. Sci.* (2000). doi:10.1016/S0376-7388(99)00338-5

185. Maaref, S. & Ayatollahi, S. The effect of brine salinity on water-in-oil emulsion stability through droplet size distribution analysis: A case study. *J. Dispers. Sci. Technol.* **39**, 721–733 (2018).

186. Davis, C. R., Martinez, C. J., Howarter, J. A. & Erk, K. A. Impact of Saltwater Environments on the Coalescence of Oil-in-Water Emulsions Stabilized by an Anionic Surfactant. *ACS ES T Water* **1**, 1702–1713 (2021).

187. 3M. 3M™ Liqui-Cel™ Data Sheets. (2018). Available at: https://www.3m.com/3M/en_US/liquicel-us/resources/data-sheets/. (Accessed: 1st November 2018)

188. Kahrilas, G. A., Blotevogel, J., Corrin, E. R. & Borch, T. Downhole Transformation of the Hydraulic Fracturing Fluid Biocide Glutaraldehyde: Implications for Flowback and Produced Water Quality. *Environ. Sci. Technol.* **50**, 11414–11423 (2016).

189. Stakne, K., Smole, M. S., Kleinschek, K. S., Jaroschuk, A. & Ribitsch, V. Characterisation of modified polypropylene fibres. *J. Mater. Sci.* **38**, 2167–2169 (2003).

190. Stachurski, J. & Michalek, M. The effect of the ζ potential on the stability of a non-polar oil-in-water emulsion. *J. Colloid Interface Sci.* **184**, 433–436 (1996).

191. USDA. *Technical Evaluation Report for the USDA Natural Organic Program: Isoparaffinic Hydrocarbon*. (2008).

192. Church, J., Paynter, D. M. & Lee, W. H. In Situ Characterization of Oil-in-Water Emulsions Stabilized by Surfactant and Salt Using Microsensors. *Langmuir* **33**, 9731–9739 (2017).

193. Kundu, P., Agrawal, A., Mateen, H. & Mishra, I. M. Stability of oil-in-water macro-emulsion with anionic surfactant: Effect of electrolytes and temperature. *Chem. Eng. Sci.* **102**, 176–185 (2013).

194. Binks, B. P., Fletcher, P. D. I. & Petsev, D. N. Stability of Oil-in-Water Emulsions in a Low Interfacial Tension System. *Landsc. Urban Plan.* **16**, 1025–1034 (2000).

195. Ríos, G., Pazos, C. & Coca, J. Destabilization of cutting oil emulsions using inorganic salts as coagulants. *Colloids Surfaces A Physicochem. Eng. Asp.* **138**, 383–389 (1998).

196. Márquez, A. L., Medrano, A., Panizzolo, L. A. & Wagner, J. R. Effect of calcium salts and surfactant concentration on the stability of water-in-oil (w/o) emulsions prepared with polyglycerol polyricinoleate. *J. Colloid Interface Sci.* **341**, 101–108 (2010).

197. Kestin, J., Khalifa, H. E. & Correia, R. J. Tables of the dynamic and kinematic viscosity of aqueous NaCl solutions in the temperature range 20â€ “ 150 °C and the pressure range 0.1â€ “ 35 MPa. *J. Phys. Chem. Ref. Data* **10**, 71–88 (1981).

198. Sutherland, G. Organic Recovery Method Using Hollow Fiber Microfilters. 1–24 (2000).

199. Kiani, A., Bhave, R. R. & Sirkar, K. K. Solvent Extraction with Immobilized Interfaces in a Microporous Hydrophobic Membrane. *J. Memb. Sci.* **20**, 125 – 145 (1984).

200. Prasad, R., Kiani, A., Bhave, R. R. & Sirkar, K. K. Further studies on solvent extraction with immobilized interfaces in a microporous hydrophobic membrane. *J. Memb. Sci.* **26**, 79–97 (1986).

201. Prasad, R. & Sirkar, K. K. Microporous Membrane Solvent Extraction. *Sep. Sci. Technol.* **22**, 619–640 (1987).

202. Prasad, R. & Sirkar, K. K. Hollow fibre solvent extraction. *J. Memb. Sci.* **50**, 153–175 (1990).

203. Majumdar, S., Guha, A. K. & Sirkar, K. K. Fuel oil desalting by hydrogel hollow fiber membrane. *J. Memb. Sci.* **202**, 253–256 (2002).

204. Prasad, R., Khare, S., Sengupta, A. & Sirkar, K. K. Novel liquid-in-pore configurations in membrane solvent extraction. *AIChE J.* **36**, 1592–1596 (1990).

205. Sirkar, K. K. Immobilized-Interface Solute-Transfer Process. (1991).

206. Franken, A. C. M., Nolten, J. A. M., Mulder, M. H. V., Bargeman, D. & Smolders, C. A. Wetting criteria for the applicability of membrane distillation. *J. Memb. Sci.* **33**, 315–328 (1987).

207. Purcell, W. R. Interpretation of centrifuge capillary pressure data. *Pet. Trans. AIME* **189**, 369–371 (1950).

208. Purcell, W. R. Capillary Pressures - Their Measurement Using Mercury and the Calculation of Permeability Therefrom. *J. Pet. Technol.* **1**, 39–48 (1949).

209. Salama, A. Critical entry pressure of a droplet pinning over multitude of pore openings. *Phys. Fluids* **33**, 032114 (2021).

210. Salama, A. Simplified Formula for the Critical Entry Pressure and a Comprehensive Insight into the Critical Velocity of Dislodgment of a Droplet in Crossflow Filtration. *Langmuir* **36**, 9634–9642 (2020).

211. Mikhail, S. Z. & Kimel, W. R. Densities and Viscosities of 1-Propanol-Water Mixtures. *J. Chem. Eng. Data* **8**, 323–328 (1963).

212. Kovvali, A. S. & Sirkar, K. K. *Chapter 7 Membrane contactors: recent developments*. *Membrane Science and Technology* **8**, (Elsevier Masson SAS, 2003).

213. 3M. *3M Liqui-Cel EXF Series Membrane Contactors: Cleaning and Storage Guidelines*. doi:10.1515/9783110281392-005